

INTERACTION BETWEEN HYDROGEN SULFIDE AND ENDOTHELIN-1 IN  
HEPATIC PERFUSION AND MITOCHONDRIAL DYNAMICS IN ENDOTOXEMIA

by

Samantha A. Pennington

A dissertation submitted to the faculty of  
The University of North Carolina at Charlotte  
in partial fulfillment of the requirements  
for the degree of Doctor of Philosophy in  
Biology

Charlotte

2018

Approved by:

---

Dr. Mark G. Clemens

---

Dr. Didier Dréau

---

Dr. Ian Marriott

---

Dr. Christine Richardson

---

Dr. Richard Chi

---

Dr. Reuben Howden

©2018  
Samantha A. Pennington  
ALL RIGHTS RESERVED

## ABSTRACT

SAMANTHA A. PENNINGTON. Interaction between hydrogen sulfide and endothelin-1 in hepatic perfusion and mitochondrial dynamics in endotoxemia. (Under the direction of DR. MARK G. CLEMENS)

A mismatch between oxygen supply and metabolic tissue demand leads to the development of hypoxia, which contributes to hepatic dysfunction and liver injury during sepsis. Recent evidence shows that hepatic H<sub>2</sub>S levels are increased during sepsis and the inhibition of endogenous H<sub>2</sub>S production significantly improves survival in septic mice; however, the precise mechanism is not known. The present study was designed to investigate the effect of H<sub>2</sub>S on hepatic microcirculation and mitochondrial dynamics during sepsis. We hypothesized that H<sub>2</sub>S contributes to hepatic dysfunction during sepsis by potentiating microvascular dysfunction and alterations in mitochondrial dynamics. Using intravital microscopy, we show that portal infusion of H<sub>2</sub>S and ET-1 is associated with sinusoidal constriction and inhibition of endogenous H<sub>2</sub>S attenuates the sensitization of the sinusoids to the constrictor effect of ET-1 and that the response to ET-1 is sex-related. Moreover, we show that endotoxemia leads to alterations in mitochondrial function, which is also sex-related. We furthered our investigation *in vitro* where we show that endotoxemia results in mitochondrial depolarization, alterations in mitochondrial dynamics, and increases in stress fiber formation, which contribute to vascular permeability observed in sepsis. We conclude that the contribution of H<sub>2</sub>S to hepatic microcirculatory and mitochondrial dysfunction is responsible, at least in part, for its deleterious effects during sepsis.

## DEDICATION

*I dedicate this dissertation to my loving husband and partner in life, James Blaine Pennington, who has been patient, encouraging, and provided unwavering support during my doctoral journey.*

## ACKNOWLEDGMENTS

I would like to thank the Novant Health Liver Research Fund and the Center for Biomedical Engineering and Science of the University of North Carolina at Charlotte for providing the funding for this research as well as Dr. Pinku Mukherjee for providing the mice used in this dissertation. This dissertation would not have been possible without the help of many individuals. I am especially grateful to my mentor, Dr. Mark Clemens, for providing the opportunity to work in his lab. His mentorship, insight, and knowledge have been invaluable throughout my doctoral research. I would also like to extend a special thanks to Dr. Didier Dréau for always making himself available to me, whether it be to discuss experimental design, aid in troubleshooting, or just for general help. I would also like to thank the rest of the members of my dissertation committee, Dr. Ian Marriott, Dr. Christine Richardson, Dr. Richard Chi, and Dr. Reuben Howden for their guidance and constructive criticism throughout this dissertation process. I am sincerely appreciative of the help I have received from various members of the Clemens laboratory throughout my tenure with a special thanks to Brittanie Height. I would also like to thank the faculty and staff of the University of North Carolina at Charlotte who had a part in the completion of my degree. Lastly, I would like to thank my parents and grandparents for instilling the love of learning in me, always supporting me throughout these years and encouraging me to chase dreams, and my husband, Blaine, who has truly been my biggest fan. His love and support are immeasurable.

## TABLE OF CONTENTS

LIST OF TABLES	viii
LIST OF FIGURES	ix
LIST OF ABBREVIATIONS	xiii
CHAPTER 1: INTRODUCTION	1
1.1 Overview	1
1.2 Hydrogen Sulfide	4
1.3 Hepatic Hydrogen Sulfide and Sepsis	7
1.4 Hepatic Microcirculation and Sepsis	8
1.5 Hepatic Mitochondrial Dysfunction and Sepsis	11
CHAPTER 2: THE RESPONSE OF HEPATOCYTES TO HYDROGEN SUFLIDE AND ENDOTHELIN-1 ON LIVER MICROCIRCULATION <i>IN VIVO</i>	15
2.1 Abstract	15
2.2 Introduction	16
2.3 Materials and Methods	19
2.4 Results	24
2.5 Discussion	28
2.6 Figures	35
CHAPTER 3: THE RESPONSE OF HEPATOCYTES TO HYDROGEN SUFLIDE AND ENDOTHELIN-1 VIA EFFECTS ON MITOCHONDIAL FUNCTION <i>IN VIVO</i>	47
3.1 Abstract	47
3.2 Introduction	48

3.3	Materials and Methods	55
3.4	Results	60
3.5	Discussion	64
3.6	Figures	72
CHAPTER 4: K <sub>ATP</sub> CHANNEL ACTIVATION BY EXOGENOUS HYDROGEN SULFIDE AND OXIDATIVE STRESS <i>IN VITRO</i>		89
4.1	Abstract	89
4.2	Introduction	90
4.3	Materials and Methods	94
4.4	Results	97
4.5	Discussion	98
4.6	Figures	103
CHAPTER 5: RESPONSE OF CELLS TO EXOGENOUS HYDROGEN SULFIDE DURING ENDOTOXEMIA <i>IN VITRO</i>		109
5.1	Abstract	109
5.2	Introduction	110
5.3	Materials and Methods	113
5.4	Results	118
5.5	Discussion	121
5.6	Figures	129
CHAPTER 6: DISCUSSION AND CONCLUSION		143
6.1	Figure	158
REFERENCES		159

## LIST OF TABLES

TABLE 1: Summary of sex-related STS effects on mitochondrial polarization and markers for mitochondrial fission and mitophagy during infusion of ET-1 during endotoxemia.	87
TABLE 2: Summary of sex-related PAG effects on mitochondrial polarization and markers for mitochondrial fission and mitophagy during infusion of ET-1 during endotoxemia.	88

## LIST OF FIGURES

FIGURE 1: Total H <sub>2</sub> S generation over time of Na <sub>2</sub> S, in the absence and in the presence of liver tissue.	35
FIGURE 2: Total H <sub>2</sub> S generation over time of STS, in the absence and in the presence of liver tissue.	36
FIGURE 3: Effect of STS on change in hepatic sinusoidal diameter.	37
FIGURE 4: Effect of STS on heterogeneity of sinusoidal diameters.	38
FIGURE 5: Effect of PAG on change in hepatic sinusoidal diameter during infusion of ET-1 during endotoxemia.	39
FIGURE 6: Effect of PAG on heterogeneity of sinusoidal diameters during infusion of ET-1 during endotoxemia.	40
FIGURE 7: Effect of STS on change in hepatic sinusoidal diameter in males and females.	41
FIGURE 8: Effect of STS on heterogeneity of sinusoidal diameters in males and females.	42
FIGURE 9: Effect of ET-1 and STS co-infusion on the hepatic sinusoids in endotoxemia.	43
FIGURE 10: Effect of PAG on change in hepatic sinusoidal diameter during infusion of ET-1 during endotoxemia in males and females.	44
FIGURE 11: Effect of PAG on change in heterogeneity of sinusoidal diameters during infusion of ET-1 during endotoxemia in males and females.	45
FIGURE 12: Effect of ET-1 infusion on the hepatic sinusoids with PAG pretreatment in endotoxemia.	46
FIGURE 13: Quantification of Rh123 staining.	72
FIGURE 14: Effect of STS on mitochondrial depolarization.	73
FIGURE 15: Effect of PAG on mitochondrial depolarization during infusion of ET-1 during endotoxemia.	74

FIGURE 16: DRP1 Western blot analysis on mitochondrial and cytosolic fractions from liver homogenates.	75
FIGURE 17: Effect of STS on mitochondrial fission.	76
FIGURE 18: Effect of PAG on mitochondrial fission during infusion of ET-1 during endotoxemia.	77
FIGURE 19: LC3B Western blot analysis from liver homogenates.	78
FIGURE 20: Effect of STS on mitophagy.	79
FIGURE 21: Effect of PAG on mitophagy during infusion of ET-1 during endotoxemia.	80
FIGURE 22: Effect of STS on mitochondrial depolarization in males and females.	81
FIGURE 23: Effect of PAG on mitochondrial depolarization during infusion of ET-1 during endotoxemia in males and females	82
FIGURE 24: Effect of STS on mitochondrial fission in males and females.	83
FIGURE 25: Effect of PAG on mitochondrial fission during infusion of ET-1 during endotoxemia in males and females.	84
FIGURE 26: Effect of STS on mitophagy in males and females	85
FIGURE 27: Effect of PAG on mitophagy during infusion of ET-1 during endotoxemia in males and females.	86
FIGURE 28: Intracellular total ROS production in response to ET-1 in endotoxemia.	103
FIGUTR 29: Intracellular mitochondrial ROS production in response to ET-1 in endotoxemia	104
FIGURE 30: Intracellular total ROS production in response to increasing doses of H <sub>2</sub> S.	105
FIGURE 31: Intracellular total ROS production in response to increasing doses of H <sub>2</sub> S with the mito-K <sub>ATP</sub> inhibitor, 5-HD.	106
FIGURE 32: Intracellular mitochondrial ROS production in response to increasing doses of H <sub>2</sub> S	107

FIGURE 33: Intracellular mitochondrial ROS production in response to increasing doses of H <sub>2</sub> S with the mito-K <sub>ATP</sub> inhibitor, 5-HD.	108
FIGURE 34: Effect of STS on mitochondrial depolarization <i>in vitro</i> .	129
FIGURE 35: The effect of ET-1 and STS on mitochondrial membrane depolarization in endotoxemia <i>in vitro</i> .	130
FIGURE 36: Effect of PAG on mitochondrial depolarization during ET-1 treatment in endotoxemia <i>in vitro</i> .	131
FIGURE 37: The effect of ET-1 and STS on mitochondrial membrane depolarization in endotoxemia <i>in vitro</i> .	132
FIGURE 38: pDRP1 Western blot analysis <i>in vitro</i> .	133
FIGURE 39: Effect of STS on mitochondrial fission <i>in vitro</i> .	134
FIGURE 40: Effect of PAG on mitochondrial fission during ET-1 treatment during endotoxemia <i>in vitro</i> .	135
FIGURE 41: LC3B Western blot analysis <i>in vitro</i> .	136
FIGURE 42: Effect of STS on mitophagy <i>in vitro</i> .	137
FIGURE 43: Effect of PAG on mitophagy during ET-1 treatment during endotoxemia <i>in vitro</i> .	138
FIGURE 44: Effect of STS on F-actin stress fiber formation in endotoxemia <i>in vitro</i> .	139
FIGURE 45: Effect of STS on F-actin stress fiber formation during ET-1 treatment in endotoxemia <i>in vitro</i> .	140
FIGURE 46: Effect of PAG on F-actin stress fiber formation in endotoxemia <i>in vitro</i> .	141
FIGURE 47: Effect of PAG on F-actin stress fiber formation in during ET-1 treatment in endotoxemia <i>in vitro</i> .	142
FIGURE 48: Illustration of current knowledge combined with research findings of this study.	158

## ABBREVIATIONS

3-MST	3-mercaptopyruvate sulfurtransferase
5-HD	5-hydroxydecanoate
ADP	adenosine diphosphate
ANOVA	analysis of variance
ATP	adenosine triphosphate
Ca <sup>2+</sup>	calcium ion
cAMP	cyclic adenosine monophosphate
cGMP	cyclic guanine monophosphate
CLP	cecal ligation and puncture
CO	carbon monoxide
CBS	cystathionine $\beta$ -synthase
CSE	cystathionine $\gamma$ -lyase
DAMPs	danger-associated molecular patterns
DCF-DA	2',7-dichlorofluorescein diacetate
DPBS	Dulbecco's phosphate-buffered saline
DRP1	dynamamin-related protein 1
DRPs	dynamamin-related proteins
eNOS	endothelial nitric oxide synthase
ETC	electron transport chain
ET-1	endothelin-1
ET <sub>A</sub>	endothelin-1 receptor subtype A

ET <sub>B</sub>	endothelin-1 receptor subtype B
ETC	electron transport chain
F-actin	filamentous
FCCP	carbonyl cyanide-p-trifluoromethoxyphenylhydrazone
Fis1	fission protein 1
GI	gastrointestinal
H <sup>+</sup>	hydrogen ion
H <sub>2</sub> DCF-DA	2',7'-dichlorodihydrofluorescein diacetate
H <sub>2</sub> S	hydrogen sulfide
HIF-1 $\alpha$	hypoxia inducible factor-1 $\alpha$
HMECs	human microvascular endothelial cells
HO	heme oxygenase
HS <sup>-</sup>	bisulfide
HSCs	hepatic stellate cells
HUVECs	human umbilical vein endothelial cells
IACUC	Institutional Animal Care and Use Committee
ICU	intensive care unit
iNOS	inducible nitric oxide synthase
I/R	ischemia/reperfusion
K <sub>ATP</sub>	ATP-sensitive potassium channel
K <sub>ca</sub>	Ca <sup>2+</sup> -activated K <sup>+</sup> channels
KCs	Kupffer cells
KHB	Kreb's hepes buffer

LC3B	light chain 3B
LPS	lipopolysaccharide
MAP	mean arterial pressure
Mid49	mitochondrial dynamic protein of 49kDa
Mid51	mitochondrial dynamic protein of 51kDa
mito-K <sub>ATP</sub>	mitochondrial ATP-sensitive potassium channel
Mff	mitochondrial fission factor
MODS	multiorgan dysfunction syndrome
MOF	multiple organ failure
mtDNA	mitochondrial DNA
Na <sub>2</sub> S	sodium sulfide
NaHS	sodium hydrosulfide
NE	norepinephrine
NRF-1, -2	nuclear respiratory factor-1, -2
NO	nitric oxide
PAG	DL-propargylglycine
PAMPs	pathogen-associated molecular patterns
PARL	presenilin-associated rhomboid-like protease
pDRP1	phosphorylated dynamin-related protein 1
PE	phenylephrine
PGC-1 $\alpha$	peroxisome proliferator-activated receptor $\gamma$ coactivator-1 $\alpha$
PI	propidium iodide
PINK1	PTEN induced putative kinase 1

RH123	rhodamine 123
ROCK1	Rho-associated protein kinase 1
ROS	reactive oxygen species
SECs	sinusoidal endothelial cells
SEM	standard error of the mean
SQR	sulfur quinone reductase
STS	sodium thiosulfate
TFAM	mitochondrial transcription factor
TIM	translocase of the inner mitochondrial membrane
TOM	translocase of the outer mitochondrial membrane
TS	thiosulfate
VE-cadherin	vascular endothelial cadherin
VOCC	voltage-operated calcium channel
VSMCs	vascular smooth muscle cells

## CHAPTER 1: INTRODUCTION

### 1.1 Overview

Sepsis is a deranged and exaggerated systemic inflammatory response to infection that can progress to multiple organ dysfunction. Sepsis-related organ failure continues to carry a significant morbidity and mortality despite decades of intensive investigation. This is largely due to the highly complex combination of immune, microvascular, and metabolic alterations that affect function of multiple organs. The liver is a critical organ in the progression of sepsis to septic shock [33]. Although liver failure is a significant complication during the late stages of sepsis, hepatocellular dysfunction is observed in early stages of disease progression [33, 37]. In early sepsis, overall delivery of oxygen to the liver is increased [192]. However, despite the increase in oxygen delivery, there is sufficient evidence demonstrating that hepatic injury is due, at least in part, to hypoxic stress [19, 50, 66, 85, 175]. Previous work from our lab and others demonstrate that disruptions in the hepatic microcirculation that succeed an inflammatory stress are a major contributor to hepatic dysfunction [18, 40, 113, 239]. In addition, mitochondria can be affected in various ways during a systemic inflammatory response, leading to mitochondrial dysfunction. Impaired liver perfusion that occurs during early sepsis leads to tissue hypoxia and insufficient oxygen levels at the mitochondrial level for use in oxidative phosphorylation of ADP to ATP [218, 219]. While the specific enzyme characteristics of Complex IV in the electron transport chain (ETC) allow it to function effectively at low oxygen concentrations, critically low levels may compromise ATP generation and potentially trigger cell death pathways [218]. The generation of excess

amounts of nitric oxide (NO), carbon monoxide (CO), hydrogen sulfide (H<sub>2</sub>S), and reactive oxygen species (ROS) directly inhibit mitochondrial respiration and cause direct damage to mitochondrial protein and other structures of the mitochondria, including the lipid membrane [15, 132, 228, 242].

The manifestations of hepatic microcirculatory dysfunction that occur during sepsis include heterogeneous tissue perfusion, focal hypoxia, mitochondrial membrane depolarization, and cell death. Given time, the inability of the hepatic microcirculation to match oxygen supply with tissue demand can result in hepatocellular injury, liver failure, and the progression of sepsis. While hepatic failure is not typically the direct cause of death in sepsis, it contains about two-thirds of the body's fixed tissue macrophages, the Kupffer cells, making it an important immune organ in magnifying injury in inflammation. In addition, the liver is the primary regulator of whole body metabolic response and a substantial reservoir of blood volume. Both the inflammatory response and the metabolic response of the liver are greatly affected by blood flow. Thus, dysfunction of blood flow in the liver is highly significant as a determinant of the systemic inflammatory response that can progress to septic shock [18, 216].

As opposed to the macrocirculation that transports blood to the organs, the microcirculation consists of smaller vessels (less than 100 $\mu$ M) that distributes blood within individual tissues, such as the sinusoids in the liver. Arterioles are the primary resistance vessels in microcirculation and because of their pre-capillary location, are responsible for modulating tissue perfusion [149]. Surrounding the arterioles are the vascular smooth muscle cells (VSMCs), which act in functional syncytium in response to various stimuli to contract or relax, resulting in variations in the diameter of the vessel

lumen. This change in vascular resistance can increase, such as during relaxation, or decrease, such as during contraction, perfusion through the capillaries. Because resistance of a fluid to flow is inversely proportional to the fourth power of the luminal diameter, even the smallest changes in blood vessel diameter can have extreme consequences on tissue perfusion.

It was originally thought that hepatic portal blood flow was exclusively regulated by total splanchnic drainage and pre-sinusoidal resistance vessels but now it is known that the hepatic sinusoid is also a significant contributor of hepatic blood flow regulation. Sinusoidal hyperconstriction occurs during sepsis and results from the hypersensitization of the hepatic sinusoid to the vasoconstrictive effects of endothelin-1 (ET-1) [18, 175]. Sinusoidal hyperconstriction is associated with heterogeneous blood flow through the sinusoids, leading to a disparity between oxygen supply and tissue metabolic demand [19]. As a result, microcirculatory failure contributes to focal hypoxia and liver injury during the progression of sepsis.

Since the discovery of the biological effects of NO and CO, it has been recognized that small gaseous molecules can act as important physiological regulators [81, 128, 181], particularly during sepsis [181, 199]. More recently, H<sub>2</sub>S was discovered to be significant gaseous mediator and was added to the class of small, biologically active gasses, called gasotransmitters [243]. It is now known that NO, CO, and H<sub>2</sub>S share several biological functions between them, specifically, their ability to cause VSMC relaxation and vasodilation [243]. However, the effect of H<sub>2</sub>S on hepatic oxygenation and microcirculation during sepsis remains to be elucidated. As a vasodilator, one would assume that H<sub>2</sub>S improves hepatic oxygen availability and microvascular function

following an inflammatory insult. Several studies demonstrate that H<sub>2</sub>S provides a protective effect following ischemia/reperfusion injury [102, 137, 212, 227], supporting this notion. On the contrary, endogenously produced H<sub>2</sub>S has been shown to be a contributor disease progression during sepsis [9, 257]. Since H<sub>2</sub>S has been shown to modulate vascular resistance, the present study was designed to investigate the contribution of H<sub>2</sub>S to microvascular and mitochondrial dysfunction during sepsis. Overall, we hypothesize that H<sub>2</sub>S contributes to hepatic sinusoidal sensitization to ET-1, leading to tissue hypoxia, and mitochondrial depolarization and an imbalance of mitochondrial dynamics results in cell death during sepsis. The findings of this study may provide evidence to further explain the mechanisms behind H<sub>2</sub>S being deleterious during the progression of sepsis, while being protective in several other pathophysiological conditions.

## 1.2 Hydrogen Sulfide

H<sub>2</sub>S is a small, colorless, flammable gas with the characteristic smell of rotten eggs. The first reports of H<sub>2</sub>S having a biological effect predate those of the other members of the gasotransmitter family and detail the lethality of exposure to elevated levels, which was demonstrated to result from potent inhibition of mitochondrial respiration. In a manner similar to that of cyanide poisoning, the main mechanism of H<sub>2</sub>S toxicity is the inhibition of cytochrome *c* oxidase in the mitochondrial ETC, thereby disrupting ATP synthesis [159].

For centuries, the toxicity of H<sub>2</sub>S was the only known physiological effect in mammals and was considered to be a metabolic waste product of two pyridoxal 5'

phosphate-dependent enzymes, cystathionine  $\beta$ -synthase (CBS) and cystathionine  $\gamma$ -lyase (CSE), during cysteine metabolism [30, 220]. Following the discovery of NO and CO as important biological mediators in mammals, the hypothesis that endogenous H<sub>2</sub>S could also be physiologically relevant was formed. In support of this hypothesis, it was demonstrated that low concentrations of NaHS, an H<sub>2</sub>S donor, lead to long-term potentiation in rat hippocampus slices, suggesting a function of H<sub>2</sub>S in the nervous system [1]. H<sub>2</sub>S was reported to cause relaxation of isolated aortic rings, providing evidence of a potential role in the cardiovascular system as well [92]. CSE<sup>-/-</sup> mice were observed to spontaneously develop hypertension, confirming the role of endogenously produced H<sub>2</sub>S as a physiologically relevant gaseous mediator [248]. It is now well established that endogenous H<sub>2</sub>S is an important mediator in the nervous, cardiovascular, pulmonary, immune, and gastrointestinal systems [242].

Although H<sub>2</sub>S is endogenously produced and a physiological important mediator, there is still substantial debate about several basic concepts in H<sub>2</sub>S chemistry and biology, including the question of what the biologically active form of H<sub>2</sub>S is. Since H<sub>2</sub>S is a weak acid in aqueous solution with a pK<sub>a1</sub> between 6.6 and 7.1 and a pK<sub>a2</sub> greater than 12 [242], dependent on experimental conditions, it is in equilibrium with the deprotonated form, HS<sup>-</sup>, with negligible amounts of S<sup>2-</sup>. Therefore, it is possible that H<sub>2</sub>S, HS<sup>-</sup>, or both exert biological functions. Each form of sulfide has different chemical properties which may allow for different biological effects. In example, the lipophilicity property of H<sub>2</sub>S permits for diffusion-mediated movement across lipid membranes. HS<sup>-</sup> is not freely permeable, leading to the possible compartmentalization of sulfide. Whether or not H<sub>2</sub>S and HS<sup>-</sup> exert differential effects is not known. Therefore, as it is currently referred to in

H<sub>2</sub>S biology, the terms H<sub>2</sub>S and sulfide, are used to refer to both H<sub>2</sub>S and HS<sup>-</sup>, collectively, in this study [165].

The physiological concentration of H<sub>2</sub>S *in vivo* is not known. Since the methods to measure the levels of H<sub>2</sub>S are still under development, initial reports that identified the physiological circulating range to be between 10-300μM appear to be an overestimation [165]. Because the lowest concentrations in this range would produce the characteristic smell of rotten eggs in blood and exhaled breath, it is likely that circulating plasma H<sub>2</sub>S concentrations are much lower or that H<sub>2</sub>S is bound in an undetectable form. It is now suggested that the level of H<sub>2</sub>S *in vivo* is the result of local rates of H<sub>2</sub>S production and disposal, which may be affected during disease states. The primary source of H<sub>2</sub>S in the nervous system is CBS, while CSE is the main source of H<sub>2</sub>S in the cardiovascular system and liver [1, 248]. A third enzyme, 3-mercaptopyruvate sulfurtransferase (3-MST) has been shown to produce a small amount of H<sub>2</sub>S but the functional significance of this enzyme on total H<sub>2</sub>S levels remains to be elucidated [208]. CSE is constitutively expressed in the liver in several different cell types including hepatocytes, hepatic stellate cells (HSCs), Kupffer cells (KCs), and sinusoidal endothelial cells (SECs) [64, 196]. As the primary recipient of blood flow, the liver is subjected to a secondary source of H<sub>2</sub>S from bacteria in the GI tract, which synthesize H<sub>2</sub>S as a metabolic byproduct producing H<sub>2</sub>S concentrations in the millimolar range [20]. This large and potentially toxic amount of sulfide is mostly sequestered and metabolized by colonic epithelial cells; however, a small portion can escape the intestinal epithelial barrier and enter the portal circulation. Due to the combination of endogenous and exogenous sources of H<sub>2</sub>S, it is likely that the liver is exposed to elevated levels of H<sub>2</sub>S, particularly during sepsis. Previous work from

our lab provided evidence that the rapid oxidation of H<sub>2</sub>S during a single pass through the liver maintains low systemic circulating levels of H<sub>2</sub>S during sepsis. The oxidation of increased levels of H<sub>2</sub>S leads to periods of liver hypoxia, resulting in a decrease in the capacity of the liver to metabolize H<sub>2</sub>S and the subsequent increase of H<sub>2</sub>S into the circulation [161].

### 1.3 Hepatic Hydrogen Sulfide Oxidation and Sepsis

In *in vivo* models of experimental sepsis, both cecal ligation and puncture (CLP) and endotoxin treatment cause an increase in hepatic CSE expression, resulting in increased hepatic capacity to synthesize H<sub>2</sub>S [257]. Damage to the intestinal cells in addition to elevated endogenous H<sub>2</sub>S concentrations has been demonstrated to reduce their ability to detoxify H<sub>2</sub>S, which may permit more diffusion of H<sub>2</sub>S into the hepatic portal circulation [233]. It was reported that colonic epithelial cells metabolize H<sub>2</sub>S via mitochondrial oxidation, which serves as protection from toxic levels of sulfide derived from the gut bacteria [130]. Since one of the main functions of the liver is oxidative catabolism of toxins within the circulation, the liver may have the capacity to dispose of H<sub>2</sub>S to protect itself from toxic accumulation of the gas. The hypothesis that H<sub>2</sub>S acts a cellular oxygen sensor is supported by several studies demonstrating an inverse relationship between O<sub>2</sub> and H<sub>2</sub>S levels [164, 167, 246]. H<sub>2</sub>S oxidation is inhibited when oxygen levels fall and allows for the accumulation of H<sub>2</sub>S. Raised levels of H<sub>2</sub>S would exert a biological function to raise oxygen levels, possibly by vasodilation of the resistance vessels, which would result in increased tissue perfusion and cellular oxygen levels. At adequate oxygen levels, oxidation of H<sub>2</sub>S resumes and overall H<sub>2</sub>S

concentrations would decrease [164]. However, it is possible that this scenario is injurious to the septic liver.

Impaired oxygen delivery and mitochondrial dysfunction leads to insufficient ATP production during sepsis [19, 41] and any physiological process that consumes hepatic oxygen may potentiate hepatic hypoxic stress. Therefore, it is very possible that hepatic oxidation of H<sub>2</sub>S during sepsis may aggravate hepatic tissue hypoxia. If the liver's capacity to metabolize H<sub>2</sub>S is inhibited during sepsis, then H<sub>2</sub>S may accumulate to toxic levels and contribute to hepatic mitochondrial dysfunction via inhibition of cytochrome *c* oxidase of the ETC. Therefore, the first part of this study was designed to determine if H<sub>2</sub>S oxidation exacerbates hepatic tissue hypoxia and to test if H<sub>2</sub>S contributes to mitochondrial dysfunction during endotoxemia.

#### 1.4 Hepatic Hydrogen Sulfide and Microcirculation During Sepsis

Failure of the microcirculation is a major contributor to the progression of sepsis. Modulating sinusoidal perfusion is not as easily modulated as capillary perfusion in other vascular beds in the body. The contractile activity of VSMCs modulate the resistance of the portal terminal venules and hepatic arterioles at presinusoidal sites. The hepatic sinusoids are involved in the regulation of tissue perfusion in the liver [17]. However, individual sinusoids do not have VSMCs; instead, they are surrounded by specialized pericytes, the HSCs, that respond to local vasoactive agents and regulate sinusoidal resistance [41, 112]. When HSCs contract, sinusoidal diameter is decreased and results in reduced blood flow through the individual sinusoids [258]. Therefore, sinusoidal

constriction is characterized by the combination of constricted and dilated sinusoids and heterogeneous sinusoidal perfusion [107].

ET-1 is a powerful twenty-one amino acid constrictor peptide and is synthesized by several cell types in the liver including the SECs, HSCs, and KCs [197, 247]. ET-1 exerts its physiological effect by binding to one of two receptor subtypes, ET<sub>A</sub> or ET<sub>B</sub>. ET<sub>A</sub> receptors are expressed on HSCs, VSMCs, and SECs and always mediate constriction while ET<sub>B</sub> receptors are expressed on SECs and are coupled to the activation of endothelial nitric oxide synthase (eNOS), mediating dilation [16, 90, 95]. Production of ET-1 is increased during inflammatory and oxidative stress conditions, including sepsis, and is correlated with disease severity [5, 214]. Previous work from our lab has shown the importance of the antagonistic relationship between ET-1 and NO in regulating liver circulation [81, 181].

Sinusoidal constriction in response to ET-1 was demonstrated to colocalize with HSCs *in vivo* [260]. Increased hepatic resistance and decreased portal flow are the result of ET-1 and phenylephrine (PE) stimulation; however, only ET-1 results in a shift in sinusoidal diameter [176, 198]. The response of the sinusoids to ET-1 causes dysfunction of the hepatic microcirculation and impaired oxygen delivery to tissues [18]. Furthermore, the hypersensitivity of the hepatic sinusoid to ET-1 during sepsis is accompanied with an increase in the heterogeneity of sinusoidal blood flow and leads to focal hypoxia and liver injury [19].

The role of eNOS-derived NO from SECs in maintaining sinusoidal tone has been demonstrated in mechanistic studies [206]. The vasoconstrictive effect of ET-1 in HSCs is counterbalanced by NO production under normal conditions [181]. It has been shown

that the ET-1/ET<sub>B</sub> interaction increases the activity of eNOS in isolated SECs *in vitro* and maintains tissue oxygenation *in vivo* [128, 181]. The delicate balance between the vasoregulatory effects of ET-1 is tipped, resulting in hypersensitization of the hepatic sinusoid to the vasoconstrictive action of ET-1. This imbalance is mostly due to a dysregulation of ET-1 stimulated eNOS activation [128]. Previous work from our lab has shown that ET-1 binding to ET<sub>B</sub> receptors on hepatic SECs becomes uncoupled from eNOS activation, thus, decreasing the compensatory vasodilation. This decrease in eNOS activation is associated with increased binding of eNOS to caveolin-1, thus inhibiting NO bioavailability [106, 127, 151, 163]. The activation of the ET<sub>B</sub> receptors during sepsis results in a beneficial effect on the hepatic microcirculation, as demonstrated using an ET<sub>B</sub> agonist on animals treated with LPS [181]. Additionally, administration of sodium nitroprusside, a nitric oxide donor, improves hepatic microcirculatory dysfunction following injury, suggesting that NO is an important contributor in the maintenance of sinusoidal perfusion [85].

It was demonstrated in livers isolated from normal and cirrhotic rats that H<sub>2</sub>S has vasodilator actions and mitigated the vasoconstrictive effect of norepinephrine (NE) [64]. In cirrhosis and fibrosis, portal hypertension poses a serious complication and a decrease in intrahepatic resistance would be favorable. In sepsis, however, portal hypertension is not a serious complication. Instead, inadequate oxygen delivery due to sinusoidal hyperconstriction is the significant complication in hepatic injury in sepsis. As a gaseous mediator with vasodilatory effects, one would predict that H<sub>2</sub>S would attenuate sinusoidal constriction. Still, sinusoidal constriction is observed in the hepatic microcirculation

despite elevated levels of endogenous H<sub>2</sub>S. Therefore, it is possible that the vasoactive effects of H<sub>2</sub>S is much more complicated.

Vasodilation mediated by H<sub>2</sub>S is largely the result of activation of K<sub>ATP</sub> channels expressed in VSMCs [264]. Activation of K<sub>ATP</sub> channels leads to hyperpolarization, inactivation of voltage-operated calcium channels (VOCC) on VSMCs, and relaxation [190]. Therefore, H<sub>2</sub>S would be beneficial to the hepatic sinusoids during sepsis if it were to behave as a vasodilator. Since the hepatic sinusoids lack VSMCs, it is possible that H<sub>2</sub>S acts on the HSCs or exerts a different effect on the sinusoids during sepsis. Conversely, it has been reported that H<sub>2</sub>S can act as a vasoconstrictor [139, 142].

### 1.5 Hepatic Mitochondrial Dysfunction During Sepsis

Multiorgan dysfunction syndrome is considered to be the end result of severe sepsis. Vascular hyporeactivity and microvascular flow abnormalities are clearly known to exist in septic patients. Increased tissue oxygen tensions have been reported in animal models [201, 236] and patients in early sepsis have been shown to exhibit a hyperdynamic state [21], which inspired the hypothesis that organ dysfunction is a result of impaired cellular usage of oxygen in addition to inadequate delivery to tissues. Because mitochondria utilize more than 90% of total body oxygen consumption for the generation of ATP within the mitochondrial respiratory chain in the process of oxidative phosphorylation, a disruption of this process with decreased ATP production as a result is a reasonable explanation for the mechanism underlying multiorgan dysfunction induced by sepsis. In cultured hepatocytes, it was shown that maximal oxygen consumption increased markedly following 6 hours of endotoxin stimulation but decreased

significantly by 24 hours [200]. In a clinical study involving septic patients, increasing sepsis severity was associated with progressive decreased in oxygen consumption [124].

Composed of a central matrix enclosed by an inner and outer membrane, mitochondria are at the crossroads of life and death. The primary roles of mitochondria are ATP production and control of cell death pathways. Other roles include  $\text{Ca}^{2+}$  and  $\text{H}^+$  homeostasis, intracellular signaling, and heat production. The mitochondrial respiratory chain is in the inner mitochondrial membrane and is composed of four individual enzyme complexes (complexes I, II, III, and IV), which transfer electrons from NADH and succinate produced by the Krebs cycle down a redox gradient, ending in the reduction of molecular oxygen to water. The transfer of electrons allows the enzyme complexes to translocate protons from the mitochondrial matrix to the intramembranous space, creating a proton gradient. ATP synthase (complex V) uses the proton gradient to generate ATP from ADP and inorganic phosphate.

Emerging research demonstrates the regulation of mitochondrial function by  $\text{H}_2\text{S}$ .  $\text{H}_2\text{S}$  exerts its actions by a chemical reaction with a wide variety of proteins. However, its actions in mammalian systems result from an interaction with three primary targets:  $\text{K}_{\text{ATP}}$  channels in the plasma membrane and mitochondria [210, 217], sulfide quinone reductase (SQR) [88] and cytochrome C oxidase in mitochondria [159]. Its vascular effects are exerted by activating  $\text{K}_{\text{ATP}}$  channels in the plasma membrane of vascular smooth muscle cells, resulting in hyperpolarization and thus, relaxation.  $\text{H}_2\text{S}$  can also be oxidized by sulfur quinone reductase, donating an electron to the mitochondrial respiratory chain leading to a clearance of  $\text{H}_2\text{S}$ , increased oxygen consumption, and potential ATP production. Conversely, its interaction with cytochrome *c* oxidase inhibits

the final transfer of electrons to molecular oxygen, resulting in inhibition of oxygen consumption and ATP production. Inhibition of the respiratory chain causes the enzyme complexes to become maximally reduced, allowing the electrons to leak from the chain and react with molecular oxygen to generate superoxide. This leak is suggested to occur at complex I and complex III. Superoxide can then rapidly react with NO to generate the powerful and detrimental oxidant, peroxynitrite, which is capable of denaturing proteins, damaging DNA, and inhibiting the respiratory chain and ATP synthase in a prolonged or irreversible fashion. Peroxynitrite production has been reported to occur during periods of inflammation in both animal sepsis models and patients in clinical studies [68, 131].

Sepsis models in the laboratory have demonstrated a decrease in mitochondrial function, including ultrastructural changes observed using electron microscopy [211]. Decreased ATP concentration and mitochondrial activity have been reported in human and animal studies [77, 143]. Decreases in ATP synthase at mRNA and protein levels were demonstrated by administering LPS in human subjects [32]. Apoptosis, or programmed cell death, is also involved in the pathogenesis of sepsis. It can be triggered through either the extrinsic or intrinsic cell death pathway and mitochondria play a role in both of these pathways. ROS cause mitochondrial damage, which can trigger the release of cytochrome *c*, the electron carrier between complex III and complex IV, to the cytosol. Once cytochrome *c* is released into the cytosol, the apoptosome can form, which reacts with caspases to initiate apoptosis.

Oxidative stress mechanisms in sepsis are complex and the pathogenesis of mitochondrial dysfunction in the disease are even more complicated. Regardless, mitochondrial impairment of ATP production is a key factor for multiorgan dysfunction

and mortality in septic patients. The biological effect of H<sub>2</sub>S is highly dependent on both concentration and initial conditions of the tissue when challenged with H<sub>2</sub>S [44, 45, 162, 163, 212, 257, 258]. Preliminary results demonstrate a complex interaction among endotoxemia and hypoxia in the liver that results in a synergistic relationship in which elevated endothelin-1 and H<sub>2</sub>S affect both blood flow and metabolic regulation in the liver. It should be noted that rodent endotoxemia is not the same as clinical sepsis. However, endotoxemia is a reproducible model of the inflammatory response seen in humans with sepsis. Previous results from our lab have shown that the vascular response seen in an endotoxin model is similar to that seen in a cecal ligation and puncture model of sepsis. An endotoxic model of sepsis is appropriate for this research study since it is focused on early molecular mechanisms. In translating our studies for more clinical relevance, we would select a different model, such as polymicrobial sepsis or a CLP model of sepsis.

## CHAPTER 2: THE RESPONSE OF HEPATOCYTES TO HYDROGEN SULFIDE AND ENDOTHELIN-1 ON LIVER MICROCIRCULATION *IN VIVO*

### 2.1 Abstract

Hydrogen sulfide (H<sub>2</sub>S) is a mediator in the regulation of blood flow and metabolism. The unique regulation of liver microvascular resistance is disturbed during the progression of sepsis, which contributes to hepatic injury. H<sub>2</sub>S has been shown to potentiate liver microvascular dysfunction in sepsis. Since vascular control is largely mediated by the endothelium, the present study was designed to examine the relationship between the effects of H<sub>2</sub>S on hepatic microcirculation and to determine the contribution of endogenous H<sub>2</sub>S to hepatic microcirculatory dysfunction in an *in vivo* endotoxin model of sepsis using confocal intravital microscopy. Since hepatic H<sub>2</sub>S levels are elevated during sepsis, DL-propargylglycine (PAG), an inhibitor of cystathionine  $\gamma$ -lyase, was used to determine the contribution of H<sub>2</sub>S to the hypersensitization of the sinusoid to the vasoconstrictive effect of endothelin-1 (ET-1). We observed that PAG pretreatment significantly attenuated the hepatic sinusoidal sensitization to ET-1 in endotoxin-treated animals. ET-1 infusion increased sinusoidal constriction to 30.3% of baseline in endotoxemic animals, which was reduced to 4.1% when pretreated with PAG ( $p < 0.05$ ). Furthermore, we show that PAG pretreatment abrogated the increase in sinusoidal perfusion heterogeneity after ET-1 infusion in endotoxin-treated animals (113.0% increase in LPS mice vs. 21.4% in PAG/LPS mice,  $p < 0.0001$ ), suggesting H<sub>2</sub>S-dependent of impairment hepatic oxygen delivery in sepsis.

## 2.2 Introduction

Dysregulated liver sinusoidal perfusion is a critical factor in the development of focal tissue hypoxia, which leads to livery injury in sepsis [18, 19, 113]. Total blood flow through the hepatic sinusoids is regulated in variations of vascular tone by extra-sinusoidal resistance vessels, which are made up of terminal portal venules and hepatic arterioles, and whole distribution is regulated within the sinusoids [260]. Vasodilatory agents, such as nitric oxide (NO) are excessively produced during sepsis, leading to the hyporesponsiveness of the extra-sinusoidal resistance vessels to the constrictor effect of catecholamines, contributing to hypotension [180]. Furthermore, hepatic sinusoidal hyperconstriction and heterogeneous perfusion during sepsis leads to a local deleterious effect on the liver [19].

Hepatic stellate cells (HSCs) surround individual sinusoids [260]. These contractile pericytes modulate hepatic sinusoidal tone by responding to a balance of vasodilatory and vasoconstrictive mediators [112]. Liver injury, such as observed in fibrosis or hepatic cirrhosis, results in the differentiation of HSCs to a phenotype matching that of myofibroblasts, which leads to increased contraction in response to the vasoactive peptide, ET-1 [198]. Increased contractile response to ET-1 has been observed following a mild inflammatory insult, such as low-dose endotoxemia or sepsis [19, 175]. Under normal conditions, NO production is increased in response to ET-1 in sinusoidal endothelial cells (SECs) and attenuates the constrictor effect of ET-1 [181]. During inflammatory stress, eNOS activity and NO production are impaired. Therefore, the constrictor effect of ET-1 is not counterbalanced by the dilator effect of NO, producing hepatic sinusoidal constriction and microvascular dysfunction. Moreover,

exacerbated sinusoidal constriction in response to ET-1 is associated with an increase in heterogeneous sinusoidal perfusion, resulting in disparity between oxygen supply and tissue metabolic demand [19, 107]. Focal hypoxia and liver injury are the results of inefficient oxygen delivery to hepatic tissue. Though it is well known that NO is a significant mediator of sinusoidal tone, it is probable that its lack is not the only contributor to microvascular dysfunction since there is a plethora of vasoactive molecules found in the hepatic microenvironment. While exogenous NO donors have been shown to restore hepatic microcirculatory function in experimental sepsis models [85], a beneficial effect of NO administration to septic patients in clinical trials still remains unclear [144, 216]. Consequently, additional research in the field of sepsis focusing on the regulation of hepatic sinusoidal perfusion is necessary to identify any additional potential therapeutic targets.

H<sub>2</sub>S, the third gasotransmitter with the characteristic smell of rotten eggs, has been shown to be increased during both sepsis and endotoxemia [45, 256]. Like its fellow gasotransmitter, NO, H<sub>2</sub>S is endogenously synthesized and acts as a vasodilator [92]. NO and H<sub>2</sub>S have differences in their mechanisms of vasodilation; NO-induced vasodilation is cGMP-dependent [99] while H<sub>2</sub>S-induced vasodilation is via K<sub>ATP</sub>-mediated hyperpolarization of vascular smooth muscle cells (VSMCs) [264]. The first study on the effect of H<sub>2</sub>S in the liver vasculature was first completed by Fiorucci, who reported that H<sub>2</sub>S significantly mitigated the increase in intrahepatic resistance during infusion of norepinephrine (NE) infusion in isolated livers from normal and cirrhotic rats [64]. Administering exogenous H<sub>2</sub>S during hepatic cirrhosis increases hepatic perfusion and reduces portal hypertension, making it a beneficial therapeutic vasodilator. Based on

this finding, it is understandable that one would characterize H<sub>2</sub>S as a vasodilator and predict that administering exogenous H<sub>2</sub>S would improve liver perfusion and be beneficial during sepsis. However, numerous studies have demonstrated that endogenous H<sub>2</sub>S contributes to progression of sepsis [9, 135, 256].

Previous results from our lab demonstrated that H<sub>2</sub>S mitigates the pressor effect of phenylephrine (PE) in an isolated and perfused liver [163]. However, we also observed that H<sub>2</sub>S had no effect on ET-1-induced increased portal pressure in the same isolated and perfused liver system. Like NE, PE exerts its effects only on the extra-sinusoidal resistance vessels, while ET-1 exerts its effects on the extra-sinusoidal and sinusoidal sites of blood flow regulation [260]. VSMC hyperpolarization in the portal venules is most likely responsible for the H<sub>2</sub>S-induced vasodilation observed during infusion of PE. However, the sinusoidal tone response to ET-1 is effected by hepatic stellate cells (HSCs), not VSMCs as this cell type is not present within the sinusoids. Since H<sub>2</sub>S affects PE pressor effects but not ET-1 pressor effects, it is possible that the vasoactivity of this gas may be different in the sinusoids than the portal venules. Therefore, this present study was designed to determine the vasoregulatory effects of exogenous and endogenous H<sub>2</sub>S on the hepatic sinusoids *in vivo*. Since H<sub>2</sub>S has been shown to be detrimental during the progression sepsis, we hypothesized that endogenous H<sub>2</sub>S is a contributor to the hypersensitization of the hepatic sinusoid to ET-1 during sepsis. Using intravital confocal microscopy, we demonstrate for the first time that co-infusion of exogenous H<sub>2</sub>S and ET-1 is associated with sinusoidal constriction and increased perfusion heterogeneity in a normal liver still contained within a live mouse animal model. Furthermore, this study shows that inhibiting endogenously produced H<sub>2</sub>S

production significantly reduces hepatic microvascular dysfunction in response to ET-1 during an endotoxic model of sepsis, leading to improved oxygen delivery in the liver. Our results challenge the notion that H<sub>2</sub>S only has the role of a vasodilator in the liver. Instead, it is likely that H<sub>2</sub>S exerts differential actions within the hepatic sinusoid than in most resistance vessels in the liver, including the portal venules. Additionally, we present a possible mechanism that explains the protective effect observed with the inhibition of endogenous H<sub>2</sub>S synthesis during the progression of sepsis.

### 2.3 Materials and Methods

**Animals:** Male and female C57Bl/6 mice (gift from Dr. Pinku Mukherjee, University of North Carolina at Charlotte, Charlotte, North Carolina) weighing 18-25 grams were used in this study. Mice were housed in a temperature-controlled environment on 12-hour light/dark cycles with free access to standard mouse chow and water. All animal manipulation was in strict adherence with the National Institute of Health guidelines and experimental protocols were approved by the Institutional Animal Care and Use Committee of the University of North Carolina at Charlotte.

**Reagents:** Sodium thiosulfate (STS), DL-propargylglycine (PAG), and lipopolysaccharide (LPS) (*E. Coli*, serotype 026:B6), endothelin-1 (ET-1), and limonene were purchased from Sigma-Aldrich. Rhodamine123 (Rh123), propidium iodide (PI), and Dulbecco's Phosphate-Buffered Saline (DPBS) 1X were purchased from ThermoFisher (Waltham, Massachusetts).

**Mitochondria Labeling:** Mitochondria were fluorescently labeled using Rh123 (525nmol/mouse). Since Rh123 is a cationic dye, it distributes electrophoretically into

the mitochondrial matrix is response to the electric potential across the inner mitochondrial membrane, which was infused via the ventral tail vein 10 minutes before intravital confocal microscopy. Rh123 was injected via the ventral tail vein using a 30-gauge needle attached to a 10cc syringe 10 minutes prior to confocal intravital microscopy.

**Confocal Intravital Microscopy:** Mice were anesthetized using 1-3% isoflurane in (J. A. Webster Veterinary Supply, Devens, Massachusetts) in oxygen. The abdomen was shaved and a laparotomy was performed to expose the liver and digestive organs. Electrocautery was used to prevent bleeding. The ligaments connecting the liver to surrounding structures (diaphragm, anterior abdominal wall, etc.) were cut to allow the liver to be exteriorized. The intestines were reflected, and a 4-ply gauze moistened with Dulbecco's phosphate-buffered saline (DBPS) 1X is placed underneath. A large mesenteric vein was cannulated with a 30-gauge needle on the end of a PE10 catheter connected to a 1cc syringe containing heparinized saline. The cannula was fixed in place with 10 $\mu$ L of Vetbond tissue adhesive and a small piece of Kimwipe. The cannula was flushed with heparinized saline to prevent clotting. The intestines were reflected over the fixed cannula and then wrapped with gauze. DPBS 1X was added to the abdominal area to prevent the intestines from drying. A length of 3-0 surgical suture is tied to the xiphoid process, which will help to retract the abdominal opening during intravital microscopy. A cotton swap dipped in limonene was applied onto the ventral side of the tail to aid in visualization of the ventral tail vein. Fluorescent indicators, Rh123 (525nmol/mouse) and PI (45nmol/mouse), were injected via the ventral tail vein using a 30-gauge needle.

For microscopy, the mouse was placed on a temperature-controlled (37-38°C) microscope stage with a viewing window over the 40X UPlanApo 0,85 objective lens of an Olympus FV500 scanning confocal microscope and was maintained under isoflurane anesthesia, administered at a dose of 1-3% in oxygen. The mouse was positioned on its right lateral side and the liver was exteriorized and the right lobe positioned over the viewing window. The ligature attached to the xiphoid process was retracted to pull the diaphragm away from the liver and was held in place with medical tape. The liver was covered with a piece of Kimwipe and moistened with DPBS 1X to minimize movement associated with breathing. The internal organs were moistened with DPBS 1X and covered with plastic wrap to prevent evaporative loss of moisture. The mesenteric cannula was connected to a syringe pump (Harvard Apparatus, Holliston, Massachusetts) to allow for infusion of treatment substances.

**Treatment Groups:** Mice were randomly divided into one of two treatment groups: 1. Saline, 2. ET-1. Then mice were further divided into one of six treatment sub-groups: 1. Control, 2. LPS, 3. STS, 4. PAG, 5. STS/LPS, 6. PAG/LPS. For the LPS sub-group, mice were administered an intraperitoneal injection of LPS (5mg/kg body weight) six hours prior to surgery. Previous reports from our lab demonstrate that PAG, the inhibitor of cystathionine  $\gamma$ -lyase (CSE), influences the hepatic vasculature within 30 minutes of administration. Therefore, the mice in the PAG sub-group were administered an intraperitoneal injection of PAG (50mg/kg body weight) 30 minutes prior to surgery. For mice receiving both LPS and PAG treatments, LPS was injected intraperitoneally 5.5 hours prior to PAG, which was injected 30 minutes prior to surgery.

**H<sub>2</sub>S Infusion:** The H<sub>2</sub>S donor, STS, was used to investigate the effect of H<sub>2</sub>S on the hepatic microcirculation. To determine the effects of infusion, saline was infused through the mesenteric cannula at a rate of 10 $\mu$ L/minute for a stabilization period of 5 minutes. Then freshly prepared STS (2  $\mu$ mol/kg body weight/minute) was infused at the same rate for a period of 10 minutes. The sinusoids were visualized using a FITC filter (excitation 488nm, emission 505nm) and a 40X UPlanApo 0,85 objective lens. Images were recorded every minute for 10 minutes, with the first image marking the beginning of the experiment, just prior to the start of STS infusion into the mesenteric vein. Images were recorded using FLUOVIEW software (Shinjuku, Tokyo, Japan).

**ET-1 Infusion:** Following the stabilization period of 5 minutes, ET-1 (1 $\mu$ mol/kg body weight/minute) was infused for a period of 10 minutes. For mice receiving both STS and ET-1, The sinusoids were visualized using a FITC filter (excitation 488nm, emission 505nm) and a 40X UPlanApo, 0,85 objective lens. Images were recorded every minute for 10 minutes, with the first image marking the beginning of the experiment, just prior to the start of ET-1 infusion into the mesenteric vein. Images were recorded using FLUOVIEW software. Offline analysis was performed using FIJI software (Laboratory for Optical and Computational Instrumentation, Madison, Wisconsin).

**Preparation of Tissue Slices:** Immediately following euthanasia of the animal, the liver was excised from the abdominal cavity and washed with 4°C Kreb's Hepes Buffer (KHB) (99mM NaCl, 4.7mM KCl, 41.2mM MgSO, 1.0mM KH<sub>2</sub>PO<sub>4</sub>, 21.9mM CaCl, 25mM NaHCO<sub>3</sub>, 20mM HEPES). Using a tissue slicer (Brendel/Vitron, Inc.), 250 $\mu$ M-thick liver slices were obtained and placed in a dish containing 4°C KHB briefly until use the same day.

**H<sub>2</sub>S Assay:** Sample volumes of 75 $\mu$ L were immediately placed into 150 $\mu$ L of 1% zinc acetate to trap H<sub>2</sub>S in solution. To this solution, 133 $\mu$ L of a 20mM N,N-dimethyl-p-phenylenediamine sulfate solution dissolved in 7.2M HCl and 133 $\mu$ L of a 30mM FeCl<sub>3</sub> solution dissolved in 1.2M HCl was added. The resulting mixture was vigorously vortexed and incubated for 20 minutes at room temperature. 300 $\mu$ L of a 10% trichloroacetic acid was added and the samples were centrifuged at 10,000  $\times$  g for 5 minutes at 4°C to precipitate proteins. Absorbance was measured at 670nm and H<sub>2</sub>S concentration was calculated against a standard curve. All chemicals were purchased from Sigma-Aldrich (St. Louis, Missouri).

**Offline Image Analysis:** Offline image analysis was performed using FIJI software. For sinusoidal diameter and heterogeneity of diameter data, 40X images recorded with a FITC filter were used. Ten blood vessels were randomly selected per image. To determine sinusoidal diameter, the total area of a vessel was obtained and divided by the length of the vessel (diameter = area/length). The mean sinusoidal diameter represents the ten vessels per animal. To determine the heterogeneity of perfusion, the standard deviation of individual vessel diameters was calculated.

**Statistical Analysis:** All data are presented as means  $\pm$  standard error of the mean (SEM). Statistical analysis was performed using GraphPad Prism software (San Diego, California). Statistical significance was assessed by one- or two-way analysis of variance (ANOVA) with independent and repeated measures used where appropriate. Sidak's and Tukey's multiple comparison *post hoc* test was used when statistical differences were detected. Statistical significance was set at  $p < 0.05$ .

## 2.4 Results

**Exogenous H<sub>2</sub>S Donor Selection:** We investigated total H<sub>2</sub>S generation of two different H<sub>2</sub>S-releasing agents, sodium sulfide (Na<sub>2</sub>S) and STS in the presence and in the absence of liver tissue. Freshly prepared 100μM Na<sub>2</sub>S generated an average of 53.3μM after 1 minute of incubation in the absence of liver tissue (Figure 1). Total H<sub>2</sub>S generated was shown to be increased to 78.6μM at 5 minutes and then decreased to 30.4μM at 10 minutes. After 20 minutes of incubation, the total amount of H<sub>2</sub>S present was shown to be decreased further to 23.7μM. In the presence of liver tissue, Na<sub>2</sub>S generated an average of 86.8μM after 1 minute and decreased over time to 38.6μM, 30.4μM, and 23.7μM at 5 minutes, 10 minutes, and 20 minutes, respectively (Figure 2). Data were from four separate experiments.

**Effect of Portal Infusion of H<sub>2</sub>S on the Hepatic Microcirculation:** We investigated the effect of portal infusion of the H<sub>2</sub>S donor, STS (2 μmol/kg body weight/minute) on the hepatic microcirculation *in vivo*. There were no significant differences in changes of sinusoidal diameters among baseline treatment groups (Figure 3). Though not statistically significant, H<sub>2</sub>S infusion decreased sinusoidal diameter from  $7.2 \pm 1.0\mu\text{m}$  to  $6.5 \pm 1.2\mu\text{m}$  following ET-1 infusion. In LPS-treated mice, H<sub>2</sub>S infusion decreased sinusoidal diameter from  $8.1 \pm 1.4\mu\text{m}$  to  $6.3 \pm 1.0\mu\text{m}$  following ET-1 infusion ( $p < 0.05$ ). Data were from six separate experiments.

**Effect of Portal Infusion of H<sub>2</sub>S on Hepatic Sinusoidal Heterogeneity:** Sinusoids neighboring constricted sinusoids have been shown to become dilated following an inflammatory insult. Therefore, we compared the variability between sinusoidal diameters within each image analyzed. Infusion of H<sub>2</sub>S was shown to have a

significant effect on sinusoidal heterogeneity in endotoxemia (Figure 4, \* =  $p < 0.05$ ).

There was no significant effect of H<sub>2</sub>S infusion compared to control but when co-infused with ET-1, H<sub>2</sub>S increased hepatic sinusoidal heterogeneity, which was potentiated in endotoxemia (\*\* =  $p < 0.01$ ). Data were from six separate experiments.

#### **Effect of PAG Pre-Treatment on the Hepatic Microcirculation During**

**Endotoxemia:** Since hyperconstriction of the hepatic sinusoid is a contributor to liver injury during endotoxemia, the non-competitive inhibitor of CSE, PAG, was used to examine the role of endogenous H<sub>2</sub>S on hepatic sinusoidal sensitization to the constrictor effect of ET-1 during endotoxemia. We found that infusion of ET-1 reduced sinusoidal diameter in control and PAG by 8.7% and 4.0%, respectively (Figure 5). While PAG pre-treatment alone had no effect on the response to ET-1, the constrictive effect of ET-1 was exacerbated in endotoxemic mice with a 37.4% reduction in sinusoidal diameter (\*\*\*\* =  $p < 0.0001$  versus control). PAG pre-treatment significantly attenuated the sensitization of the sinusoid to the constrictor effect of ET-1 in endotoxemic mice, resulting in a 10.4% decrease in sinusoidal diameter, similar to what was observed in control (\*\*\*\* =  $p < 0.0001$  versus LPS). Data were from six separate experiments.

#### **Effect of PAG Pre-Treatment on Hepatic Sinusoidal Heterogeneity During**

**Endotoxemia:** We assessed the variability of hepatic sinusoidal diameters among treatment groups (Figure 6). LPS-treated mice produced a significant increase in the standard deviation of the means of sinusoidal diameters per image with infusion of ET-1 ( $5.7 \pm 3.6\mu\text{m}$  versus  $8.4 \pm 2.7\mu\text{m}$  for control, \*\*\*\* =  $p < 0.0001$ ). Pretreatment with PAG abrogated the increase in heterogeneity of sinusoidal diameters during ET-1 infusion ( $8.4 \pm 2.9\mu\text{m}$  versus control). Data were from six separate experiments.

### **Sex Differences of Portal Infusion of H<sub>2</sub>S on the Hepatic Microcirculation:**

We furthered our investigation of the effect of portal infusion of the H<sub>2</sub>S-releasing agent, STS, by splitting up the pooled data into male and female sets to assess sex differences. Baseline data for both males and females showed no significant differences among treatment groups (Figure 7). While endotoxemic male mice showed a 23.9% decrease in hepatic sinusoidal diameter compared to control (\*\*\* =  $p < 0.001$ ), this reduction was only 19.4% in female mice (\*\* =  $p < 0.01$ ). A 10-minute period of ET-1 and H<sub>2</sub>S co-infusion did not result in a significant difference in vessel diameter in females but did in males (20.6% reduction versus control, \*\*\* =  $p < 0.001$ ). Moreover, in STS/LPS groups accompanied with infusion of ET-1, males showed a potentiated reduction in sinusoidal diameter (31.1% reduction versus control, \*\*\*\* =  $p < 0.0001$ ) whereas there was no difference observed in females. Data were from six separate experiments (three male, three female).

### **Sex Differences of Portal Infusion of H<sub>2</sub>S on Hepatic Sinusoidal**

**Heterogeneity:** The variability between hepatic sinusoidal diameters between male and female mice was evaluated (Figure 8). Though females did not have any significant differences among baseline treatment groups, the male STS/LPS group showed a significant effect on heterogeneity of sinusoidal diameters ( $6.8 \pm 2.5\mu\text{m}$  versus  $7.5 \pm 1.9\mu\text{m}$  for control, \*\*\* =  $p < 0.001$ ). Co-infusion of H<sub>2</sub>S and ET-1 resulted in an increase in the standard deviation of the means of sinusoidal diameter for males ( $8.8 \pm 2.3\mu\text{m}$  versus control, \* =  $p < 0.05$ ) but not females. In animals treated with LPS and co-infused with H<sub>2</sub>S and ET-1, sinusoidal perfusion heterogeneity was increased for both males ( $4.9 \pm 4.0\mu\text{m}$  versus control, \*\* =  $p < 0.01$ ) and females ( $7.1 \pm 2.9\mu\text{m}$  versus  $6.3 \pm 1.8\mu\text{m}$  for

control, \*\* =  $p < 0.01$ ). Moreover, differences in hepatic sinusoidal diameter and heterogeneity of perfusion between treatment groups can be observed in images of the vasculature (Figure 9). Data were from six separate experiments (three male, three female).

**Sex Differences of PAG Pre-Treatment on Hepatic Microcirculation During Endotoxemia:** We demonstrated that portal infusion of ET-1 for a duration of 10 minutes resulted in significant reductions in hepatic sinusoidal diameters for endotoxemic males and females (Figure 10), with males showing a greater sensitization to ET-1 than females (23.9% decrease versus control males, \*\*\*\* =  $p < 0.0001$ ; 19.4% decrease versus control females, \*\* =  $p < 0.01$ ). The constrictive effect of ET-1 was abrogated with PAG pre-treatment for both males. There were no significant differences among any of the treatment groups for baseline for either sex. Data were from six separate experiments (three male, three female).

**Sex Differences of PAG Pre-Treatment on Hepatic Sinusoidal Heterogeneity During Endotoxemia:** It was determined that there were no significant effects among baseline treatment groups or in PAG groups for males or females when evaluating the variability of hepatic sinusoidal diameters (Figure 11). When endotoxemic mice were pretreated with PAG, the increased sinusoidal perfusion heterogeneity was attenuated with ET-1 infusion ( $8.2 \pm 3.1\mu\text{m}$  versus  $5.4 \pm 3.3\mu\text{m}$  for LPS males, \*\* =  $p < 0.01$ ;  $7.6 \pm 2.1\mu\text{m}$  versus  $5.7 \pm 3.5\mu\text{m}$  for LPS females, \*\*\* =  $p < 0.001$ ). Additionally, there was a noticeable difference between treatment groups for hepatic sinusoidal diameter heterogeneity based on the visual appearance of the microvasculature (Figure 12). Data were from six separate experiments (three male, three female).

## 2.5 Discussion

The present study investigated whether H<sub>2</sub>S regulates sinusoidal perfusion within the hepatic microcirculation. We showed that pretreatment with the non-competitive inhibitor of cystathionine  $\gamma$ -lyase (CSE), the enzyme that produces H<sub>2</sub>S, mitigates the hypersensitization of the hepatic sinusoid to the vasoconstrictive effect of ET-1 during endotoxemia. Additionally, we report for the first time that there are sex differences in sinusoidal perfusion and microvascular dysfunction in the liver in endotoxemia.

NO, carbon monoxide (CO), and H<sub>2</sub>S make up the “gasotransmitters,” a group of endogenously synthesized gases that function as mediators in an array of physiological and pathophysiological functions [243]. H<sub>2</sub>S is the newest member of the “gasotransmitters” and is primarily synthesized during cysteine metabolism by two pyridoxal 5' phosphate-dependent enzymes, cystathionine  $\beta$ -synthase (CBS) and CSE. CSE is the major source of endogenous H<sub>2</sub>S in the liver and in the cardiovascular system [30, 92, 220]. H<sub>2</sub>S regulates blood flow by modulating vascular resistance. Several *in vivo* experimental models have provided evidence for the role of H<sub>2</sub>S as a vasodilator, including isolated aortic rings and mesenteric artery beds [38, 92]. In contrast to NO and CO, the vasorelaxant effect of H<sub>2</sub>S is not mediated by the cGMP pathway [83, 99]. Instead, H<sub>2</sub>S activates ATP-sensitive K<sup>+</sup> channels (K<sub>ATP</sub>) and/or Ca<sup>2+</sup>-activated K<sup>+</sup> channels (K<sub>Ca</sub>) [1, 13]. However, CSE<sup>-/-</sup> mice have been reported to spontaneously develop hypertension, which suggests that H<sub>2</sub>S is an important contributor in vasoregulation [252].

There is a large body of evidence that demonstrates that the primary action of H<sub>2</sub>S in the vasculature is vasodilatory [114, 136, 242]. However, biphasic responses to H<sub>2</sub>S

have been reported [49, 232]. In the rat mesenteric arterial bed, low concentrations of H<sub>2</sub>S ( $\leq 100\mu\text{M}$ ) elicited contraction while high concentrations promoted relaxation [49]. Similar observations have been reported in the mouse aorta [232] and the rat gastric artery [125].

H<sub>2</sub>S-releasing agents are widely used in the field of H<sub>2</sub>S physiology and pharmacology and it is important to be aware of potential problems associated with the choice of donor to generate H<sub>2</sub>S in *in vitro* and *in vivo* experiments. Inorganic salts, such as Na<sub>2</sub>S have been used as an exogenous H<sub>2</sub>S donor in many research studies. Sulfide salts are advantageous due to their ability to boost the concentration of H<sub>2</sub>S quickly. However, these compounds release H<sub>2</sub>S spontaneously during solution preparation, making it difficult to precisely control the total H<sub>2</sub>S concentration. The time that lies between when the solution is prepared and the time that a biological effect is measured can have an effect on results. The uncontrolled and rapid release of H<sub>2</sub>S can cause severe damage to *in vitro* and *in vivo* research models when H<sub>2</sub>S concentrations accumulate to toxic levels. Moreover, H<sub>2</sub>S can be lost from solution very rapidly due to volatilization under normal laboratory conditions [265]. The effective time sulfide salts remains in tissues is short and it was reported that H<sub>2</sub>S was lost from freshly prepared solutions with a half-life value of about 5 minutes [54]. Also, sulfide salts obtained commercially always contain a substantial amount of impurities. These issues outlined should be considered when selecting sulfide salts as an H<sub>2</sub>S-releasing agent in research.

It was initially assumed that cysteine was the primary source of H<sub>2</sub>S biosynthesis. However, it has been reported that thiols, including glutathione, homocysteine, cystathionine, and methionine can produce H<sub>2</sub>S directly [39, 145, 168]. A more recent

approach to administering H<sub>2</sub>S in experimental models is the use of sodium thiosulfate (STS, Na<sub>2</sub>S<sub>2</sub>O<sub>3</sub>). H<sub>2</sub>S is serially oxidized to persulfide, thiosulfate (TS, S<sub>2</sub>O<sub>3</sub>), sulfite and sulfate [88, 105]. STS is an intermediate in oxidative H<sub>2</sub>S metabolism that can also be reduced by rhodanese to generate H<sub>2</sub>S. Additionally, STS requires the presence of tissue in order for H<sub>2</sub>S to be liberated [166]. Because tissue is required for metabolism of STS and subsequent H<sub>2</sub>S production to occur, concentrations of H<sub>2</sub>S do not reach toxic levels as seen with sulfide salts. Therefore, STS was selected as the H<sub>2</sub>S donor for all parts of this research.

Using confocal intravital microscopy, we observed a reduction in hepatic sinusoidal diameter during portal infusion of H<sub>2</sub>S. Previous studies from our lab reported that sinusoidal constriction in response to ET-1 produces heterogeneous blood flow at the level of individual sinusoids within the hepatic microcirculation [108, 162]. In our study, H<sub>2</sub>S infusion increased the heterogeneity of the means of sinusoidal diameters, confirming previous results of increased heterogeneity of flow. H<sub>2</sub>S as a vasoconstrictor of the hepatic sinusoids suggests that there is a fundamentally different mechanism for the regulation of vascular tone in the microcirculation of the liver compared to other resistance vessels. H<sub>2</sub>S activates the K<sub>ATP</sub> channels in VSMCs, leading to hyperpolarization and results in relaxation and vasodilation [231]. Notably, vasodilation by H<sub>2</sub>S is reversible with treatment of the K<sub>ATP</sub> channel inhibitor, glibenclamide [264]. VSMCs are located around the portal terminal venules and hepatic arterioles in the liver. It has been shown that H<sub>2</sub>S mitigates vasoconstriction induced by norepinephrine (NE) in isolated liver models and increases the hepatic arterial buffer response [64, 210]. These results suggest that H<sub>2</sub>S functions as a vasodilator in the liver where there are VSMCs

present. However, the hepatic sinusoids lack VSMCs and sinusoidal tone is primarily modulated by specialized pericytes, the HSCs. HSCs, which surround individual sinusoids, respond to local balances between vasodilators and vasoconstrictors to modulate sinusoidal tone [112]. When the balance between vasodilators and vasoconstrictors is tipped, HSCs cause contraction or relaxation to alter sinusoidal tone. It is well known that during sepsis there is an imbalance between NO and the vasoconstrictive effect of ET-1, leading to sinusoidal hyperconstriction [18]. In an isolated, perfused liver model, it was demonstrated that H<sub>2</sub>S could be beneficial as a treatment in hepatic cirrhosis by reducing portal hypertension and increasing hepatic perfusion since it was shown that H<sub>2</sub>S attenuated catecholamine-induced vasoconstriction [64]. Based on this finding, it is understandable that one would predict that the vasodilatory effect of H<sub>2</sub>S would also be beneficial during sepsis. However, previous studies from our lab show that H<sub>2</sub>S differentially regulates the effect of phenylephrine (PE) and ET-1 in an isolated, perfused liver system [163]. Therefore, H<sub>2</sub>S may have a different effect on the hepatic sinusoids than on the portal venules. Previous results from our lab also demonstrated that inhibiting the H<sub>2</sub>S-synthesizing enzyme, CSE, attenuates hepatic microcirculatory dysfunction in an endotoxin model of sepsis [162].

In the hepatic sinusoid, the vasoconstrictive effect of ET-1 is the result of an interaction with ET<sub>A</sub> and ET<sub>B</sub> receptors found on HSCs [95]. Vasoconstriction is counterbalanced by ET-1 interaction with ET<sub>B</sub> receptors on SECs, which stimulate eNOS activity and bioavailability of NO [181]. Inflammatory stress elicits an increase in ET-1 levels [5, 190] but NO production stimulated by ET-1 from SECs is impaired. Impairment of NO production is the result of an increase in caveolin-1, which has been

shown to inhibit eNOS activity [128]. The vasoconstrictive effect of ET-1 is not counterbalanced, leading to hepatic sinusoidal hypersensitization. Sinusoidal hyperconstriction causes development of heterogeneous sinusoidal perfusion and focal hypoxia [107]. As a result, individual sinusoids that are constricted are under-perfused, leading to local ischemia, while adjacent sinusoids are dilated and over-perfused. Although total hepatic blood flow may remain unchanged, the heterogeneous hepatic perfusion in the microcirculation fails to match oxygen supply with metabolic tissue demand, leading to liver dysfunction and injury.

For this study, we injected male and female mice intraperitoneally with LPS (5mg/kg body weight) for 6 hours as our endotoxemic model of sepsis. We assessed the effect of exogenous H<sub>2</sub>S as well as PAG pretreatment on changes in the hepatic microcirculation during endotoxemia. In contrast with previous studies from our lab that demonstrated an effect of portal infusion of H<sub>2</sub>S [162], we did not observe any alterations in the hepatic microcirculation with STS alone. This study used STS as the H<sub>2</sub>S-releasing agent and not Na<sub>2</sub>S, it is possible that H<sub>2</sub>S did not accumulate to the same concentrations *in vivo* even though the concentrations administered were the same. In addition, previous studies used rats whereas this study used mice, thus, it is possible that the responses are species-related. Since STS requires tissue to release H<sub>2</sub>S, levels of the noxious gas do not become elevated enough to elicit the same effect as observed in previous studies where Na<sub>2</sub>S was the selected H<sub>2</sub>S-releasing agent.

It has been demonstrated that ET-1 leads to sinusoidal constriction, which colocalizes with HSCs [260]. It was also shown that portal infusion of ET-1 results in an increase in the heterogeneity of perfusion through the sinusoids [107]. Other studies

reported that inflammatory stress, sepsis included, potentiates the vasoconstrictive effect induced by ET-1 in the hepatic microcirculation [18, 108, 175]. Moreover, there is evidence that sinusoidal hyperconstriction and heterogeneous perfusion results in impaired oxygen delivery to hepatic tissues and focal hypoxia and liver injury [19]. In this study, we have shown that endotoxin significantly increases sinusoidal constriction and heterogeneity of sinusoidal perfusion following portal infusion of ET-1. This effect was reversed with one intraperitoneal injection of PAG 30 minutes prior to administration of LPS. In LPS-treated mice, PAG pretreatment decreased hyperconstriction of the sinusoids and attenuated sinusoidal perfusion heterogeneity following a 10-minute period of ET-1 infusion.

When we further analyzed our data by sex, it was observed that females were less sensitive to ET-1 in endotoxemia. In addition, when H<sub>2</sub>S was co-infused with ET-1, male showed a significant reduction in sinusoidal diameter where females did not for both baseline and in endotoxemia. Differences among the sexes also applied to sinusoidal perfusion heterogeneity. Co-infusion of H<sub>2</sub>S and ET-1 showed an increase in the standard deviation of the means of sinusoidal diameter for males but not females.

The results of this study provide evidence for one possible protective mechanism of inhibiting CSE during sepsis. A rapid-releasing H<sub>2</sub>S donor, sodium hydrosulfide (NaHS), has been shown to reverse the protective effect of PAG, suggesting that PAG is dependent on H<sub>2</sub>S [176, 255, 258]. Importantly, PAG pretreatment has been shown to be protective on the inflammatory response during sepsis [255].

There are conflicting reports of the vasoregulatory roles of H<sub>2</sub>S in the hepatic microcirculation. In chronic conditions, such as hepatic cirrhosis and fibrosis, H<sub>2</sub>S may

be beneficial as it acts as a vasodilator in the portal venules to improve hepatic perfusion and reduce portal hypertension. However, during sepsis, dysfunction of the hepatic microcirculation occurs primarily at the sinusoidal level, which become hyperconstricted with heterogeneous blood flow. For the first time, we show sex differences in the effect of both exogenous and endogenous H<sub>2</sub>S in sinusoidal resistance vessels. We demonstrated that pretreatment with the inhibitor of endogenous H<sub>2</sub>S-synthesizing enzyme, CSE, significantly improves hepatic microcirculatory function following ET-1 infusion during an endotoxemia model of sepsis. Our results suggest that the observed protective effect of PAG pretreatment during sepsis may be the result of improved sinusoidal perfusion.

## 2.6 Figures

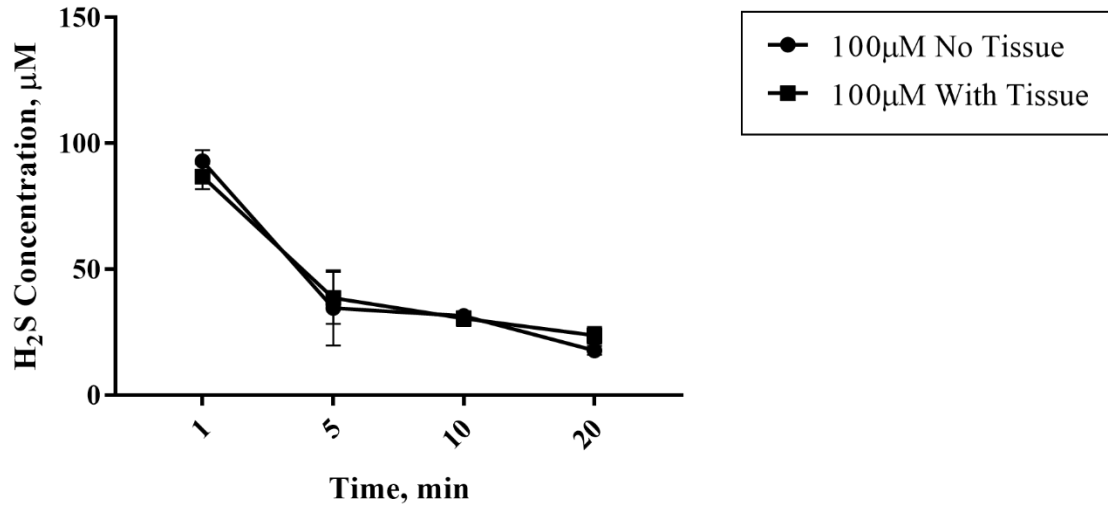


Figure 1: Total H<sub>2</sub>S generation over time of Na<sub>2</sub>S, in the absence and in the presence of liver tissue. The amount of H<sub>2</sub>S generated was monitored over time to determine the effect of liver tissue on the efficacy of H<sub>2</sub>S-releasing agent, Na<sub>2</sub>S. The total amount of H<sub>2</sub>S generated was determined by calculating the amount of H<sub>2</sub>S present in solution after incubation times of 1 minute, 5 minutes, 10 minutes, and 20 minutes with freshly prepared 100 µM Na<sub>2</sub>S in the absence and in the presence of liver tissue. Data are presented as the means  $\pm$  SEM from four separate experiments.

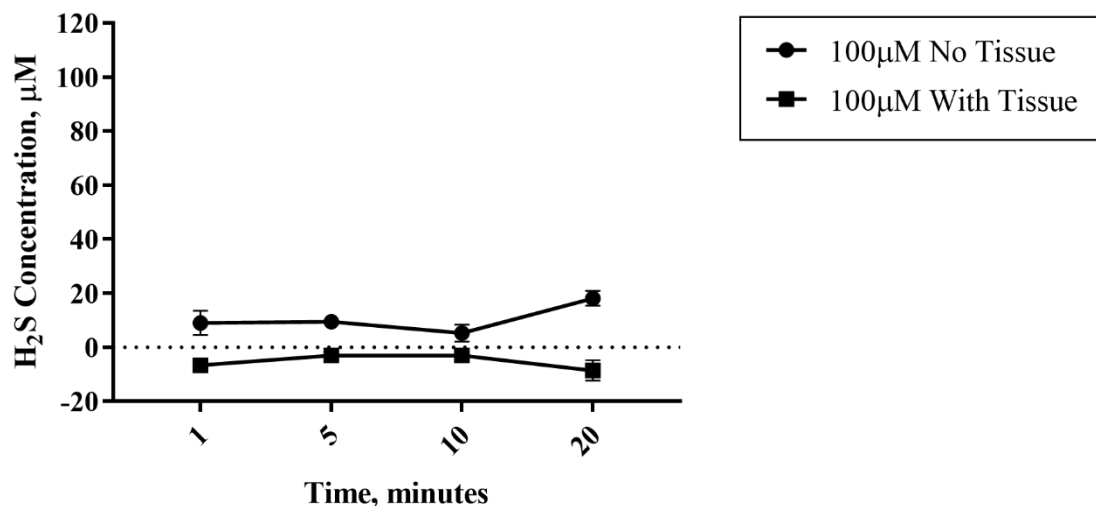


Figure 2: Total H<sub>2</sub>S generation over time of STS, in the absence and in the presence of liver tissue. The amount of H<sub>2</sub>S generated was monitored over time to determine the effect of liver tissue on the efficacy of H<sub>2</sub>S-releasing agent, STS. The total amount of H<sub>2</sub>S generated was determined by calculating the amount of H<sub>2</sub>S present in solution after incubation times of 1 minute, 5 minutes, 10 minutes, and 20 minutes with freshly prepared 100 µM STS in the absence and in the presence of liver tissue. Data are presented as the means  $\pm$  SEM from four separate experiments.

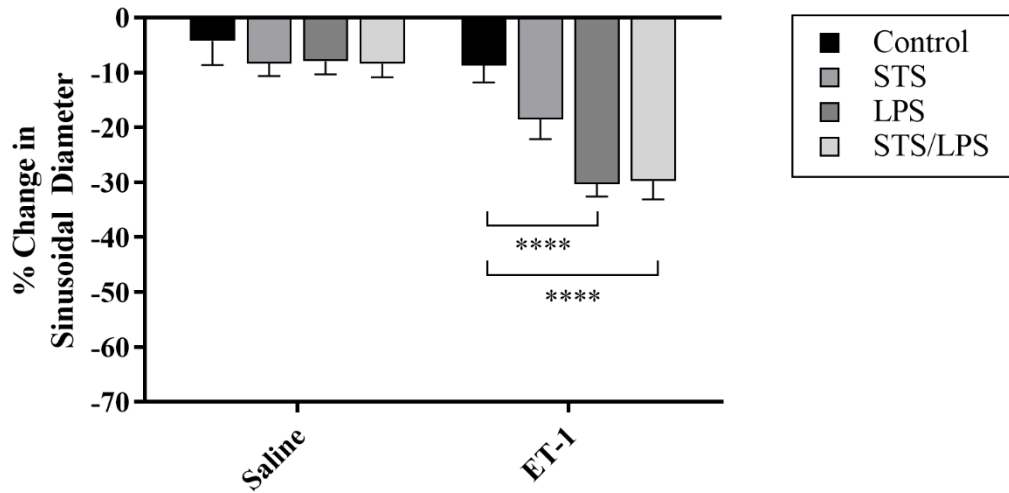


Figure 3: Effect of STS on change in hepatic sinusoidal diameter. Images of the hepatic sinusoids were recorded before, during, and 10 minutes following infusion of H<sub>2</sub>S donor, STS. Infusion of STS decreased sinusoidal diameter when co-infused with ET-1 in endotoxemia for pooled sexes. Data are presented as the means  $\pm$  SEM from six separate experiments. Statistical analysis was performed using two-way ANOVA with Sidak's multiple comparison *post hoc* test. \*\*\*\* =  $p < 0.0001$ .

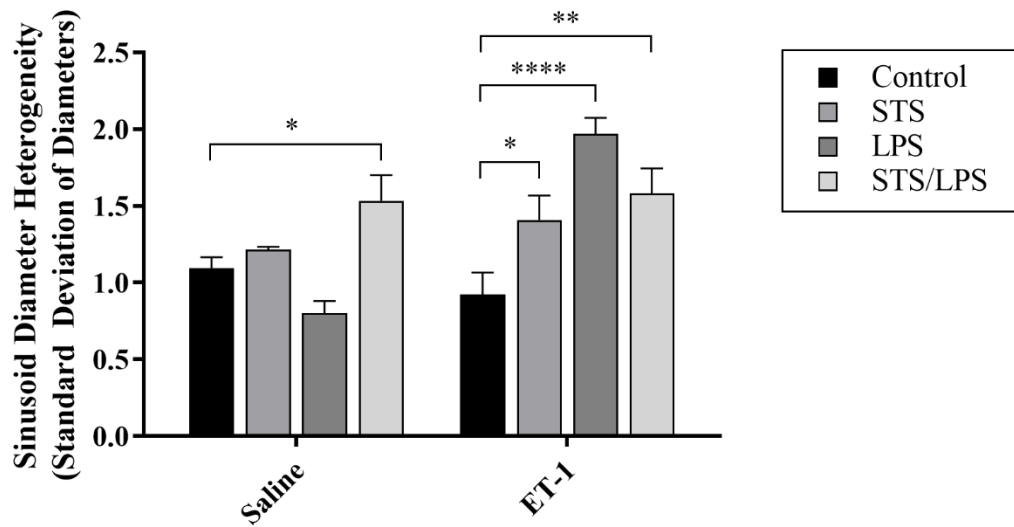


Figure 4: Effect of STS on heterogeneity of sinusoidal diameters. Images of the hepatic sinusoids were recorded before, during, and 10 minutes following infusion of H<sub>2</sub>S donor, STS. Infusion of STS increased heterogeneity of sinusoidal diameter in endotoxemia for pooled sexes. Data are presented as the means  $\pm$  SEM from six separate experiments. Statistical analysis was performed using two-way ANOVA with Sidak's multiple comparison *post hoc* test. \* =  $p < 0.05$ , \*\* =  $p < 0.01$ , \*\*\*\* =  $p < 0.0001$ .

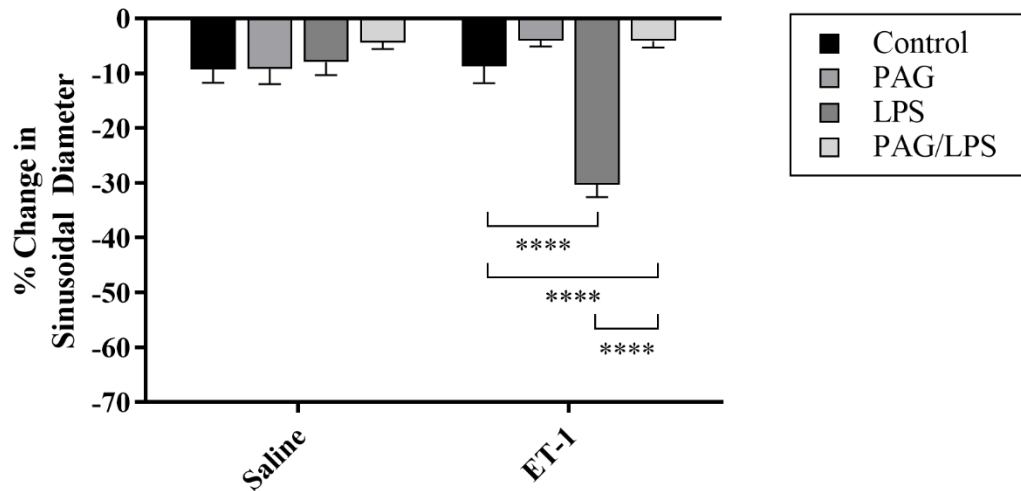


Figure 5: Effect of PAG on change in hepatic sinusoidal diameter during infusion of ET-1 during endotoxemia. Mice were pretreated with PAG for 30 minutes with or without LPS treatment for 6 hours. Images of the hepatic sinusoids were recorded before, during, and 10 minutes following infusion of ET-1. PAG attenuates sinusoidal hyperconstriction following ET-1 infusion during endotoxemia for pooled sexes. Data are presented as the means  $\pm$  SEM from six separate experiments. Statistical analysis was performed using two-way ANOVA with Tukey's *post hoc* test. \*\*\*\* =  $p < 0.0001$ .

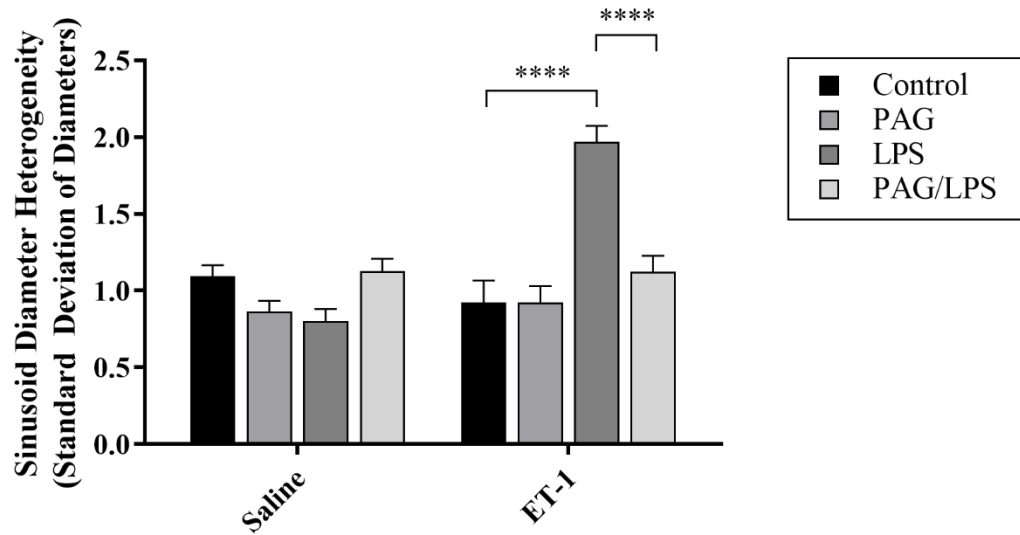


Figure 6: Effect of PAG on heterogeneity of sinusoidal diameters during infusion of ET-1 during endotoxemia. Mice were pretreated with PAG for 30 minutes with or without LPS treatment for 6 hours. Images of the hepatic sinusoids were recorded before, during, and 10 minutes following infusion of ET-1. PAG attenuates increased heterogeneity of sinusoidal diameter following ET-1 infusion in endotoxemia for pooled sexes. Data are presented as the means  $\pm$  SEM from six separate experiments. Statistical analysis was performed using two-way ANOVA with Tukey's *post hoc* test. \*\*\*\* =  $p < 0.0001$ .

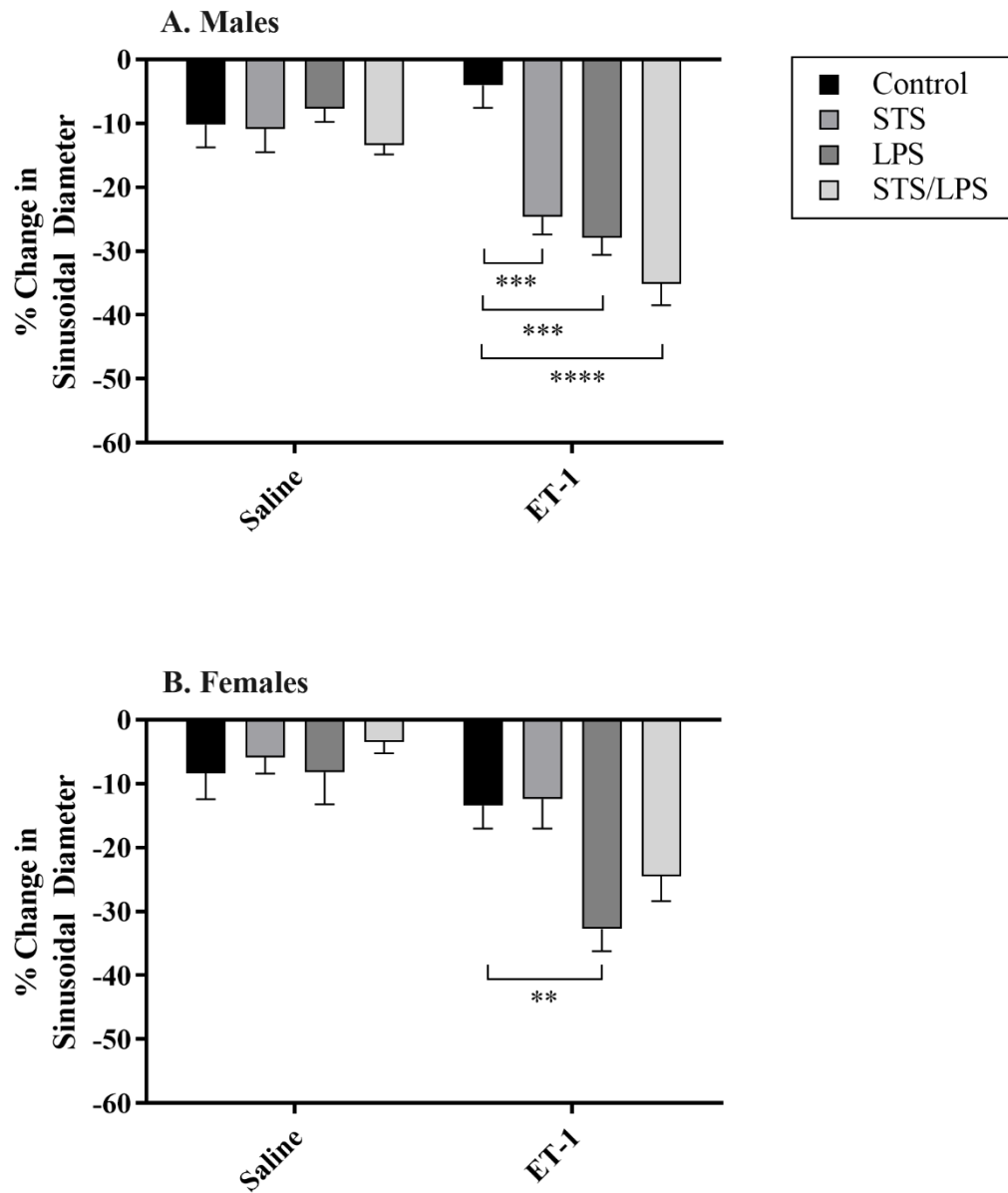


Figure 7: Effect of STS on change in hepatic sinusoidal diameter in males and females. Images of the hepatic sinusoids were recorded before, during, and 10 minutes following infusion of H<sub>2</sub>S donor, STS. Infusion of STS decreased sinusoidal diameter when co-infused with ET-1, which was potentiated in endotoxemia. Data are presented as the means  $\pm$  SEM from three separate experiments. Statistical analysis was performed using two-way ANOVA with Sidak's *post hoc* test. \*\* =  $p < 0.01$ , \*\*\* =  $p < 0.001$ , \*\*\*\* =  $p < 0.0001$ .

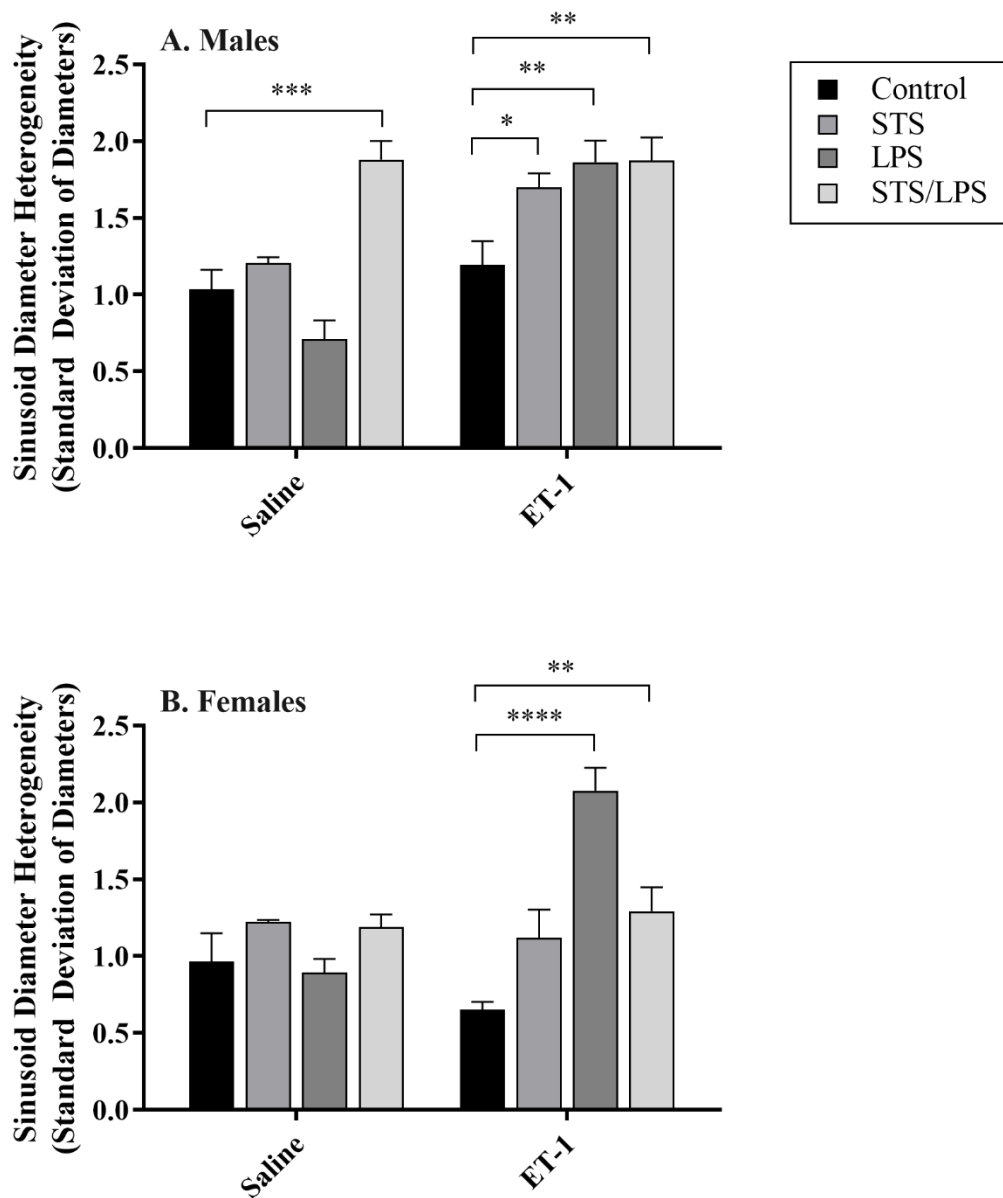


Figure 8: Effect of STS on heterogeneity of sinusoidal diameters in males and females. Images of the hepatic sinusoids were recorded before, during, and 10 minutes following infusion of H<sub>2</sub>S donor, STS. Infusion of STS increased heterogeneity of sinusoidal diameter in endotoxemia. Data are presented as the means  $\pm$  SEM from three separate experiments. Statistical analysis was performed using two-way ANOVA with Sidak's *post hoc* test. \* =  $p < 0.05$ , \*\* =  $p < 0.01$ , \*\*\* =  $p < 0.001$ , \*\*\*\* =  $p < 0.0001$ .

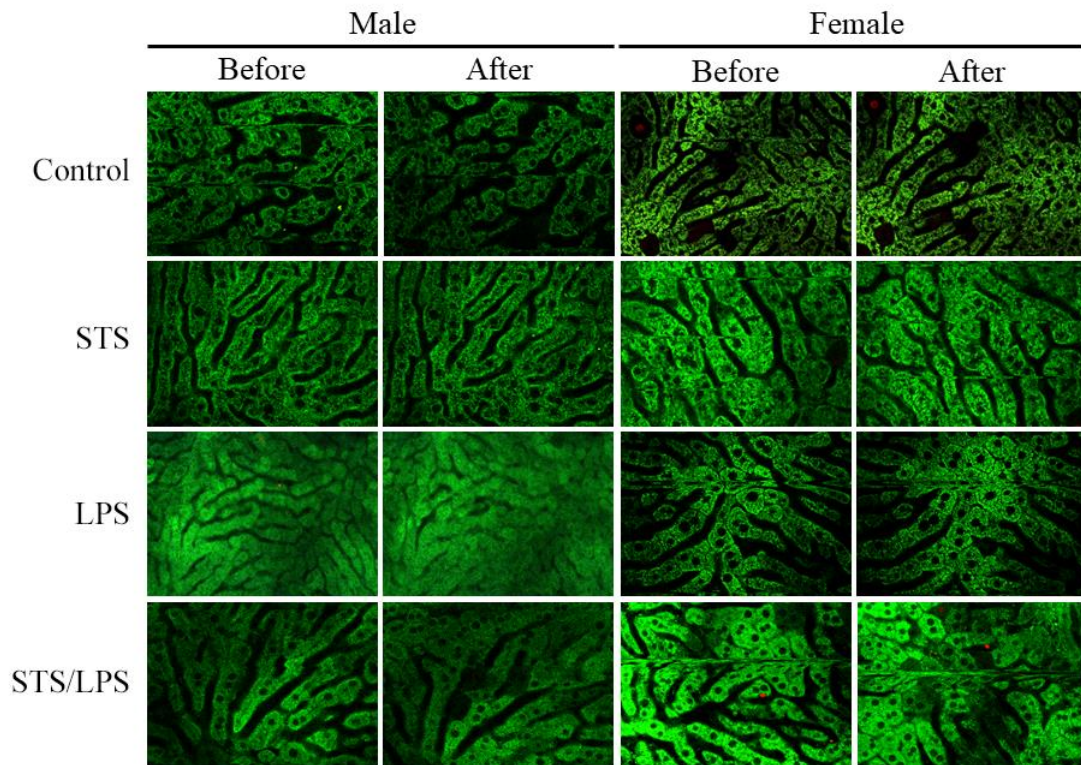


Figure 9: Effect of ET-1 and STS co-infusion on the hepatic sinusoids in endotoxemia. Sinusoids were visualized to determine the effect of ET-1 and STS co-infusion on endotoxemic male and female mice. Representative images are shown before and after co-infusion of ET-1 ( $1\mu\text{mol/kg}$  body weight/minute) and STS ( $2\mu\text{mol/kg}$  body weight/minute).

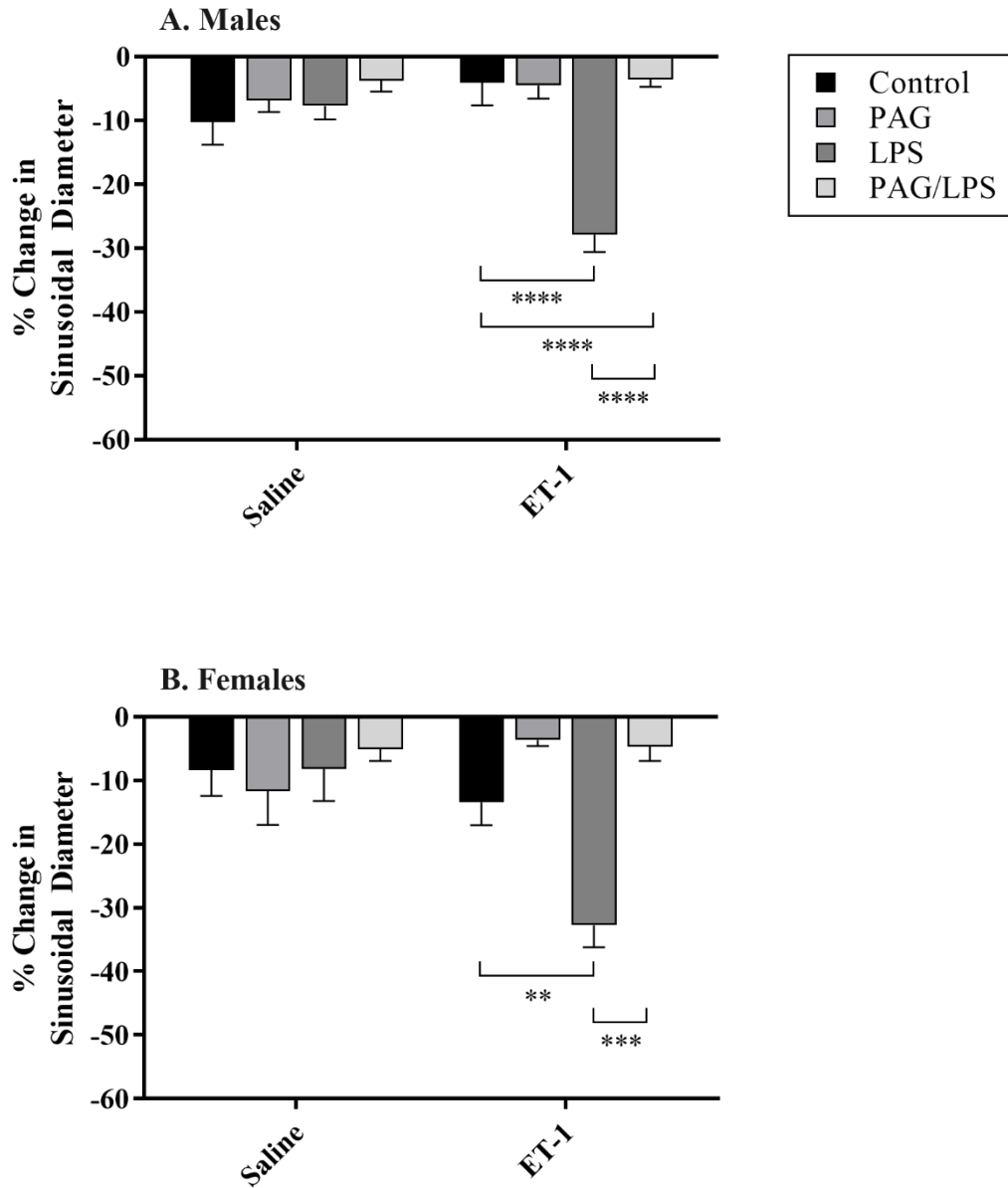


Figure 10: Effect of PAG on change in hepatic sinusoidal diameter during infusion of ET-1 during endotoxemia in males and females. Mice were pretreated with PAG for 30 minutes with or without LPS treatment for 6 hours. Images of the hepatic sinusoids were recorded before, during, and 10 minutes following infusion of ET-1. PAG attenuates sinusoidal hyperconstriction following ET-1 infusion during endotoxemia. Data are presented as the means  $\pm$  SEM from three separate experiments. Statistical analysis was performed using two-way ANOVA with Tukey's *post hoc* test. \*\* =  $p < 0.01$ , \*\*\* =  $p < 0.001$ , \*\*\*\* =  $p < 0.0001$ .

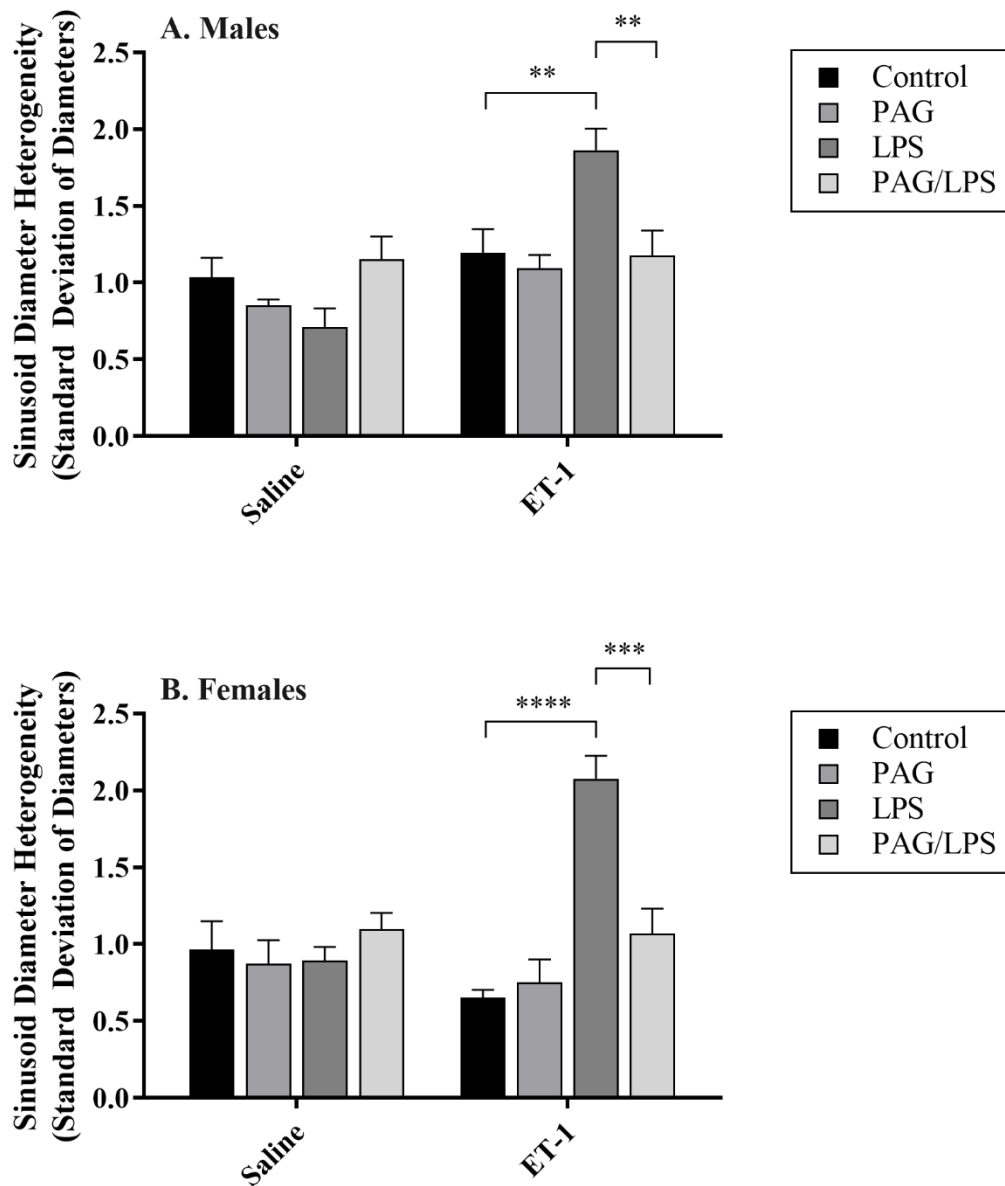


Figure 11: Effect of PAG on change in heterogeneity of sinusoidal diameters during infusion of ET-1 during endotoxemia in males and females. Mice were pretreated with PAG for 30 minutes with or without LPS treatment for 6 hours. Images of the hepatic sinusoids were recorded before, during, and 10 minutes following infusion of ET-1. PAG attenuates sinusoidal hyperconstriction following ET-1 infusion during endotoxemia. Data are presented as the means  $\pm$  SEM from three separate experiments. Statistical analysis was performed using two-way ANOVA with Tukey's *post hoc* test. \*\* =  $p < 0.01$ , \*\*\* =  $p < 0.001$ , \*\*\*\* =  $p < 0.0001$ .

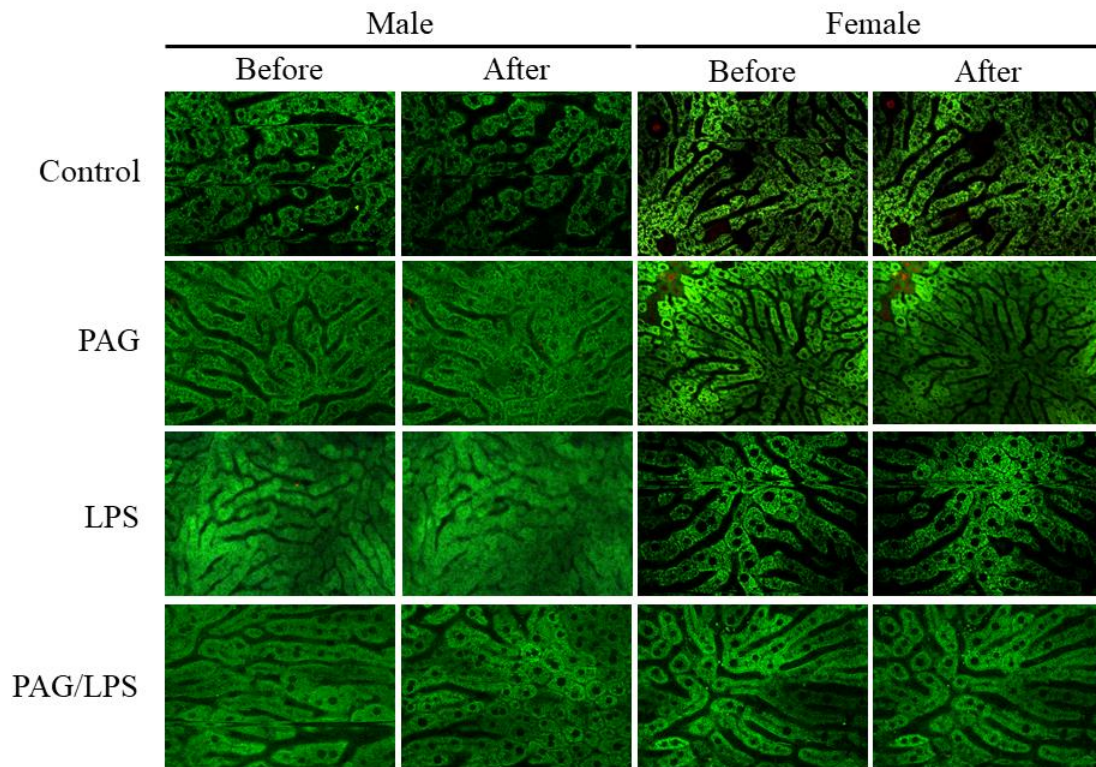


Figure 12: Effect of ET-1 infusion on the hepatic sinusoids with PAG pretreatment in endotoxemia. Sinusoids were visualized to determine the effect of ET-1 infusion on endotoxemic male and female mice, with or without the inhibitor of CSE, PAG. Representative images are shown before and after infusion of 1  $\mu\text{mol/kg}$  body weight/minute infusion of ET-1.

## CHAPTER 3: THE RESPONSE OF HEPATOCYTES TO HYDROGEN SULFIDE AND ENDOTHELIN-1 ON MITOCHONDRIAL FUNCTION *IN VIVO*

### 3.1 Abstract

Impaired blood flow that occurs in early sepsis results in insufficient oxygen at the mitochondrial level to drive oxidative phosphorylation and a potential to trigger cell death pathways. Furthermore, the generation of excessive amount of hydrogen sulfide ( $H_2S$ ) and reactive oxygen species (ROS) directly inhibit the mitochondrial electron transport chain (ETC), subsequent ATP generation, and can cause damage to the mitochondrial proteins and DNA. The ability to clear dysfunctional mitochondria via the process of mitophagy may be critical in the pathogenesis of sepsis. Mitophagy involves the selective degradation of dysfunctional mitochondria before they can activate apoptotic pathways and cause the death of the cell. Therefore, mitophagy serves as an early protective mechanism. The present study was designed to examine the effects of both exogenous and endogenous  $H_2S$  on hepatic mitochondrial function and dynamics in an *in vivo* endotoxin model of sepsis using confocal intravital microscopy. Since hepatic  $H_2S$  levels are elevated during sepsis, DL-propargylglycine (PAG), the inhibitor of cystathionine  $\gamma$ -lyase, was used to determine the contribution of  $H_2S$  to changes in mitochondrial depolarization. We observed that mitochondrial depolarization was significantly increased in endotoxin-treated males but not females, which was attenuated with PAG pretreatment. When examining mitochondrial dynamics, results showed that  $H_2S$  decreased mitophagy by 20.7% in males but had no significant effect in females. Endotoxemic females showed a 17.4% increase in mitophagy while males showed a 14.9% decrease, suggesting a possible protective mechanism that is present in females

but not males. Furthermore, we show that PAG pretreatment induced mitophagy by 40.8% in LPS-treated males but not females, suggesting a role for endogenous H<sub>2</sub>S in mitochondrial dysfunction in the progression of sepsis that is sex-related.

### 3.2 Introduction

Defined as the systemic inflammatory response to infection, sepsis is the result of organ dysfunction and is the predominant cause of mortality in the intensive care unit (ICU). Patients who die of sepsis typically succumb to the resultant multi-organ failure and not the initial acute inflammation. Multiple organ failure (MOF) is regarded as the terminal result of severe, continual inflammation but the exact mechanisms by which inflammation results in organ dysfunction remain elusive. Decreases in oxygen extraction and lactic acidosis are hallmarks of sepsis and lead to the conclusion that MOF was caused by tissue hypoxia caused by disturbances in the microvasculature. Without adequate oxygen delivery, cells are unable to generate adenosine triphosphate (ATP) to meet the metabolic demand, leading to organ failure.

It is well known that vascular hyporeactivity to catecholamine vasopressors and microvascular dysfunction exist in septic patients. However, significant tissue hypoxia may not be the cause of multiorgan failure. Increased tissue oxygen tensions have been reported in various tissues and organs, including the muscle, gut, and bladder in both animal studies [201, 236] and septic patients in early sepsis [21]. These findings prompted the investigation of an alternate hypothesis in which impaired cellular usage of oxygen, rather than inadequate oxygen delivery, leads to organ dysfunction. The process of oxidative phosphorylation, used by the mitochondrial respiratory chain, utilizes more

than 90% of total body oxygen consumption. It is possible that a decrease in ATP production as a result of a disruption in oxidative phosphorylation, is a mechanism underlying organ dysfunction in the progression of sepsis. In support of this cellular dysoxia theory, it was reported that maximal oxygen consumption increased significantly in hepatocytes exposed to endotoxin for 6 hours but decreased markedly by 24 hours [200]. It was also observed that sepsis severity was associated with decreases in oxygen consumption in a patient study [124].

Mitochondria are intracellular organelles and composed of a central matrix enclosed by an inner and outer mitochondrial membrane. Mitochondria have several primary functions including the production of ATP, control cell death pathways, calcium and H<sup>+</sup> homeostasis, intracellular signaling, and heat production. The mitochondrial electron transport chain (ETC) is composed of four individual protein complexes (complexes I-IV) that transfer electrons from NADH and succinate down a redox gradient ending with the reduction of molecular oxygen to water. Electron transfer enables complex I, complex III, and complex IV to translocate protons from the inner mitochondrial matrix to the intramembranous space, which generates a proton gradient in the process. Complex V, or ATP synthase, uses this proton gradient to generate ATP from adenosine diphosphate (ADP) and inorganic phosphate.

A systemic inflammatory response can be triggered by microbial antigens or by intrinsic factors released into the general circulation because of trauma or other injury. These factors, danger-associated molecular patterns (DAMPs) are released in response to stress, injury to tissue, or cell death. DAMPs can be intracellular constituents, such as heat shock proteins, histones, DNA, and mitochondria [230, 263]. Pattern recognition

receptors, such as the Toll-like receptors, recognize DAMPs and modulate gene transcription of inflammatory proteins, including cytokine and cytokine receptors. Cytokines trigger activation or suppression of multiple intracellular pathways to modulate function. The systemic inflammatory response can affect mitochondria in multiple ways. Intrinsic and extrinsic fluid loss and decreased fluid intake, myocardial depression, microcirculatory dysfunction and loss and vascular tone lead to impaired blood perfusion and tissue hypoxia in the progression of sepsis [218, 219]. Though complex IV of the mitochondrial respiratory chain can function effectively at low oxygen concentrations, critically low levels of oxygen compromises ATP production and may lead to cell death pathways via the release of cytochrome *c* [218]. Furthermore, excess NO, CO, and H<sub>2</sub>S, and reactive oxygen species (ROS) inhibit mitochondrial respiration and ATP production.

Three gases are produced endogenously in the body: nitric oxide (NO), carbon monoxide (CO), and hydrogen sulfide (H<sub>2</sub>S). These “gasotransmitters” have important roles in the regulation of mitochondrial signaling [15, 132, 242]. In particular, H<sub>2</sub>S effects are highly divergent, dependent on local concentrations, and are observed as a characteristic biphasic dose-response curve. Many H<sub>2</sub>S effects at low concentrations have been shown to be beneficial while high concentrations of the noxious gas are toxic [229]. On the molecular level, H<sub>2</sub>S toxicity is due to the inhibition of cytochrome *c* oxidase or complex IV of the mitochondrial respiratory chain [89, 182]. Complex IV catalyzes the transfer of electrons from cytochrome *c* to molecular oxygen. It has been demonstrated that high concentrations of H<sub>2</sub>S reversibly and competitively binds to complex IV, inhibiting molecular oxygen and resulting in an accumulation of electrons, mitochondrial membrane depolarization, and suppression of ATP synthesis. In contrast,

H<sub>2</sub>S is a substrate for the oxidative phosphorylation, donating electrons to the ETC at the level of sulfur quinone reductase (SQR), stimulating electron flow and ATP production. When comparing H<sub>2</sub>S to other substrates of the ETC, the electron yield is low (two molecules of sulfide are needed to provide two electrons) and is costly (sulfide requires three times more oxygen). Therefore, sulfide oxidation yield in energy per oxygen atom consumed is low when compared with NADH and FADH<sub>2</sub>. However, this low energy yield is balanced by several properties of H<sub>2</sub>S: 1) H<sub>2</sub>S can freely diffuse across membranes, allowing it to reach mitochondria without requiring transporters, 2) H<sub>2</sub>S does not require biological preparation, contrasting with NADH and FADH<sub>2</sub>, which are derived via the Krebs's cycle 3) the affinity of SQR is high so that the total H<sub>2</sub>S that is released is ultimately oxidized.

Mitochondria exist in a dynamic state, where mitochondrial networks are constantly elongating (fusion) and dividing (fission). These two events must remain in balance to provide an equilibrium of small, fragmented mitochondria and long, connected mitochondria. This delicate balance is thought to be critical for mitochondrial homeostasis, cell stability, and cell survival [31, 235]. Mitochondrial fission is responsible for the segregation of dysfunctional mitochondria that contain damaged proteins and mitochondrial DNA (mtDNA) and depolarized membrane while mitochondrial fusion plays a role in the equilibrium of matrix metabolites, intact mtDNA, and membrane components, such as the protein complexes included in the respiratory chain [56, 91, 179]. Both fission and fusion are regulated by a family of dynamin-related proteins (DRPs), which modulate the mitochondrial network to ensure a healthy and connected network as well as the distribution of mitochondria to specific sites within the

cell [24]. The master modulator of mitochondrial fission is dynamin-related protein 1 (DRP1). DRP1 is distributed diffusely throughout the cytosol and when activated through post-translational modification, sequesters to the outer mitochondrial membrane [129]. DRP1 then reacts with four proteins bound to the mitochondria acting as receptors including mitochondrial dynamic protein of 49kDa (Mid49) and 51kDa (Mid51), mitochondrial fission protein 1 (Fis-1), and mitochondrial fission factor (Mff) to constrict and cleave the mitochondria [172, 173, 221]. Furthermore, dysregulation of DRP1 has been shown to interact with mitochondrial biogenesis. In a breast cancer cell line, DRP1 upregulation was associated with metabolically less active mitochondria. The number of mitochondria was reduced accompanied with an upregulation of mitochondrial biogenesis markers, including peroxisome proliferator-activated receptor  $\gamma$  coactivator 1- $\alpha$  (PCG-1 $\alpha$ ), nuclear respiratory factor 1 (NRF1), and mammalian mitochondrial transcription factor (TFAM) [266].

Macroautophagy, commonly referred to as autophagy, is the degradation of large cellular constituents, such as organelles, through both selective and nonselective mechanisms. The process of degrading mitochondria through macroautophagy is termed mitophagy and occurs in several steps: 1) detection of dysfunctional mitochondria, 2) segregation of dysfunctional mitochondria from healthy mitochondria via mitochondrial fission, 3) recruitment of the phagophore, and 4) degradation via autophagic processes. In conjunction with mitochondrial biogenesis, mitophagy ensures a healthy mitochondrial network through mitochondrial turnover. It is important to clear dysfunctional mitochondria to limit cellular damage by ROS production and apoptosis. The PINK1/Parkin-mediated mitophagy pathway is the most well-known [147, 157]. PINK1

contains a mitochondrial-targeting domain that is transported into the intramembranous space via the translocase of the outer mitochondrial membrane (TOM) where it is integrated into the inner mitochondrial membrane via the translocase of the inner mitochondrial membrane (TIM) and rapidly processed and degraded by the mitochondrial membrane peptidase and presenilin-associated rhomboid-like protease (PARL). In healthy mitochondria, PINK1 concentration is maintained at low levels through its rapid degradation [150]. However, TIM-mediated import of proteins is dependent on mitochondrial membrane potential. When mitochondria become depolarized, PINK1 can no longer be inserted into the mitochondria, preventing its subsequent proteolytic cleavage and degradation [104]. PINK1 accumulates on depolarized mitochondria, become phosphorylated, and activates several proteins, including Parkin and ubiquitin [109, 122, 157, 170]. Upon activation, Parkin ubiquitinates a myriad of outer mitochondrial membrane proteins to promote mitophagy [170]. The phagophore is recruited and binding to the dysfunction, segregated mitochondrion is mediated by light chain 3B (LC3B) binding domain. DRP1 is considered to be associated with mitophagy by fractionating mitochondria into sizes ideal for autophagosome engulfment.

This present study was designed to determine the mitochondrial effects of exogenous and endogenous H<sub>2</sub>S on the hepatic sinusoidal endothelial cells (SECs) *in vivo*. Since H<sub>2</sub>S has been shown to be detrimental during the progression sepsis, we hypothesized that endogenous H<sub>2</sub>S is a contributor to the mitochondrial depolarization of the SECs within the hepatic sinusoid during sepsis. Using intravital confocal microscopy, we demonstrate for the first time that both sepsis and infusion of exogenous H<sub>2</sub>S are associated with decreased mitophagy in male livers but not in female livers,

suggesting a difference in response among sexes. By examining expression of proteins involved in mitochondrial fission and subsequent mitophagy, we present a possible mechanism that explains the sex differences observed in the microvascular response to sepsis and ET-1.

### 3.3 Materials and Methods

**Animals:** Male and female C57Bl/6 mice (gift from Dr. Pinku Mukherjee, University of North Carolina at Charlotte, Charlotte, North Carolina) weighing 18-25 grams were used in this study. Mice were housed in a temperature-controlled environment on 12-hour light/dark cycles with free access to standard mouse chow and water. All animal manipulation was in strict adherence with the National Institute of Health guidelines and experimental protocols were approved by the Institutional Animal Care and Use Committee of the University of North Carolina at Charlotte.

**Reagents:** Sodium thiosulfate (STS), DL-propargylglycine (PAG), and lipopolysaccharide (LPS) (E. Coli, serotype 026:B6), endothelin-1 (ET-1), and limonene were purchased from Sigma-Aldrich. Rhodamine123 (Rh123), propidium iodide (PI), and Dulbecco's Phosphate-Buffered Saline (DPBS) 1X were purchased from ThermoFisher (Waltham, Massachusetts).

**Mitochondria Labeling:** Mitochondria were fluorescently labeled using Rh123 (525nmol/mouse). Since Rh123 is a cationic dye, it distributes electrophoretically into the mitochondrial matrix in response to the electric potential across the inner mitochondrial membrane, which was infused via the ventral tail vein 10 minutes before intravital confocal microscopy. Rh123 was injected via the ventral tail vein using a 30-gauge needle attached to a 10cc syringe 10 minutes prior to confocal intravital microscopy.

**Labeling of Nonviable Cells:** Nonviable cells were fluorescently labeled using PI (45nmol/mouse). While PI is excluded from live, cells, it permeates dead cells and stains

chromosomes. PI was injected the ventral tail vein with Rh123 using a 30-gauge needle attached to a 10cc syringe 10 minutes prior to confocal intravital microscopy.

**Confocal Intravital Microscopy:** Mice were anesthetized using 1-3% isoflurane in (J. A. Webster Veterinary Supply, Devens, Massachusetts) in oxygen. The abdomen was shaved and a laparotomy was performed to expose the liver and digestive organs. Electrocautery was used to prevent bleeding. The ligaments connecting the liver to surrounding structures (diaphragm, anterior abdominal wall, etc.) were cut to allow the liver to be exteriorized. The intestines were reflected, and a 4-ply gauze moistened with Dulbecco's phosphate-buffered saline (DBPS) 1X is placed underneath. A large mesenteric vein was cannulated with a 30-gauge needle on the end of a PE10 catheter connected to a 1cc syringe containing heparinized saline. The cannula was fixed in place with 10 $\mu$ L of Vetbond tissue adhesive and a small piece of Kimwipe. The cannula was flushed with heparinized saline to prevent clotting. The intestines were reflected over the fixed cannula and then wrapped with gauze. DPBS 1X was added to the abdominal area to prevent the intestines from drying. A length of 3-0 surgical suture is tied to the xiphoid process, which will help to retract the abdominal opening during intravital microscopy. A cotton swap dipped in limonene was applied onto the ventral side of the tail to aid in visualization of the ventral tail vein. Fluorescent indicators, Rh123 (75mmol/mouse) and PI (7mmol/mouse), were injected via the ventral tail vein using a 30-gauge needle.

For microscopy, the mouse was placed on a temperature-controlled (37-38°C) microscope stage with a viewing window over the 40X UPlanApo 0,85 objective lens of an Olympus FV500 scanning confocal microscope and was maintained under isoflurane

anesthesia, administered at a dose of 1-3% in oxygen. The mouse was positioned on its right lateral side and the liver was exteriorized and the right lobe positioned over the viewing window. The ligature attached to the xiphoid process was retracted to pull the diaphragm away from the liver and was held in place with medical tape. The liver was covered with a piece of Kimwipe and moistened with DPBS 1X to minimize movement associated with breathing. The internal organs were moistened with DPBS 1X and covered with plastic wrap to prevent evaporative loss of moisture. The mesenteric cannula was connected to a syringe pump (Harvard Apparatus, Holliston, Massachusetts) to allow for infusion of treatment substances.

**Treatment Groups:** Mice were randomly divided into one of two treatment groups: 1. Saline, 2. ET-1. Then mice were further divided into one of six treatment sub-groups: 1. Control, 2. LPS, 3. STS, 4. PAG, 5. STS/LPS, 6. PAG/LPS. For the LPS sub-group, mice were administered an intraperitoneal injection of LPS (5mg/kg body weight) six hours prior to surgery. Previous reports from our lab demonstrate that PAG, the inhibitor of cystathionine  $\gamma$ -lyase (CSE), influences the hepatic vasculature within 30 minutes of administration. Therefore, the mice in the PAG sub-group were administered an intraperitoneal injection of PAG (50mg/kg body weight) 30 minutes prior to surgery. For mice receiving both LPS and PAG treatments, LPS was injected intraperitoneally 5.5 hours prior to PAG, which was injected 30 minutes prior to surgery.

**H<sub>2</sub>S Infusion:** The H<sub>2</sub>S donor, STS, was used to investigate the effect of H<sub>2</sub>S on the hepatic microcirculation. To determine the effects of infusion, saline was infused through the mesenteric cannula at a rate of 10 $\mu$ L/minute for a stabilization period of 5 minutes. Then freshly prepared STS (2  $\mu$ mol/kg body weight/minute) was infused for a

period of 10 minutes at the same rate. The sinusoids were visualized using a FITC filter (excitation 488nm, emission 505nm) and a 40X UPlanApo 0,85 objective lens. Images were recorded every minute for 10 minutes, with the first image marking the beginning of the experiment, just prior to the start of STS infusion into the mesenteric vein. Images were recorded using FLUOVIEW software (Shinjuku, Tokyo, Japan).

**ET-1 Infusion:** Following the stabilization period of 5 minutes, ET-1 (1 $\mu$ mol/kg body weight/minute) was infused for a period of 10 minutes. For mice receiving both STS and ET-1, The sinusoids were visualized using a FITC filter (excitation 488nm, emission 505nm) and a 40X UPlanApo, 0,85 objective lens. Images were recorded every minute for 10 minutes, with the first image marking the beginning of the experiment, just prior to the start of ET-1 infusion into the mesenteric vein. Images were recorded using FLUOVIEW software. Offline analysis was performed using FIJI software (Laboratory for Optical and Computational Instrumentation, Madison, Wisconsin).

**Offline Image Analysis:** Offline image analysis was performed using FIJI software. For sinusoidal diameter and heterogeneity of diameter data, 40X images recorded with FITC and Texas Red filters were used. Five hepatocyte areas of interest were randomly selected per image. To determine the degree of mitochondrial depolarization, areas of interest were measured for standard deviation of Rh123 green fluorescence. Since nuclei and the sinusoids are black in acquired images, these areas were not included in any analysis. To determine cell viability, the number of PI-positive cells were counted and divided by the total number of cells in each image.

**Mitochondrial Isolation:** Following euthanasia of the animal under anesthesia, the liver was removed from the abdominal cavity and washed with mitochondria isolation

buffer (10.0mM Tris/MOPS, 1.0mM EGTA/Tris, 0.2M sucrose). The liver was homogenized in additional mitochondria isolation buffer using a Teflon homogenizer and centrifuged at 800×g for 10 minutes at 4°C to pellet nuclei and any remaining whole cells. The supernatant was recentrifuged at 800×g for 10 minutes at 4°C to further purify the mitochondrial fraction. The supernatant was centrifuged at 10,000×g for 10 minutes at 4°C to pellet the mitochondria. The supernatant was saved and serves as the cytosolic fraction. Mitochondrial and cytosolic fractions were stored at -20°C for subsequent protein analysis.

**Determination of Changes in Mitochondrial Dynamics:** Protein concentration of mitochondrial and cytosolic fractions prepared from liver homogenate were determined by the BCA protein assay. Equal amounts of protein from each sample were separated on an SDS polyacrylamide gel and transferred onto a nitrocellulose membrane. After incubation with a primary antibody for the protein of interest (DRP1 for mitochondrial fission, LC3B I/II for mitophagy), the blots were probed with an appropriate secondary antibody and developed with enhanced chemiluminescence reagents. The relative amount of the target protein were normalized ( $\alpha$ -actin for cytosolic fractions and ATP5 for mitochondrial fractions) and analyzed with FIJI software.

**Protein Expression Analysis:** Relative expression of target proteins were determined by Western blot and densitometric analysis with FIJI software.

**Statistical Analysis:** All data are presented as means  $\pm$  standard error of the mean (SEM). Statistical analysis was performed using GraphPad Prism software (San Diego, California). Statistical significance was assessed by one- or two-way analysis of variance (ANOVA) with independent and repeated measures used where appropriate. Dunnett's

or Tukey's multiple comparison *post hoc* test was used when statistical differences were detected. Statistical significance was set at  $p < 0.05$ .

### 3.4 Results

**Quantifying Mitochondrial Depolarization:** To quantify the extent of mitochondrial membrane depolarization, we measured the standard deviation of Rh123 staining. In preliminary data, cultured human umbilical vein endothelial cells (HUVECs) were stained with Rh123 and prepared for intravital confocal microscopy. In control cells, green Rh123 fluorescence was punctate in virtually every cell, indicating mitochondrial polarization. Since the measured area of interest in control cells showed punctate green Rh123 staining against a black background, the standard deviation was high in numerical value (Figure 13). To induce mitochondrial membrane depolarization, HUVECs were treated with 100nM carbonyl cyanide-p-trifluoromethoxyphenylhydrazone (FCCP), a known uncoupler of mitochondrial respiration. After FCCP treatment, mitochondria began to depolarize and the green Rh123 fluorescence appeared diffuse throughout the entire cell. The standard deviation of measured area of interests for depolarized mitochondria were low in numerical value because the cells showed diffuse green Rh123 staining without a black background.

**Effect of Portal Infusion of H<sub>2</sub>S on Mitochondrial Membrane Potential:** We investigated the effect of portal infusion of the H<sub>2</sub>S donor, STS (2  $\mu$ mol/kg body weight/minute) on the mitochondria of the SECs *in vivo*. There were no significant differences in mitochondrial membrane potential among baseline or ET-1 treatment groups (Figure 14). Data were from six separate experiments.

**Effect of PAG Pretreatment on Mitochondrial Membrane Potential:** The non-competitive inhibitor of CSE, PAG, was used to examine the role of endogenous H<sub>2</sub>S on the mitochondria of the SECs during endotoxemia. PAG pretreatment showed no significant differences in mitochondrial membrane potential among baseline or ET-1 treatment groups (Figure 15). Data were from six separate experiments.

**Effect of H<sub>2</sub>S on Mitochondrial Fission:** The relationship between mitochondrial morphology and function have been shown to be involved in shaping cellular function. Therefore, we assessed the degree of mitochondrial fission by Western blot analysis for DRP1 protein expression in harvested liver tissue (Figure 16). Mitochondrial fission was expressed as the ratio of mitochondrial DRP1 protein expression to cytosolic DRP1 protein expression. There were no significant differences of mitochondrial fission among ET-1 treatment groups (Figure 17). In baseline groups, H<sub>2</sub>S infusion decreased mitochondrial fission by 3.0-fold in endotoxemia (\*\* =  $p < 0.01$ ). Data were from six separate experiments.

**Effect of PAG Pretreatment on Mitochondrial Fission:** We assessed the degree of mitochondrial fission among treatment groups (Figure 18). LPS-treated mice showed a significant decrease in the expression of mitochondrial fission protein, DRP1 (\* =  $p < 0.05$ ). Pretreatment with PAG was shown to further decrease DRP1 expression (\* =  $p < 0.05$ ).

**Effect of Portal Infusion of H<sub>2</sub>S on Mitophagy:** Dysfunctional mitochondrial fragments are removed from functional mitochondrial networks via mitochondrial fission and eliminated via mitophagy. Therefore, we furthered our investigation on the role of mitochondrial dynamics in the progression of sepsis by examining the degree of

mitophagy, quantified as the protein expression of LC3B in harvested liver tissue by Western blot analysis (Figure 19). Mitophagy was expressed as the ratio of LC3BII protein expression to LC3BI protein expression. There were no significant differences among baseline treatment groups (Figure 20). Co-infusion of STS and ET-1 in endotoxemia resulted in the upregulation of mitophagy (1.4-fold increase from control, \*\* =  $p < 0.01$ ). Data were from six separate experiments.

**Effect of PAG Pretreatment on Mitophagy:** We assessed the LC3BII/LC3BI protein expression among treatment groups (Figure 21). We found no significant differences among treatments for baseline or ET-1 groups. Data were from six separate experiments.

#### **Sex Differences in Portal Infusion of H<sub>2</sub>S on Mitochondrial Membrane**

**Potential:** We furthered our investigation on the effect of portal infusion of the H<sub>2</sub>S-releasing agent, STS, by segregating the pooled data into male and female sets to assess sex differences (Figure 22, Table 1). LPS-treated males showed a 32.6% decrease in mitochondrial membrane potential compared to control for baseline (\* =  $p < 0.05$ ) and a 43.1% decrease in mitochondrial membrane potential compared to control for ET-1 (\* =  $p < 0.05$ ). Females showed no significant differences among any treatment group. Data were from six separate experiments (three male, three female).

#### **Sex Differences in PAG Pretreatment on Mitochondrial Membrane**

**Potential:** Changes in mitochondrial membrane potential in male and female mice with the inhibitor for endogenous H<sub>2</sub>S was evaluated (Figure 23, Table 2). Though females did not show any significant differences among treatment groups for baseline or ET-1, endotoxemic males exhibited a decrease in the standard deviation of the means of Rh123

staining ( $11.8 \pm 0.9$  versus  $20.0 \pm 1.3$  for control,  $* = p < 0.05$ ). Data were from six separate experiments (three male, three female).

**Sex Differences in Portal Infusion of H<sub>2</sub>S on Mitochondrial Fission:** ET-1 data for both males and females showed no significant differences among treatment groups (Figure 24). LPS treatment did not result in a significant difference in mitochondrial fission in males but showed a 2.4-fold decrease in females, expressed as the mitoDRP1/cytoDRP1 protein expression ratio ( $* = p < 0.05$ ). Furthermore, H<sub>2</sub>S infusion during endotoxemia lead to a potentiated decrease in mitochondrial fission in females ( $** = p < 0.01$ ) but not males. Data were from six separate experiments (three male, three female).

**Sex Differences in PAG Pretreatment on Mitochondrial Fission:** There were no significant differences observed among any treatment groups for males (Figure 25). However, females pretreated with PAG showed a 2.6-fold decrease in mitoDRP1/cytoDRP1 protein expression in the baseline group ( $* = p < 0.05$ ), which was further decreased in endotoxemia (4.0-fold decrease from control,  $* = p < 0.05$ ). There were no significant differences for female ET-1 treatment groups. Data were from six separate experiments (three male, three female).

**Sex Differences in Portal Infusion of H<sub>2</sub>S on Mitophagy:** The degree of mitophagy, expressed as the LC3BII/LC3BI ratio of protein expression, was evaluated for both males and females (Figure 26). Though males did not show any significant differences among ET-1 treatment groups, the female STS/LPS group showed a significant effect on LC3BII/LC3BI protein expression (1.8-fold decrease from control,  $**** = p < 0.0001$ ). Infusion of H<sub>2</sub>S resulted in a decrease in mitophagy for males (1.2-

fold decrease from control,  $** = p < 0.01$ ) but not female baseline groups. Endotoxemic animals showed decreased mitophagy in males (1.1-fold decrease from control,  $* = p < 0.05$ ) but increased mitophagy in females (1.3-fold increase from control,  $*** = p < 0.001$ ) for baseline groups. Furthermore, endotoxemic females subjected to a 10-minute period of H<sub>2</sub>S infusion showed increased LC3BII/LC3BI protein expression (1.7-fold increase from control) while males did not for baseline groups. Data were from six separate experiments (three male, three female).

**Sex Differences in PAG Pretreatment on Mitophagy:** We demonstrated that portal infusion of H<sub>2</sub>S for a duration of 10 minutes resulted in a significant decrease in mitophagy for endotoxemic females but not males (Figure 27), with females showing a 31.6% reduction in LC3BII/LC3BI protein expression ( $** = p < 0.01$ ). While males showed no significant differences among ET-1 treatment groups, females demonstrated a significant effect with PAG pretreatment alone (41.6% increase versus control females,  $** = p < 0.01$ ) and in combination with LPS (33.3% increase versus control females,  $* = p < 0.01$ ). Compared to LPS alone, endotoxemic males pretreated with PAG showed an 85.7% increase in LC3BII/LC3BI protein expression ( $**** = p < 0.0001$ ) while endotoxemic females pretreated with PAG showed a 36.8% decrease ( $**** = p < 0.0001$ ). Data were from six separate experiments (three male, three female).

### 3.5 Discussion

The present study investigated whether hydrogen sulfide (H<sub>2</sub>S) regulates mitochondrial function and mitochondrial dynamics within the hepatic sinusoidal endothelial cells (SECs). We demonstrated that portal infusion of the H<sub>2</sub>S-releasing

agent, STS, results in reduced mitochondrial fission in endotoxemia. We show that pretreatment with the non-competitive inhibitor of cystathionine  $\gamma$ -lyase (CSE), the enzyme that produces  $H_2S$ , attenuates LPS-induced mitochondrial fission. Additionally, we report for the first time that there are sex differences in mitochondrial membrane potential and mitochondrial dynamics, namely mitochondrial fission and mitophagy, in the liver in endotoxemia.

“Gasotransmitters” are small molecules of endogenous gases with important roles in physiological functions [241]. The metabolism of these gaseous molecules is controlled enzymatically and they have the property of diffusion across biological membranes with specific targets, making them mediators of many biological processes [243]. Gasotransmitters have short half-lives but are damaging to tissue when present in excess amounts [189]. Only three gasses have been defined as gasotransmitters and include nitric oxide (NO), carbon monoxide, (CO), and  $H_2S$ . These gaseous mediators exert fine, modulatory control over a plethora of cellular functions by regulating a variety of intracellular signaling processes [136].

The third gaseous mediator and identified the latest,  $H_2S$  is a colorless, flammable gas with the characteristic smell of rotten eggs. Approximately five times more toxic than CO,  $H_2S$  is synthesized endogenously via two pathways. In the non-enzymatic pathway of  $H_2S$  production, thiols and thiol-containing molecules are reduced to yield  $H_2S$  while endogenous enzymes produce the noxious gas in the enzymatic pathway. Two pyridoxal 5-phosphate-dependent enzymes, cystathionine  $\beta$ -synthase (CBS), primarily expressed in the brain, and CSE, expressed in the peripheral tissues are responsible for synthesizing  $H_2S$  using L-cysteine as a substrate. CBS catalyzes the transfer from serine

to homocysteine to produce cystathionine while CSE converts cystathionine to cysteine. Both CBS and CSE catalyze a  $\beta$ -disulfide elimination reaction, resulting in the production of pyruvate,  $\text{NH}_4^+$ , and thiocysteine. Thiocysteine then reacts with cysteine or other thiols to produce  $\text{H}_2\text{S}$ . Moreover, cysteine aminotransferase catalyzes the reaction of L-cysteine with  $\alpha$ -ketoglutarate to produce 3-mercaptopyruvate, from which sulfur is removed by 3-mercaptopyruvate sulfurtransferase (3-MST), producing  $\text{H}_2\text{S}$ . While CBS and CSE are cytosolic, 3-MST is localized in both the mitochondria and in the cytosol [136].

$\text{H}_2\text{S}$  is a powerful antioxidant [102] and has a role in the regulation of energy metabolism. Lower concentrations of  $\text{H}_2\text{S}$  donate electrons to the mitochondrial respiratory chain and can function as an inorganic source of energy in mammalian cells [26]. However, specifically in the mitochondria,  $\text{H}_2\text{S}$  dose-response follows a bell-shaped curve where high concentration of  $\text{H}_2\text{S}$  results in cytotoxicity and suppression of mitochondrial respiration via inhibition of complex IV in the electron transport chain (ETC) [229, 261].

Using confocal intravital microscopy, we visualized and quantified changes in mitochondrial membrane potential using the fluorophore, Rhodamine 123 (Rh123). Rh123 is a cationic fluorescent stain that partitions itself in the most electronegative parts of the cell, the mitochondria. Green Rh123 staining of healthy, polarized mitochondria appears punctate and the measured standard deviation of the area of interest is high in numerical value. When mitochondria lose their electronegativity, becoming depolarized, Rh123 no longer sequesters in the mitochondria and diffuses into the cytosol. The

resulting image is diffuse green stain throughout the entire cell and the measured standard deviation of the area of interest is low in numerical value.

In the hepatocyte chords of the sinusoid, we did not observe any significant changes in mitochondrial membrane potential with infusion of H<sub>2</sub>S among any of the treatment groups when male and female data were pooled together. However, when data was analyzed using sex as a variable, we observed a reduction in the standard deviation of Rh123 staining for LPS-treated males, indicating mitochondrial membrane depolarization, but not females. The degree of mitochondrial depolarization is increased following stimulation with LPS in murine macrophages-like cells [55]. Mitochondrial structural damage and dysfunction are recognized as important factors in the progression of sepsis and are associated with the severity of organ dysfunction and disease outcome [12]. Patients with severe sepsis have been shown to have mitochondrial functional deficiencies, including decreased ATP production and complex I activity, which is linked to sepsis outcomes [28]. Increased levels of mitochondrial reactive oxygen species (ROS) during sepsis can lead to mitochondrial depolarization, inhibit oxidative phosphorylation and ATP production, which tips the balance of energy metabolism and tissue demand. This can result in systemic inflammation and multiple organ failure ensues [8, 72]. Furthermore, excessive ROS can impair mitochondrial morphology and inhibit mitochondrial biogenesis [209, 234, 262].

We further investigated the role of exogenous H<sub>2</sub>S on mitochondrial dynamics, namely mitochondrial fission and mitophagy. Mitochondrial fission is essential for the transfer of mitochondria to daughter cells during mitosis and the detachment of damaged DNA, proteins, and metabolites of the mitochondria. As the main regulator of

mitochondrial fission, dynamin-related protein 1 (DRP1), is a cytosolic GTPase and is recruited to the outer mitochondrial membrane. At the site of mitochondrial fission, it forms a multimeric ring-like structure that constricts and cleaves mitochondria in a GTPase-dependent manner [115]. Following intravital confocal microscopy, animals were euthanized and tissue homogenates were prepared from harvested livers. Because DRP1 remains in the cytosol until recruitment to the mitochondria, liver homogenates were subjected to differential centrifugation to yield mitochondrial and cytosolic subcellular fractions for Western blot analysis. We observed a downregulation of DRP1 recruitment in mitochondria from animals infused with exogenous H<sub>2</sub>S in endotoxemia. Inhibition of endogenously produced H<sub>2</sub>S also resulted in a reduction of mitochondrial fission in endotoxemia. Furthermore, when data were divided according to sex, males showed no significant differences among any treatment for baseline or ET-1 groups. In contrast, females showed decreased mitochondrial fission following a 10-minute period of H<sub>2</sub>S infusion alone and with LPS treatment. We also assessed the effect of PAG pretreatment on changes in hepatic mitochondrial dynamics. PAG pretreatment had no significant effect on mitochondrial fission for any treatment for males. However, pretreatment with PAG reduced the expression of mitochondrial fission protein, DRP1, in mitochondrial fractions for females when administered alone and in endotoxemia.

Interestingly, portal infusion of ET-1 had no significant effect, regardless of sex. It has been suggested that ET-1 results in the upregulation of Rho-associated protein kinase 1 (ROCK1) expression, which increases LIMK2 expression and impairs DRP1-mediated mitochondrial fission in neuronal death [118]. However, it is unlikely that the

time allowed for ET-1 infusion would be enough for the upregulation of LIMK2. Further work will need to be done to elucidate if this is the case for liver tissue.

Mitochondria that are damaged and dysfunctional are deleterious to the cell. Therefore, degradation of mitochondria is crucial to the overall livelihood of the cell. Selective mitochondrial degradation is executed by mitophagy, which is regulated by several proteins, including PTEN induced putative kinase 1 (PINK1), Parkin, and light chain 3B (LC3B). Parkin is a ubiquitin ligase that functions downstream of PINK1 in a pathway capable of detecting and eliminating dysfunctional mitochondria [183]. When mitochondria become damaged, PINK1 accumulation on the outer mitochondrial membrane leads to phosphorylation of polyubiquitin chains and recruitment of Parkin from the cytosol. Activation of Parkin induces ubiquitination of additional mitochondrial outer membrane proteins, yielding more ubiquitin substrate from PINK1 and creating a potent feedback amplification loop. Phosphoubiquitin chains on the outer mitochondrial membrane recruit autophagy receptors, which recruit autophagy machinery, including LC3B, to induce mitophagy [133]. In this study, we estimated mitophagy by determining the protein expression ratio of active LC3B (LC3BII) to inactive LC3B (LC3BI). We demonstrated by Western blot analysis that co-infusion of H<sub>2</sub>S and ET-1 for a 10-minute period results in an upregulation of LC3BII in endotoxemia. Furthermore, we observed sex differences upon dividing our pooled data according to sex. Exogenous H<sub>2</sub>S administration via portal infusion resulted in a downregulation of LC3BII in males but not females. Males also showed a reduction of activated LC3B in endotoxemia compared to female data, which showed an increase. Furthermore, H<sub>2</sub>S infusion in endotoxemia resulted in increased mitophagy for both baseline and ET-1 treatment groups in females

but not males. We also assessed the effect of inhibiting endogenous H<sub>2</sub>S on mitophagy in endotoxemia. PAG treatment alone resulted in a reduction in the protein expression of activated LC3B in both males and females. Females, but not males, treated with LPS for 6 hours showed an increase in selective mitophagy, suggesting a protective effect against cell death by release of cytochrome *c* from damaged mitochondria. When pretreated with PAG, males showed an increase in selective mitochondrial degradation while females showed a decrease. In addition, we observed no significant differences among the treatments when combined with ET-1 infusion for males. This is in contrast to females, which show an upregulation of activated LC3B for PAG alone and in endotoxemia.

Mitochondrial dysfunction and subsequent disruption in energy metabolism are linked with multiple organ failure and increased mortality in septic patients [67]. Mitochondrial fission and fusion work in concert to maintain the shape, size, and number of mitochondria and their physiological function [35, 223]. This dynamic relationship is thought to function as a rescue mechanism with fusion allowing damaged mitochondria to recover functionally by coupling to healthy mitochondria while fission induces fractionation of the organelle when the damage is too excessive to rescue the cell [35, 174, 223]. The imbalance of mitochondrial fusion and fission has been reported to potentiate the progression of sepsis and that inhibition of DRP1 prevented mitochondrial respiration dysfunction and apoptosis in hepatocytes [80]. In males, we observed mitochondrial membrane depolarization in endotoxemia with no significant changes in mitochondrial fission or mitophagy. Female data showed no mitochondrial membrane depolarization in endotoxemia with decreased mitochondrial fission (though not significant) and decreased mitophagy. Regarding mitochondrial function, it appears as

though female mice exhibited responses to endotoxin insult that resulted in better outcomes. The impact of sex on sepsis is highly controversial. A survival advantage for females [254] has been reported in animal studies but is contradictory to human clinical data on sepsis-related mortality [46, 60, 97, 156]. An epidemiological study demonstrated that males are more likely to develop sepsis than females but females have a higher mortality than males [203] while another reported a lower risk of mortality for females [3]. A meta analysis was conducted on publications that investigated sex differences in relation to sepsis-related incidence and sepsis-related mortality [3] indicating that the current compilation of clinical sepsis studies evaluating differences among the sexes are inconclusive and complex.

The results of the present study provide evidence for sex differences in mitochondrial dysfunction and dynamics in endotoxemia. However, the impact that sex has on prognosis of sepsis remains a matter of debate and additional clinical studies will need to be completed to further elucidate this topic.

### 3.6 Figures

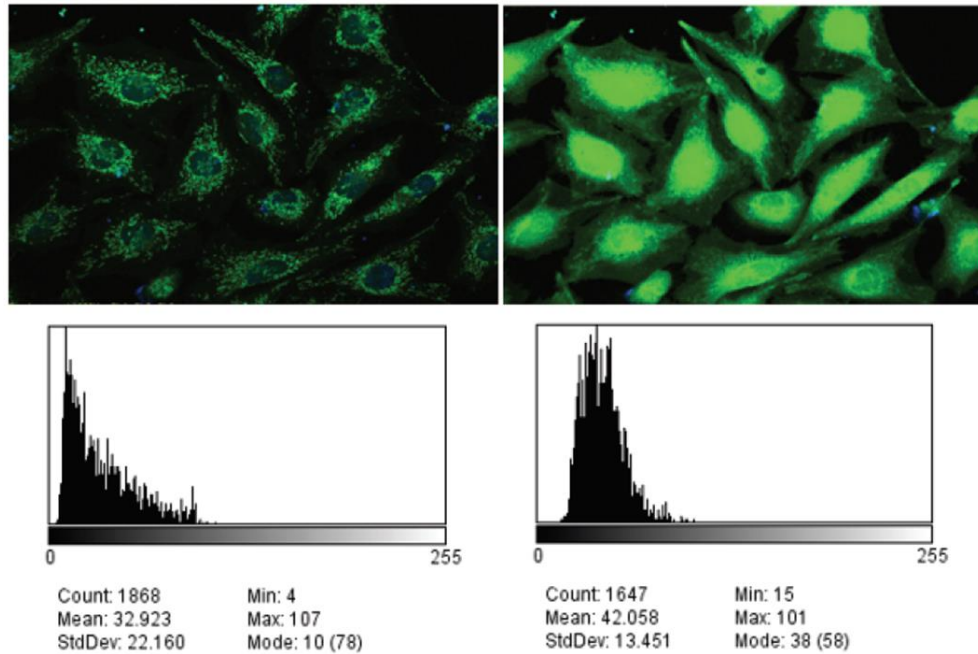


Figure 13: Quantification of Rh123 staining. Cultured HUVECs were imaged before (left) and after stimulation with the uncoupling agent, FCCP (right). To quantify the extent of mitochondrial membrane depolarization, the standard deviation of Rh123 staining was measured for each image. Cells show punctate green Rh123 prior to stimulation with FCCP, indicating mitochondria polarization. Following FCCP treatment, mitochondria depolarize and diffuse green Rh123 staining results. Standard deviation measurement was higher in polarized mitochondria than in depolarized mitochondria.

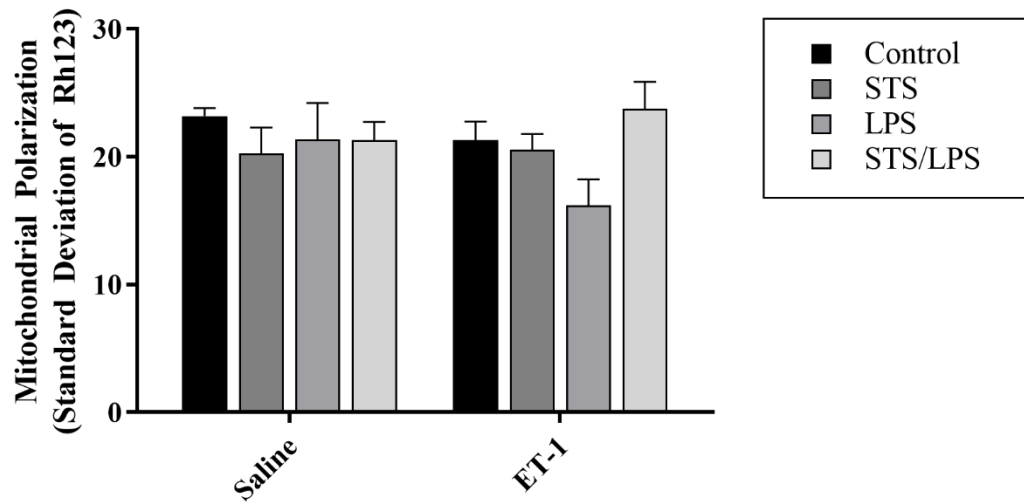


Figure 14: Effect of STS on mitochondrial polarization. Images of the hepatic sinusoids were recorded before, during, and 10 minutes following infusion of H<sub>2</sub>S donor, STS. Infusion of STS had no effect on mitochondrial polarization, quantified as the standard deviation of Rh123 staining, in endotoxemia for pooled sexes. Data are presented as the means  $\pm$  SEM from six separate experiments.

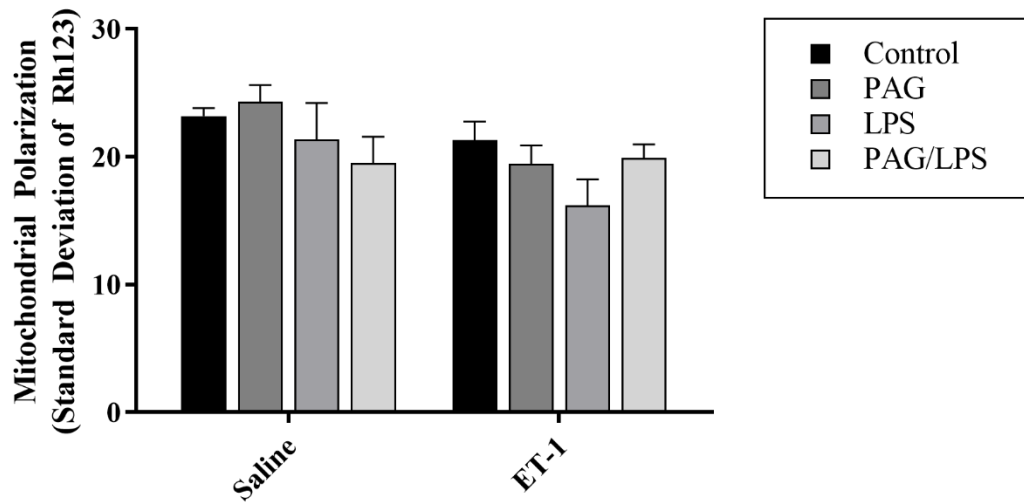


Figure 15: Effect of PAG on mitochondrial polarization during infusion of ET-1 during endotoxemia. Mice were pretreated with PAG for 30 minutes with or without LPS treatment for 6 hours. Images of the hepatic sinusoids were recorded before, during, and 10 minutes following infusion of ET-1. PAG had no effect on mitochondrial polarization, quantified as the standard deviation of Rh123 staining, in endotoxemia for pooled sexes. Data are presented as the means  $\pm$  SEM from six separate experiments.

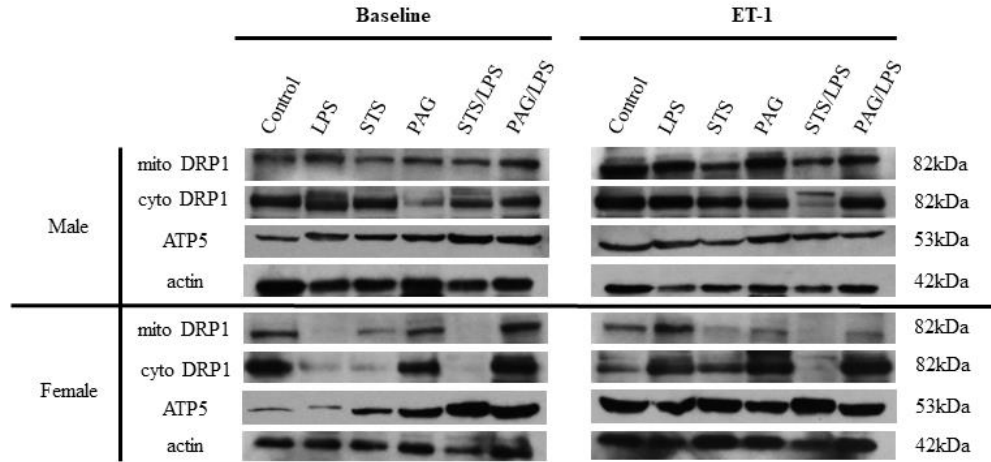


Figure 16: DRP1 Western blot analysis on mitochondrial and cytosolic fractions from liver homogenates. Following intravital confocal microscopy experiments, liver tissue was homogenized and subjected to differential centrifugation to obtain mitochondrial and cytosolic fractions. Total protein was determined by BCA. DRP1 protein expression was determined by Western blot analysis on mitochondrial and cytosolic fractions. Densities of mito DRP1 and cyto DRP1 were normalized to ATP5 and actin, respectively. Blots presented are representative of six separate experiments (3 male, 3 female).

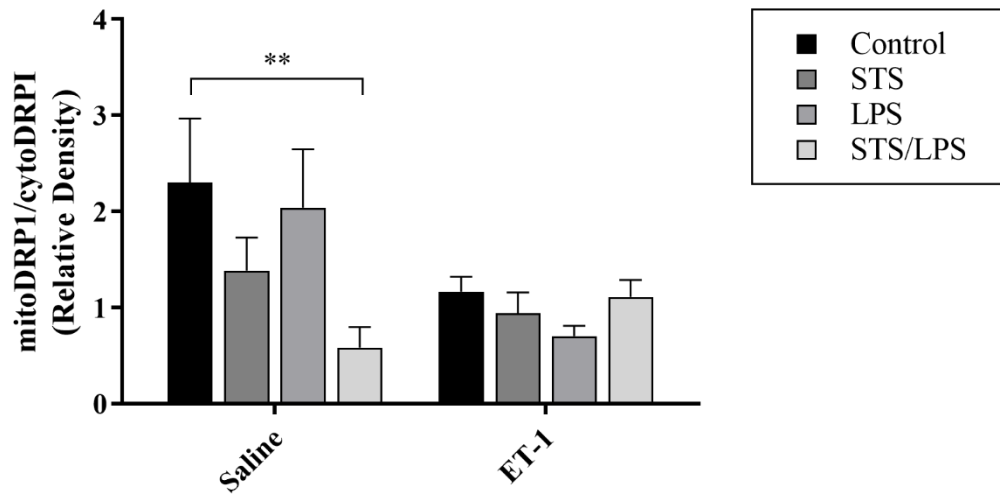


Figure 17: Effect of STS on mitochondrial fission. Following intravital confocal microscopy experiments, liver tissue was homogenized and subjected to differential centrifugation to obtain mitochondrial and cytosolic fractions. DRP1 protein expression was determined by Western blot analysis and mitochondrial fission was expressed as the ratio of mitochondrial DRP1 to cytosolic DRP1. Infusion of STS resulted in a significant decrease of mitochondrial fission in endotoxemia for pooled sexes. Data are presented as the means  $\pm$  SEM from six separate experiments. Statistical analysis was performed using two-way ANOVA with Sidak's multiple comparison *post hoc* test. \*\* =  $p < 0.01$ .

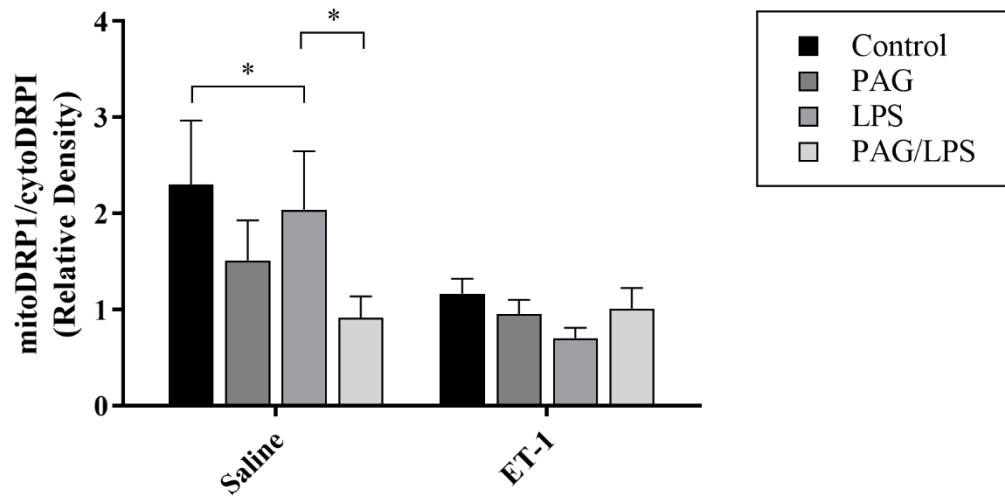


Figure 18: Effect of PAG on mitochondrial fission during infusion of ET-1 during endotoxemia. Mice were pretreated with PAG for 30 minutes with or without LPS treatment for 6 hours. Following intravital confocal microscopy experiments, liver tissue was homogenized and subjected to differential centrifugation to obtain mitochondrial and cytosolic fractions. DRP1 protein expression was determined by Western blot analysis and mitochondrial fission was expressed as the ratio of mitochondrial DRP1 to cytosolic DRP1. Endotoxemia caused a decrease in mitochondrial fission, which was potentiated with PAG pretreatment for pooled sexes. Data are presented as the means  $\pm$  SEM from six separate experiments. Statistical analysis was performed using two-way ANOVA with Sidak's multiple comparison *post hoc* test. \* =  $p < 0.05$ .

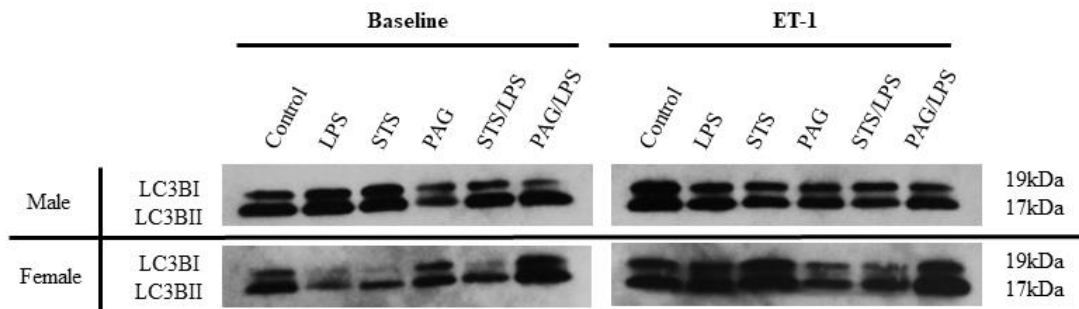


Figure 19: LC3B Western blot analysis from liver homogenates. Following intravital confocal microscopy experiments, liver tissue harvested and homogenized. Total protein was determined by BCA. LC3BII and LC3BI protein expression was determined by Western blot analysis. Blots presented are representative of six separate experiments (3 male, 3 female).

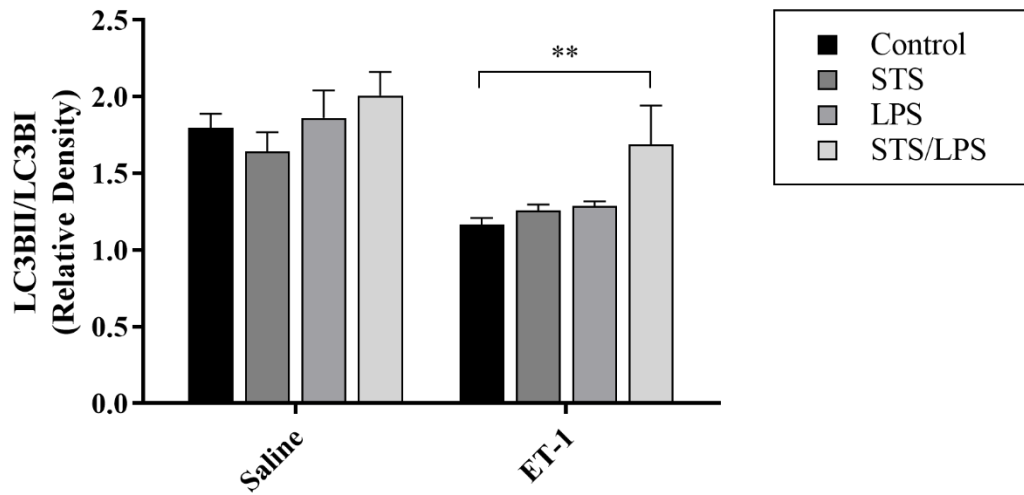


Figure 20: Effect of STS on mitophagy. Following intravital confocal microscopy experiments, liver tissue was homogenized. LC3BII and LC3BI protein expression was determined by Western blot analysis on mitophagy was expressed as the ratio of LC3BII to LC3BI. Co-infusion of STS and ET-1 resulted in a significant increase of mitophagy in endotoxemia for pooled sexes. Data are presented as the means  $\pm$  SEM from six separate experiments. Statistical analysis was performed using two-way ANOVA with Dunnett's *post hoc* test. \*\* =  $p < 0.01$ .

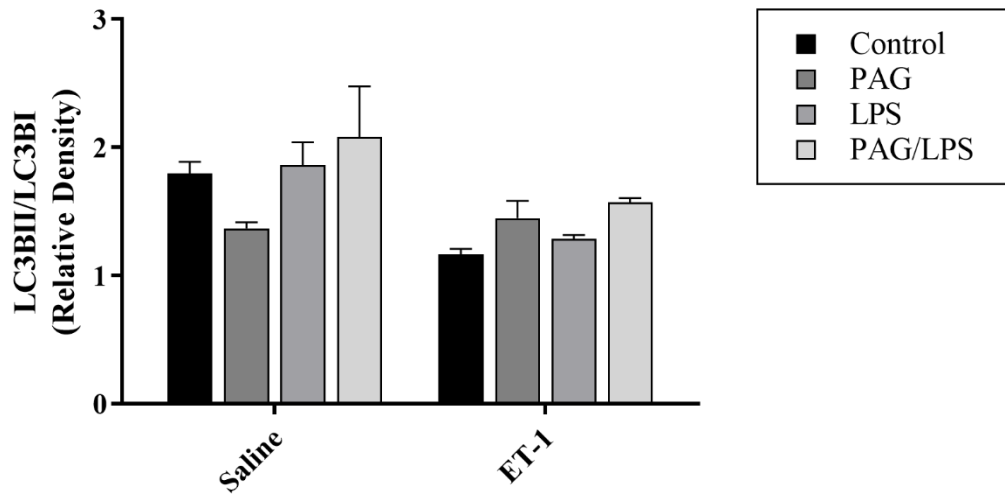


Figure 21: Effect of PAG on mitophagy during infusion of ET-1 during endotoxemia. Mice were pretreated with PAG for 30 minutes with or without LPS treatment for 6 hours. Following intravital confocal microscopy experiments, liver tissue was homogenized. LC3BII and LC3BI protein expression was determined by Western blot analysis on mitophagy was expressed as the ratio of LC3BII to LC3BI. PAG pretreatment had no effect on mitophagy in endotoxemia. Data are presented as the means  $\pm$  SEM from six separate experiments.

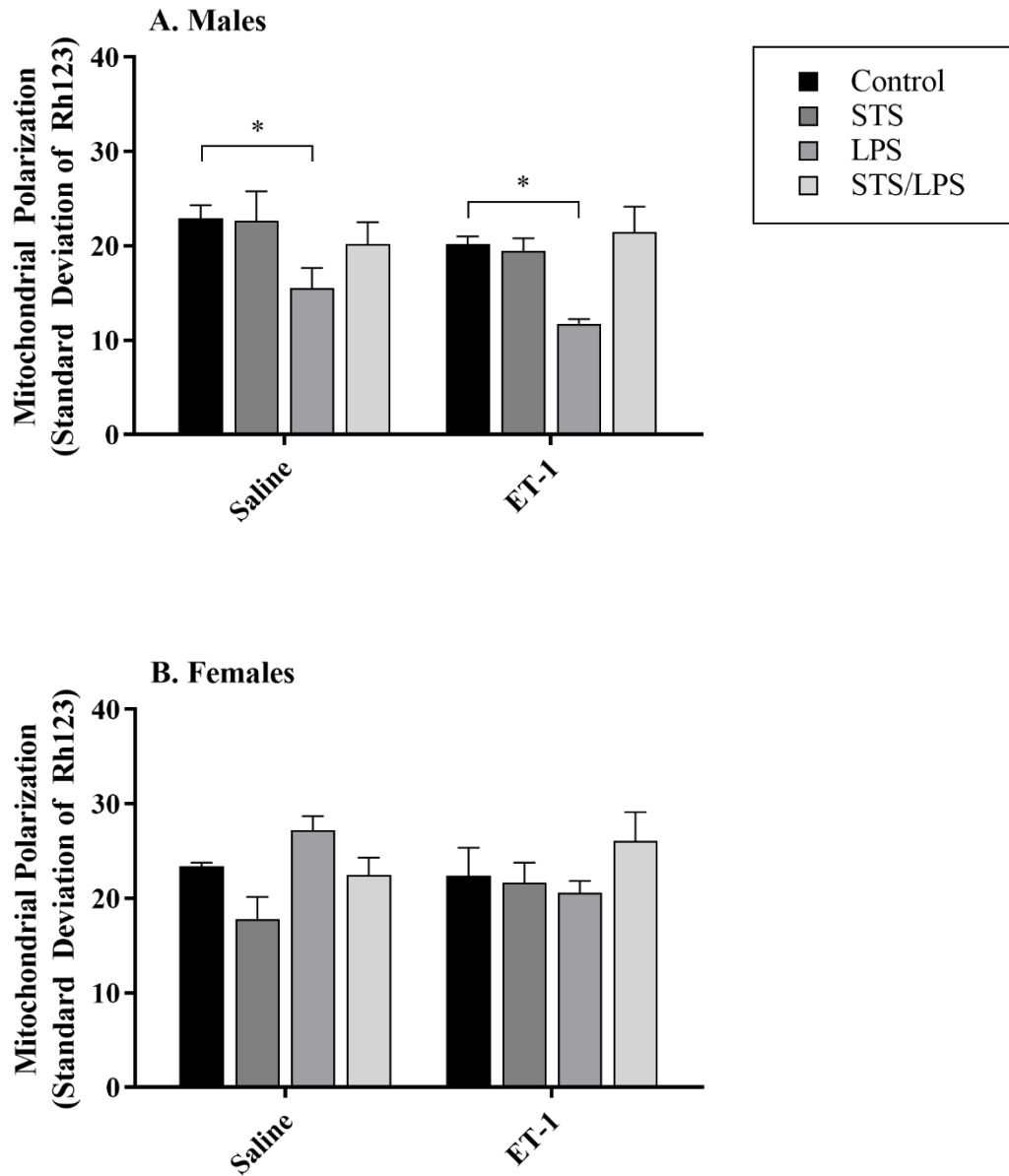


Figure 22: Effect of STS on mitochondrial polarization in males and females. Images of the hepatic sinusoids were recorded before, during, and 10 minutes following infusion of H<sub>2</sub>S donor, STS. Data are presented as the means  $\pm$  SEM from three separate experiments. Statistical analysis was performed using two-way ANOVA with Dunnett's *post hoc* test. \* =  $p < 0.05$ .

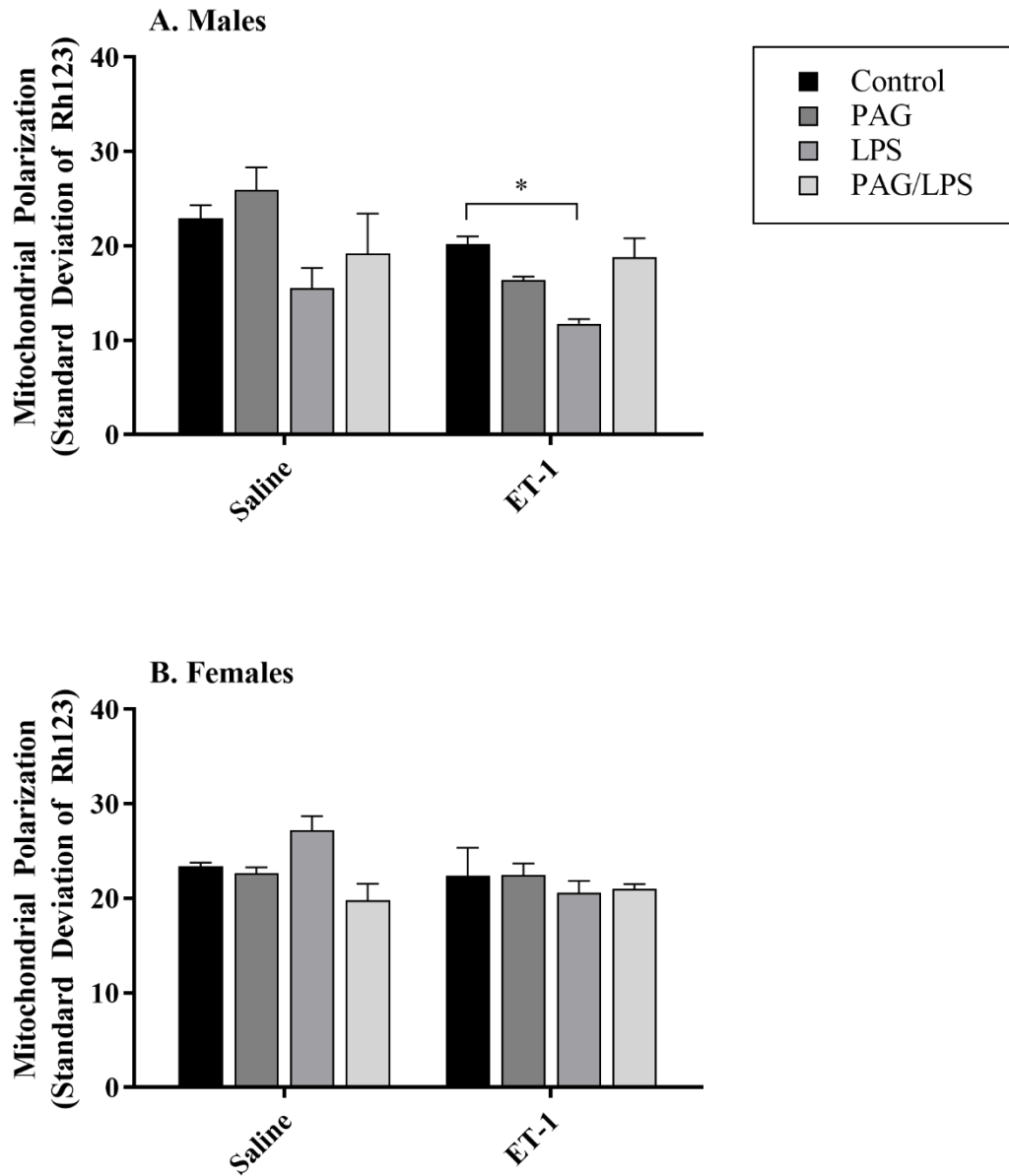


Figure 23: Effect of PAG on mitochondrial polarization during infusion of ET-1 during endotoxemia in males and females. Mice were pretreated with PAG for 30 minutes with or without LPS treatment for 6 hours. Images of the hepatic sinusoids were recorded before, during, and 10 minutes following infusion of ET-1. Data are presented as the means  $\pm$  SEM from three separate experiments. Statistical analysis was performed using two-way ANOVA with Tukey's *post hoc* test. \* =  $p < 0.05$ .

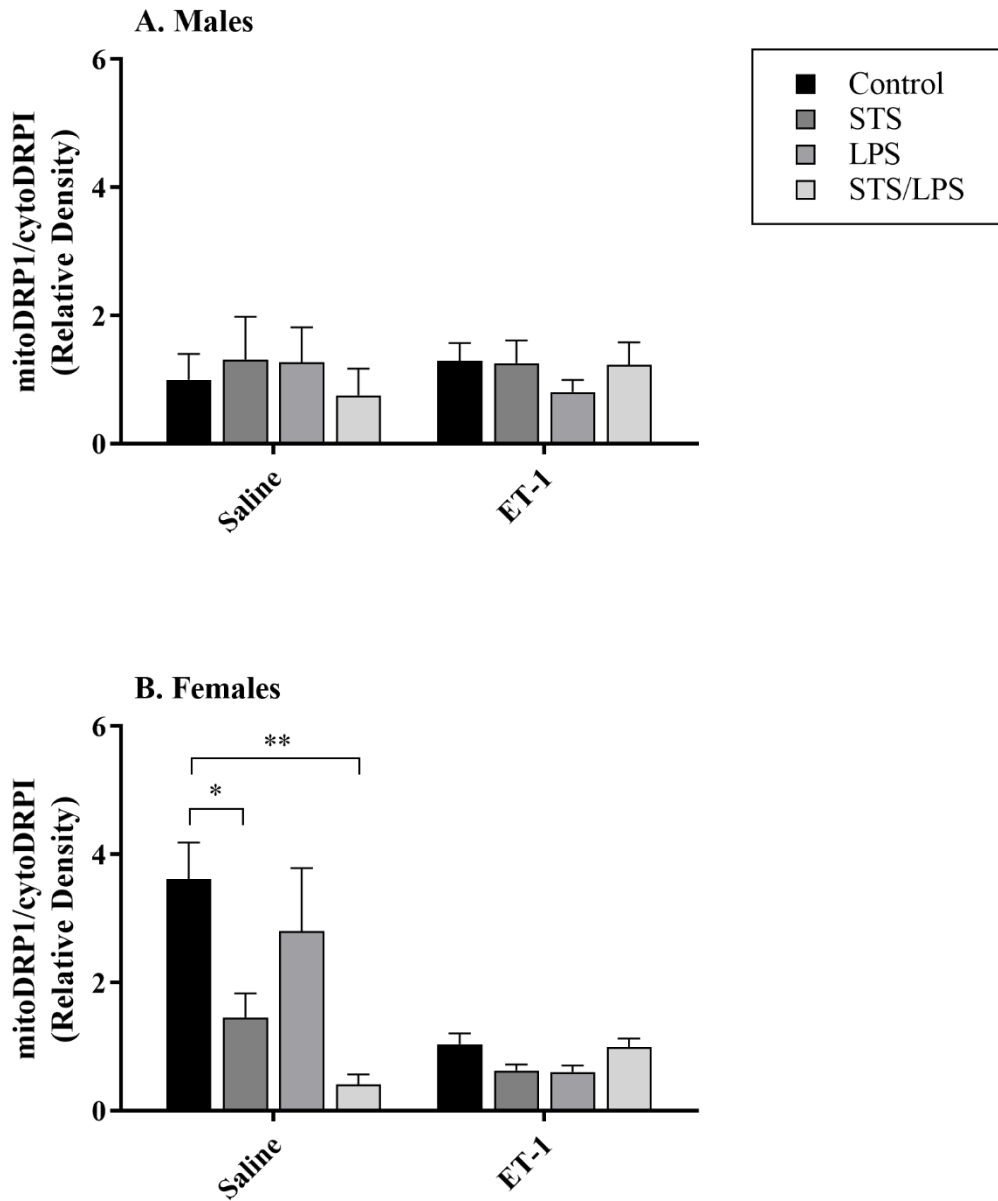


Figure 24: Effect of STS on mitochondrial fission in males and females. Following intravital confocal microscopy experiments, liver tissue was homogenized and subjected to differential centrifugation to obtain mitochondrial and cytosolic fractions. DRP1 protein expression was determined by Western blot analysis and mitochondrial fission was expressed as the ratio of mitochondrial DRP1 to cytosolic DRP1. Data are presented as the means  $\pm$  SEM from three separate experiments. Statistical analysis was performed using two-way ANOVA with Dunnett's *post hoc* test. \* =  $p < 0.05$ , \*\* =  $p < 0.01$ .

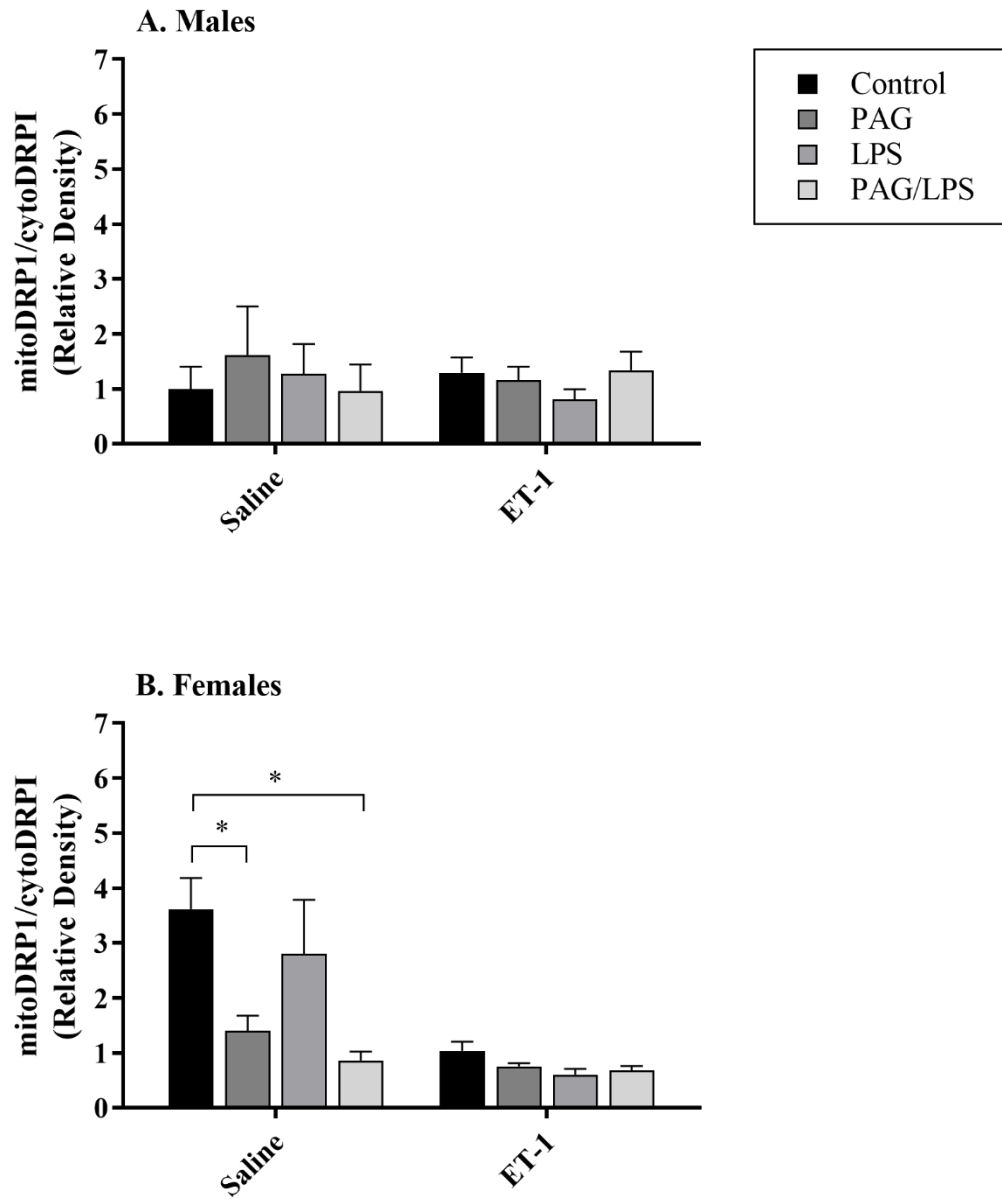


Figure 25: Effect of PAG on mitochondrial fission during infusion of ET-1 during endotoxemia in males and females. Mice were pretreated with PAG for 30 minutes with or without LPS treatment for 6 hours. Following intravital confocal microscopy experiments, liver tissue was homogenized and subjected to differential centrifugation to obtain mitochondrial and cytosolic fractions. DRP1 protein expression was determined by Western blot analysis and mitochondrial fission was expressed as the ratio of mitochondrial DRP1 to cytosolic DRP1. Data are presented as the means  $\pm$  SEM from three separate experiments. Statistical analysis was performed using two-way ANOVA with Tukey's *post hoc* test. \* =  $p < 0.05$ .

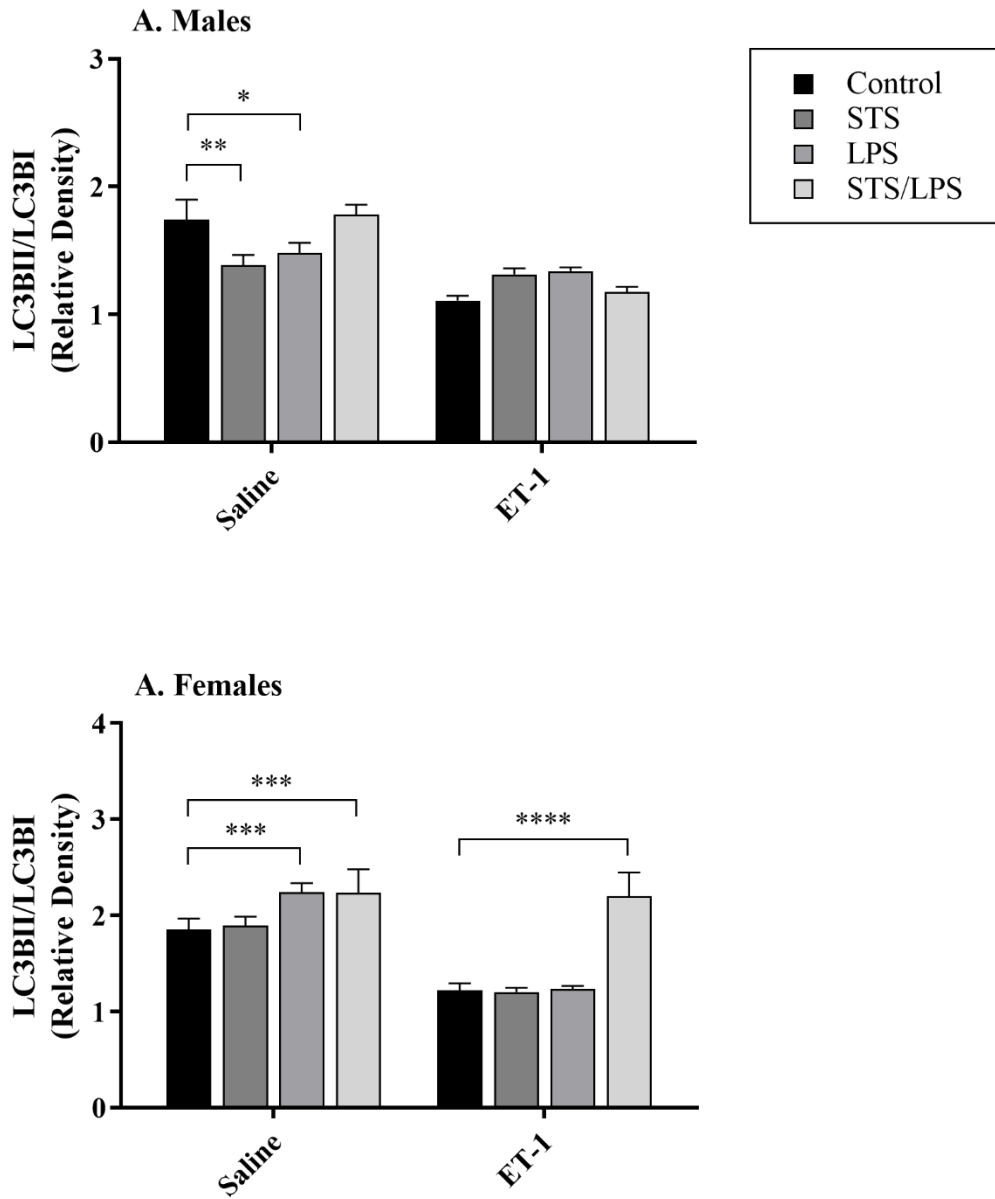


Figure 26: Effect of STS on mitophagy in males and females. Following intravital confocal microscopy experiments, liver tissue was homogenized. LC3BII and LC3BI protein expression was determined by Western blot analysis on mitophagy was expressed as the ratio of LC3BII to LC3BI. Both STS infusion and LPS treatment resulted in decreased mitophagy in saline but not ET-1. Data are presented as the means  $\pm$  SEM from three separate experiments. Statistical analysis was performed using two-way ANOVA with Dunnett's *post hoc* test. \* =  $p < 0.05$ , \*\* =  $p < 0.01$ , \*\*\* =  $p < 0.001$ , \*\*\*\* =  $p < 0.0001$ .

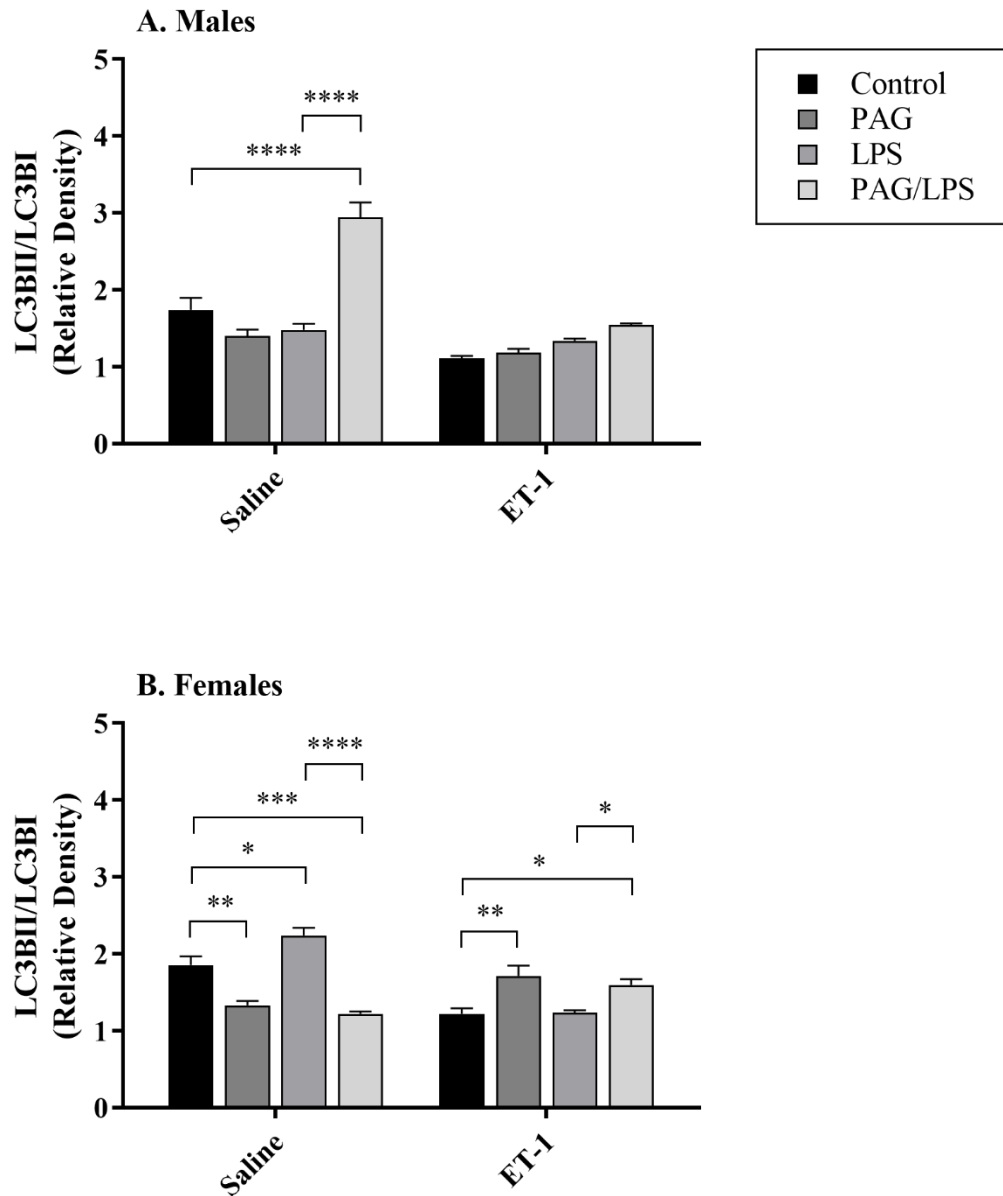


Figure 27: Effect of PAG on mitophagy during infusion of ET-1 during endotoxemia in males and females. Mice were pretreated with PAG for 30 minutes with or without LPS treatment for 6 hours. Following intravital confocal microscopy experiments, liver tissue was homogenized. LC3BII and LC3BI protein expression was determined by Western blot analysis and mitophagy was expressed as the ratio of LC3BII to LC3BI. Data are presented as the means  $\pm$  SEM from three separate experiments. Statistical analysis was performed using two-way ANOVA with Tukey's *post hoc* test. \* =  $p < 0.05$ , \*\*\*\* =  $p < 0.0001$ .

Table 1: Summary of sex-related STS effects on mitochondrial polarization and markers for mitochondrial fission and mitophagy during infusion of ET-1 during endotoxemia.

Treatment		Baseline		ET-1	
		Males	Females	Males	Females
STS	Mito. Polarization (Std Dev Rh123)	=	=	=	=
	mito-DRP1/cyto-DRP1 (Relative Density)	=	↓	=	=
	LC3BII/LC3BI (Relative Density)	↓↓	=	=	=
LPS	Mito. Polarization (Std Dev Rh123)	↓	=	↓	=
	mito-DRP1/cyto-DRP1 (Relative Density)	=	=	=	=
	LC3BII/LC3BI (Relative Density)	↓	↑↑↑	=	=
STS/LPS	Mito. Polarization (Std Dev Rh123)	=	=	=	=
	mito-DRP1/cyto-DRP1 (Relative Density)	=	↓↓	=	=
	LC3BII/LC3BI (Relative Density)	=	↑↑↑	=	↑↑↑↑

Table 2: Summary of sex-related PAG effects on mitochondrial polarization and markers for mitochondrial fission and mitophagy during infusion of ET-1 during endotoxemia.

Treatment		Baseline		ET-1	
		Males	Females	Males	Females
PAG	Mito. Polarization (Std Dev Rh123)	=	=	=	=
	mito-DRP1/cyto-DRP1 (Relative Density)	=	↓	=	=
	LC3BII/LC3BI (Relative Density)	=	↓↓	=	↑↑
LPS	Mito. Polarization (Std Dev Rh123)	=	=	↓	=
	mito-DRP1/cyto-DRP1 (Relative Density)	=	=	=	=
	LC3BII/LC3BI (Relative Density)	=	↑	=	=
PAG/LPS	Mito. Polarization (Std Dev Rh123)	=	=	=	=
	mito-DRP1/cyto-DRP1 (Relative Density)	=	↓	=	=
	LC3BII/LC3BI (Relative Density)	↑↑↑↑	↓↓↓	=	↑

## CHAPTER 4: K<sub>ATP</sub> CHANNEL ACTIVATION BY EXOGENOUS HYDROGEN SULFIDE AND OXIDATIVE STRESS *IN VITRO*.

### 4.1 Abstract

It is well accepted that the microcirculation is hypersensitized to the constrictor effect of endothelin-1 (ET-1) following endotoxin insult. Decreased activation of endothelial nitric oxide synthase (eNOS) by ET-1 may be, at least in part, responsible for the hyperconstrictive response observed. Also, eNOS can be uncoupled to produce superoxide (O<sub>2</sub><sup>-</sup>) as a result, leading to further hyperconstriction and tissue injury due to ET-1 in endotoxemia. In this present study, we first determined the effect of lipopolysaccharide (LPS) on reactive oxygen species (ROS) production and whether ET-1 altered this response *in vitro*. The gaseous mediator, hydrogen sulfide (H<sub>2</sub>S) is an important regulator of the cardiovascular system and has been shown to exhibit cardioprotective effects against hypoxic injury through the activation of mitochondrial potassium (mito-K<sub>ATP</sub>) channels, reduction of oxidative stress, and dampening of inflammatory responses. The activation of mito-K<sub>ATP</sub> channels are suggested to be crucial in the cardioprotective effects observed with H<sub>2</sub>S treatment in hypoxic studies. Therefore, we furthered our studies *in vitro* and investigated the role H<sub>2</sub>S had on ROS formation and whether inhibiting mitochondria-specific K<sub>ATP</sub> channels altered this response. We observed a biphasic H<sub>2</sub>S dose-response curve for ROS production in response to mito-K<sub>ATP</sub> channel inhibition, indicating that exogenously administered H<sub>2</sub>S exhibits a protective effect against oxidative stress *in vitro*.

## 4.2 Introduction

Bacterial endotoxemia elicits an inflammatory response like that observed in the progression of sepsis and includes alterations in vascular regulation and cell injury. Endotoxic stress, in the form of LPS administration, precipitates changes in vascular reactivity to mediators, such as ET-1. ET-1 is a potent peptide constrictor whose production is increased in inflammatory and oxidative stress [247]. ET-1 elicits its actions on the microcirculation through the binding of its two receptor subtypes. ET<sub>A</sub> receptor subtype is expressed on hepatic stellate cells (HSCs) and vascular smooth muscles cells (VSMCs) and always mediates constriction while ET<sub>B</sub> receptor subtype, expressed on hepatic sinusoidal endothelial cells (HSECs) and is coupled to eNOS activation to mediate dilation [16, 250, 251, 259].

Recent work from our lab has demonstrated that endotoxemia uncouples ET-1 binding to ET<sub>B</sub> receptors on HSECs from eNOS activation, preventing compensatory vasodilation. The production of H<sub>2</sub>S and increased binding of eNOS to caveolin-1 is associated with the decrease in eNOS activation [163]. Since eNOS activation is decreased, nitric oxide (NO) production would also be decreased as a result. NO production by eNOS requires activation by calcium-calmodulin, phosphorylation, and availability of substrate and cofactor, L-arginine and tetrahydrobiopterin [7, 47, 116]. When substrate and cofactor supplies are not adequate, the superoxide formed from the donation of an electron from nicotinamide adenine dinucleotide phosphate (NADPH) to molecular oxygen is released instead of combined with L-arginine to produce NO and L-citrulline. Moreover, superoxide may combine with available NO to form peroxynitrite [222]. Therefore, the decreasing NO bioavailability and uncoupling of ET-1 binding to

its receptors from eNOS activation are contributing factors to vascular dysfunction via the production of ROS and reactive nitrogen species (RNS).

Studies on pulmonary hypertension have demonstrated that ET-1 can activate NADPH oxidase, leading to increased superoxide production that can subsequently react with NO to form RNS but it was not known whether ET-1 contributes to ROS production in endotoxemia. Therefore, we tested whether ROS was produced in endotoxemia and if ET-1 stimulation altered the effect of LPS on ROS production in cultured human microvascular endothelial cells (HMECs).

Despite decades of investigation, sepsis remains as the leading cause of death in the intensive care units (ICUs) [10] with the pathogenesis of the disease still obscure. In addition to hyperinflammation, micro- and microcirculatory failure, and mitochondrial dysfunction, sepsis is also characterized by excessive production of oxidants. Redox reactions are fundamental for a plethora of biochemical mechanisms necessary for physiological cell function and oxidants and antioxidants play important roles.

Antioxidants are substances that donate electrons whereas oxidants are substances that accept electrons [119]. Free radicals are important participants in host defense against bacterial infections [244], the regulation of vascular tone, cell adhesion, and oxygen sensing [58]. Superoxide, hydrogen peroxide, and hydroxyl radicals are ROS involved in the pathogenesis of sepsis. RNS in sepsis include the free radical, NO, and peroxynitrite. Both ROS and RNS are important for host defense and bacterial clearance. LPS-induced NOS expression leads to increased NO production by L-arginine. Increased NO levels inhibits cytochrome *c* oxidase (complex IV) and generates hydrogen peroxide in the mitochondria [185]. Moreover, NADPH oxidase and the electron transport chain (ETC)

in the mitochondria are sources for additional intracellular superoxide levels [100, 238]. To maintain cellular homeostasis, oxidant scavengers make up an antioxidant defense system. Under normal physiological conditions, there is a balance between oxidant production and their removal by oxidant scavengers. Excess oxidant concentration creates an imbalance to antioxidant defense and results in oxidative stress and tissue injury. Studies have demonstrated that survivors of sepsis had greater antioxidant potential than non-survivors [48] and antioxidant deficiency correlates with mortality [110].

Mitochondria have important roles in redox regulation as they are both sources and targets of oxidants. Mitochondria are also at the cornerstone of programmed cell death and cell death is involved in the pathogenesis of sepsis. Damage to the mitochondria by ROS can release cytochrome *c* and cause mitochondrial membrane depolarization. The release of the mitochondrial ETC protein, cytochrome *c*, into the cytosol leads to the activation of caspases and the formation of the apoptosome, terminating in DNA fragmentation and cytolysis [141]. In contrast, activation of the  $K_{ATP}$  channels in the mitochondria has been shown to prevent lethal ischemic injury *in vivo*, suggesting that these channels play a key role in cardioprotective effects against hypoxic injury. The precise mechanisms by which mito- $K_{ATP}$  channels protects against apoptosis still require further investigation. However, the activation and opening of the mito- $K_{ATP}$  channels may act quite early in the apoptotic cascade by inhibiting cytochrome *c* release and mitochondrial membrane depolarization. These are the earliest alterations in the cascade and the two events are closely associated [79]. It has been demonstrated that mito- $K_{ATP}$  channel activation with diazoxide inhibits activation of mitochondrial

apoptotic pathways induced by oxidative stress by delaying mitochondrial membrane depolarization in a dose-dependent manner [4]. In addition, it was also shown that the mito-K<sub>ATP</sub> channel inhibitor, 5-hydroxydecanoate (5-HD) abolishes the antiapoptotic effect of diazoxide, suggesting that mito-K<sub>ATP</sub> channel activation protects against apoptosis [4].

Dysregulation of cell death pathways is involved in the pathogenesis of sepsis and is an important contributor to multiple organ failure. It was reported that plasma sulfide levels in septic patients are very elevated and could be a predictor of intensive care unit (ICU) survival [120]. High plasma sulfide levels were shown to be correlated with blood pressure and cardiac function and patients with higher plasma sulfide during ICU admission had increased mortality than patients with lower sulfide levels. Endogenous production of H<sub>2</sub>S is time-dependent during the progression of sepsis and excessive production of H<sub>2</sub>S was only present in the early stages of a cecal ligation and puncture model of sepsis [255]. Furthermore, it was demonstrated in a different study that plasma H<sub>2</sub>S levels were also elevated in an endotoxin model of sepsis in addition to increased cystathionine  $\gamma$ -lyase (CSE) gene expression and enzymatic activity [257]. It is also known that H<sub>2</sub>S acts as an ROS scavenger *in vitro* [44].

Oxidative stress induces apoptosis and contributes to tissue injury. Therefore, the objective of this present study was to evaluate if exogenous H<sub>2</sub>S increased ROS production *in vitro*. Since many other effects associated with H<sub>2</sub>S have been attributed to K<sub>ATP</sub> channel activation [227], we also investigated whether the mechanism of action of H<sub>2</sub>S on ROS production was mediated via mito-K<sub>ATP</sub> channel activation.

### 4.3 Materials and Methods

**HMEC Cell Culture:** HMECs were a gift from Dr. Vijay Kumar Kalra (University of Southern California, Los Angeles, California). Cells were cultured in MCDB 131 growth medium without L-glutamine, 10% heat-inactivated fetal bovine serum (FBS) (Serum Source, Charlotte, North Carolina), 10% penicillin-streptomycin (ThermoFisher, Waltham, Massachusetts), 10% GlutaMAX (Life Technologies, Carlsbad, California), 10ng/mL endothelial growth factor, and 1 $\mu$ g/mL hydrocortisone. Cells were maintained in a T75 tissue culture-treated flask and seeded on collage-coated 24-well tissue culture-treated plates at a density of  $0.05 \times 10^6$  cells per well and allowed to attach overnight. Cells were quiesced the following day in 0.1% FBS medium overnight. On the day of the experiment, medium was refreshed with 1% FBS medium. All cells were maintained in 5% CO<sub>2</sub>/95% air at 37°C.

**HUVEC Cell Culture:** HUVECs, obtained from ATCC (Manassas, Virginia), were cultured in vascular cell basal medium (ATCC) supplemented with an endothelial cell growth kit (5ng/mL vascular endothelial growth factor, 5ng/mL endothelial growth factor, 5ng/mL fibroblast growth factor, 15ng/mL insulin-like growth factor, 10mM L-glutamine, 0.75U/mL heparin sulfate, 1 $\mu$ g/mL hydrocortisone, 50 $\mu$ g/mL ascorbic acid), 10% penicillin-streptomycin, and 10% FBS. Cells were maintained in a T75 tissue culture-treated flask and seeded on collage-coated 24-well tissue culture-treated plates at a density of  $0.05 \times 10^6$  cells per well and allowed to attach overnight. Cells were quiesced the following day in 0.1% FBS medium overnight. On the day of the experiment, medium was refreshed with 1% FBS medium. For intravital confocal microscopy experiments, cells were seeded in 6-well tissue culture-treated plates

containing collagen-coated 25mM glass coverslips at a density of  $0.3 \times 10^6$  cells per well and allowed to attach overnight. Cells were quiesced the following day in 0.1% FBS medium overnight. On the day of the experiment, medium was refreshed with 1% FBS medium. All cells were maintained in 5% CO<sub>2</sub>/95% air at 37°C.

**Reagents:** Sodium thiosulfate (STS), lipopolysaccharide (LPS) (E. Coli, serotype 026:B6), endothelin-1 (ET-1), and 5-hydroxydecanoate (5-HD) were purchased from Sigma-Aldrich (St. Louis, Missouri). Hoechst, 2',7-dichlorofluorescein diacetate (DCF-DA), and MitoSOX were purchased from ThermoFisher.

**Synergistic Effect of ET-1 and LPS:** Cells seeded in 24-well tissue culture-treated plates were incubated with or without LPS for 6 hours. Cell culture medium was removed and cells were incubated with a 4µM Hoechst + 25µM DCF-DA staining solution for 20 minutes in 5% CO<sub>2</sub>/95% air at 37°C. Cells were washed three times with Hank's Balanced Salt Solution (HBSS, Life Technologies, Carlsbad, California) pre-warmed to 37°C. Warmed HBSS was placed in each well. The tissue culture plate containing loaded cells was placed in a multi-well fluorescence plate reader with the temperature maintained at 37°C. The excitation and emission filters were set at 360/40 and 460/40, respectively. The fluorescence intensity from Hoechst staining from each well was recorded to normalize for cell count prior to the addition of MitoSOX. MitoSOX staining solution was added to each well to a final concentration of 0.5µM. The excitation filters were then set at 485/20 and 525/20 and the emission filters were set at 530/25 and 590/35, respectively, for simultaneous measurement of DCF and MitoSOX fluorescent intensities. The fluorescent intensities from each well were measured and recorded for 30 minutes.

**H<sub>2</sub>S Dose-Response and Mito-K<sub>ATP</sub> Channel Inhibition:** Cells seeded in 24-well tissue culture-treated plates were incubated with or without a mitochondria-specific K<sub>ATP</sub> channel inhibitor, 5-HD (Cayman Chemical, Ann Arbor, Michigan) for 10 minutes. Cell culture medium was removed and cells were incubated with a 4 $\mu$ M Hoechst + 25 $\mu$ M DCF-DA staining solution for 20 minutes 5% CO<sub>2</sub>/95% air at 37°C. Cells were washed three times with Hank's Balanced Salt Solution (HBSS, Life Technologies, Carlsbad, California) pre-warmed to 37°C. Warmed HBSS was placed in each well. The tissue culture plate containing loaded cells was placed in a multi-well fluorescence plate reader with the temperature maintained at 37°C. The excitation and emission filters were set at 360/40 and 460/40, respectively. The fluorescence intensity from Hoechst staining from each well was recorded to normalize for cell count prior to the addition of MitoSOX. MitoSOX staining solution was added to each well to a final concentration of 0.5 $\mu$ M. Cells were then treated with increasing concentrations of the H<sub>2</sub>S donor, sodium thiosulfate (STS, final concentrations of 0 $\mu$ M, 1 $\mu$ M, 10 $\mu$ M, 100 $\mu$ M, and 1000 $\mu$ M). The excitation filters were then set at 485/20 and 525/20 and the emission filters were set at 530/25 and 590/35, respectively, for simultaneous measurement of DCF and MitoSOX fluorescent intensities. The fluorescent intensities from each well were measured and recorded for 30 minutes.

**Statistical Analysis:** All data are presented as means  $\pm$  standard error of the mean (SEM). Statistical analysis was performed using GraphPad Prism software (San Diego, California). Statistical significance was assessed by one- or two-way analysis of variance (ANOVA) with independent and repeated measures used where appropriate. Dunnett's

multiple comparison *post hoc* test was used when statistical differences were detected. Statistical significance was set at  $p < 0.05$ .

#### 4.4 Results

**Effect of ET-1 on ROS Production in Endotoxemia:** Since plasma ET-1 levels has been shown to be elevated in septic patients and oxidative stress is important in the pathogenesis of sepsis, we tested whether ET-1 causes ROS production in an endotoxemic model of sepsis. Stimulation with ET-1 alone showed an increase in total ROS production, though not significant (Figure 28). However, ET-1 stimulation following endotoxin incubation for 6 hours resulted in a 2.6-fold increase in intracellular ROS levels, indicated by elevated DCF fluorescence ( $*** = p < 0.001$ ). There were no observed differences among any treatment groups for MitoSOX fluorescence, suggesting that the mitochondria are not major contributors to ROS production in response to ET-1 in endotoxemia (Figure 39). Data were from triplicate wells of four separate experiments.

**Effect of Mito- $K_{ATP}$  Channel Inhibition on Total ROS Production with Increasing Doses of  $H_2S$ :** Since one of the primary targets of  $H_2S$  in the mammalian system are the  $K_{ATP}$  channels in the mitochondria, we tested the effect of exogenous  $H_2S$  on ROS production. We observed a bell-shaped curve, typically seen in  $H_2S$  dose-response experiments (Figure 29) with no significant increases in total ROS production for any of the doses compared to control ( $0\mu M$  STS). However, the inhibition of mito- $K_{ATP}$  channels with 5-HD resulted in a bell-shaped dose-response curve, peaking at the  $1\mu M$  STS dose for total intracellular ROS formation ( $* = p < 0.05$ ) compared to the  $0\mu M$

dose, indicated by DCF fluorescence (Figure 30). Data were from triplicate wells of four separate experiments.

**Effect of Mito-K<sub>ATP</sub> Channel Inhibition on Mitochondrial ROS Production with Increasing Doses of H<sub>2</sub>S:** To determine if the mitochondria contributed to the total intracellular ROS formed upon incubation with H<sub>2</sub>S alone and with the mito-K<sub>ATP</sub> inhibitor, we determined the change in fluorescent intensities of MitoSOX, which targets mitochondrially-sourced ROS. Our results show that intracellular ROS levels are increased at H<sub>2</sub>S donor, STS, doses of 10μM, 100μM, and 1000μM (\* = p < 0.05) compared to the 0μM dose (Figure 31). Pre-treatment with 5-HD potentiated the production of ROS by mitochondria (Figure 32). Resulting dose-response bell-curve graph, demonstrating significant increases in mitochondrially-sourced ROS at all doses of STS not equal to 0μM, with the most potent doses being 10μM and 100μM (\*\* = p < 0.01, \*\*\* = p < 0.001, \*\*\*\* = p < 0.0001). Data were from triplicate wells of four separate experiments.

#### 4.5 Discussion

The vascular endothelium is a major site of vascular regulation in both normal physiological and stressed conditions, including both the regulation of inflammatory cell adhesion and the formation of endothelium-dependent vasoactive substances such as nitric oxide (NO) and endothelin-1 (ET-1). Reactive oxygen signaling has long been known to be a contributor to vascular injury in states of inflammatory stress, such as sepsis, but the source of oxidants has typically been said to be neutrophils and macrophages since these immune cells are involved in oxidative burst in early sepsis.

Our results demonstrate that endotoxemia leads to the production of reactive oxygen species (ROS) in response to ET-1. Previous studies from our lab have demonstrated that ET-1-stimulated endothelial nitric oxide synthase (eNOS) activity is inhibited in endotoxemia in both *in vivo* and *in vitro* models [106, 128, 163]. This inhibition is the result, at least in part, to increased hydrogen sulfide (H<sub>2</sub>S) production [162].

ROS generation contributes to tissue injury following lipopolysaccharide (LPS) insult. However, these ROS are produced by infiltrating neutrophils and macrophages or by NADPH oxidase in inflammatory cells in addition to other cell types [29]. The Kupffer cells (KCs), fixed macrophages in the liver, are an important source of ROS. Despite reactive oxygen having a short half-life, they can still be functionally important even if produced in moderate amounts. Previous work from our lab has demonstrated that reactive oxygen elicits a significant impact on endothelial cells, resulting in alterations in the regulation of local circulation. Uncoupling of eNOS from ET-1 binding to ET<sub>B</sub> receptor subtypes results in the formation of superoxide instead of NO and this is due to limited supplies of substrate or cofactor. Inflammatory stresses, such as sepsis, leads to high inducible nitric oxide synthase (iNOS). Elevated iNOS activity results in high consumption of L-arginine substrate and consequently, an inadequate supply of substrate for eNOS to utilize. Oxidative stress has been implicated in vascular dysregulation in response to an inflammatory stress. Endotoxin is associated with inflammation, activation of the immune system, and increased production of ROS. Studies from our lab have previously shown that ET-1-induced NO production in SECs is disrupted by LPS [106, 128, 162]. Since ET-1 can act as both a vasodilator and a vasoconstrictor, any imbalance in its effect can tip the scale in favor of a potentiated

vasodilatory effect or a potentiated vasoconstriction effect. We have previously demonstrated that LPS pretreatment suppresses ET-1-induced NO production by eNOS and that increased ROS production is a result of ET-1 in endotoxemia [81]. In addition, NO can be scavenged as it is being produced, further limiting NO bioavailability.

Our knowledge regarding H<sub>2</sub>S has significantly improved over the last two decades. H<sub>2</sub>S, a colorless, flammable, water-soluble gas is gaining attention as an endogenous gaseous mediator with diverse roles in many physiological and pathophysiological processes. One of the primary targets of H<sub>2</sub>S in the mammalian system are the K<sub>ATP</sub> channels in addition to eNOS, and cytochrome *c* oxidase and the combinatory effect H<sub>2</sub>S elicits on all its targets affect vascular tone. There is mounting evidence that H<sub>2</sub>S is an activator of K<sub>ATP</sub> channels [126, 155, 177, 225, 264]. Opening of mitochondrial K<sub>ATP</sub> channels (mito-K<sub>ATP</sub>) appears to have two consequences: 1) when the mitochondrial membrane potential is high, as seen in normal physiologic conditions, activation of mito-K<sub>ATP</sub> channels leads to potassium influx and increases mitochondrial ROS production [75], and 2) when the mitochondrial membrane potential is low, as seen in ischemia, opening of the mito-K<sub>ATP</sub> channels adds a parallel potassium conductance pathway to prevent contraction of the matrix and expansion of the intramembranous space [57, 121].

The activation of mito-K<sub>ATP</sub> channels leads to an influx of potassium and swelling of the mitochondrial matrix [76]. The swelling of the matrix is modest and is not consequential in that it does not lead to mitochondrial outer membrane rupture or coupling [121]. In this present study, we showed that exogenous H<sub>2</sub>S does not have a significant effect on total ROS at any concentration of STS administered. However,

inhibiting mito-K<sub>ATP</sub> channels results in a biphasic dose response curve for mitochondrial ROS production at all concentrations of H<sub>2</sub>S. Therefore, the opening of the mito-K<sub>ATP</sub> channels plays an important role in the regulation of mitochondrial function and attenuates oxidative stress, specifically, mito-K<sub>ATP</sub> channels modulate mitochondrial ROS. Another primary target of H<sub>2</sub>S in the mitochondria is sulfur quinone reductase (SQR), which oxidizes H<sub>2</sub>S and feeds additional electrons into the mitochondrial respiratory chain [82] and increases ROS production at the site of complex III [187]. ROS from H<sub>2</sub>S oxidation by SQR could also be a contributor to the increased ROS we observed in our studies.

Therefore, it is probable that exogenous H<sub>2</sub>S activation of mito-K<sub>ATP</sub> channels resulted in modest potassium influx, which altered the pH of the mitochondrial matrix, making it alkaline, and caused the increased ROS production we observed in this present study. The data from this study are consistent with the view that a modest influx of potassium because of mito-K<sub>ATP</sub> opening alkalinizes the mitochondrial matrix and leads to elevated levels of mitochondria ROS. Furthermore, our results demonstrate that the inhibition of mito-K<sub>ATP</sub> channels with 5-hydroxydecanoate (5-HD) pretreatment lead to an exacerbated increase in mitochondrial ROS, indicated by the increase in MitoSOX fluorescence. Another primary target of H<sub>2</sub>S in the mitochondria is sulfur quinone reductase (SQR), which oxidizes H<sub>2</sub>S and feeds additional electrons into the electron transport chain (ETC) by reducing ubiquinone [82]. Donated electrons increase the flux of the ETC in addition to increasing ROS production at the site of complex III [187]. Reactive oxygen as a result of H<sub>2</sub>S oxidation by SQR could also be a contributor to the increased ROS observed from our studies.

The results of this present *in vitro* study add mechanistic insights into the causes of vascular dysregulation, in part due to ROS production in response to ET-1, in sepsis. Earlier studies discussed in this dissertation provide further evidence of microvascular dysfunction indicated by hypersensitization to ET-1 in endotoxemia. Moreover, this study provides evidence for the molecular mechanisms H<sub>2</sub>S has on mitochondria, specifically activation of mito-K<sub>ATP</sub> channels and mitochondrial ROS production.

#### 4.6 Figures

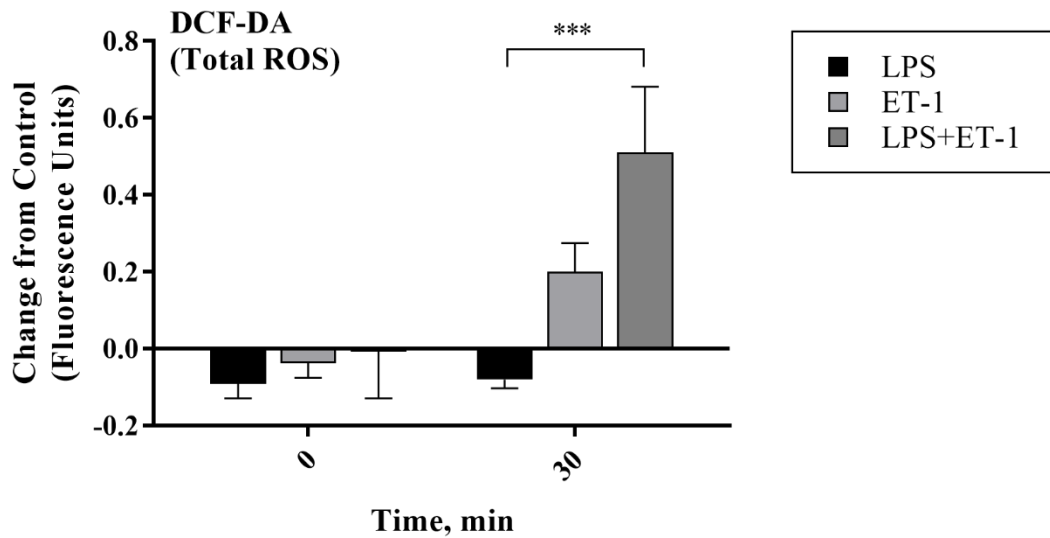


Figure 28: Intracellular total ROS production in response to ET-1 in endotoxemia. HMECs were stimulated with LPS alone or in combination with ET-1. Cells were loaded with DCF-DA and change in fluorescent intensities was measured after 30 minutes and normalized to cell number. Data are presented as the means  $\pm$  SEM from triplicate wells in four separate experiments. Statistical analysis was performed using two-way ANOVA with Dunnett's *post hoc* test. \*\*\* =  $p < 0.001$ .

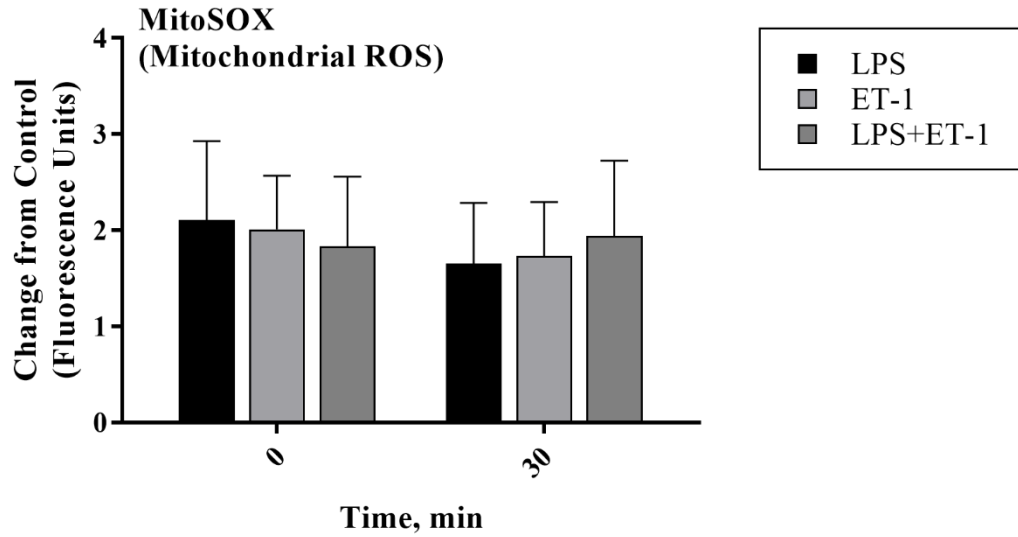


Figure 29: Intracellular mitochondrial ROS production in response to ET-1 in endotoxemia. HMECs were stimulated with LPS alone or in combination with ET-1. Cells were loaded with MitoSOX and change in fluorescent intensities was measured after 30 minutes and normalized to cell number. Data are presented as the means  $\pm$  SEM from triplicate wells in four separate experiments.

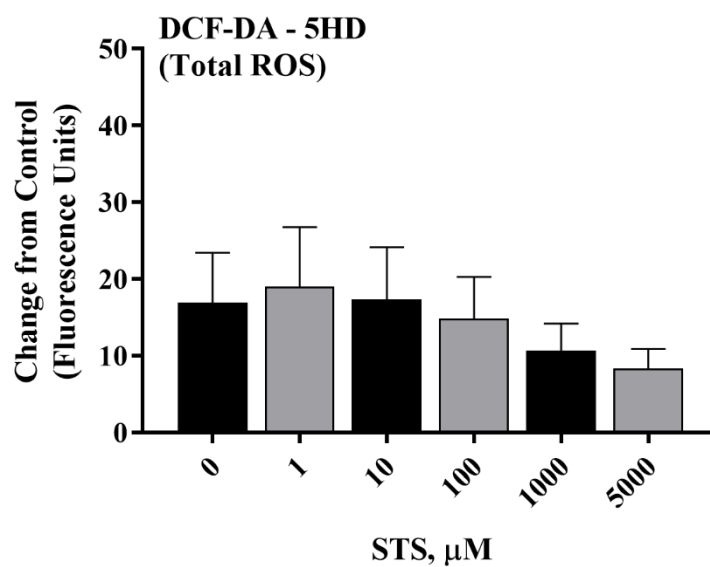


Figure 30: Intracellular total ROS production in response to increasing doses of H<sub>2</sub>S. Cells were loaded with DCF-DA and incubated with increasing doses of H<sub>2</sub>S. Change in fluorescent intensities was measured after 30 minutes and normalized to cell number. Data are presented as the means  $\pm$  SEM from triplicate wells in four separate experiments.

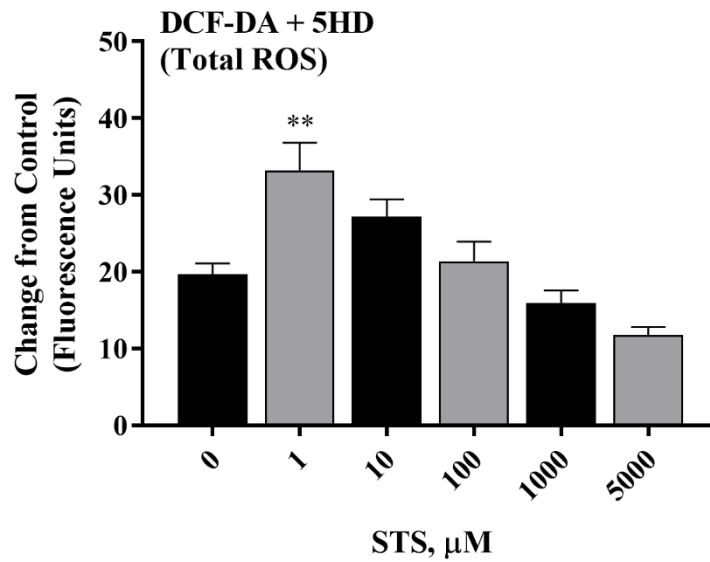


Figure 31: Intracellular total ROS production in response to increasing doses of H<sub>2</sub>S with the mito-K<sub>ATP</sub> inhibitor, 5-HD. Cells were loaded with DCF-DA and incubated with increasing doses of H<sub>2</sub>S. Change in fluorescent intensities was measured after 30 minutes and normalized to cell number. Data are presented as the means  $\pm$  SEM from triplicate wells in four separate experiments. Statistical analysis was performed using two-way ANOVA with Dunnett's *post hoc* test. \*\* =  $p < 0.01$  compared to 0 $\mu\text{M}$  STS.

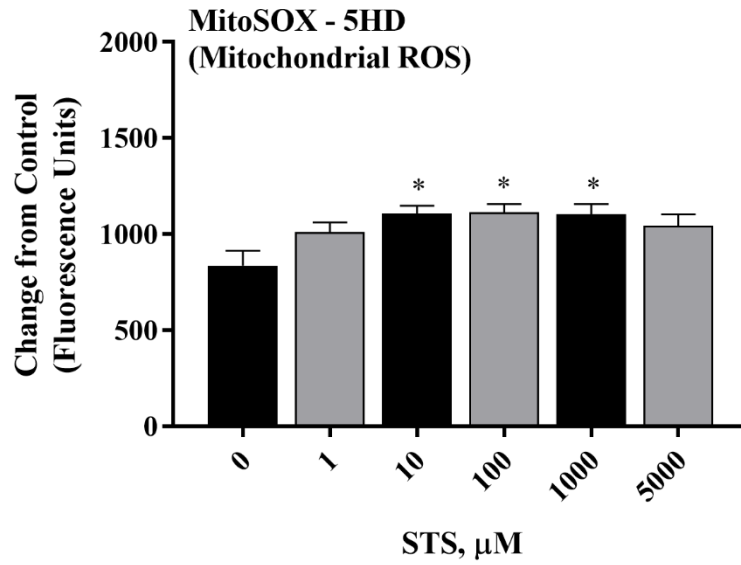


Figure 32: Intracellular mitochondrial ROS production in response to increasing doses of  $\text{H}_2\text{S}$ . Cells were loaded with MitoSOX and incubated with increasing doses of  $\text{H}_2\text{S}$ . Change in fluorescent intensities was measured after 30 minutes and normalized to cell number. Data are presented as the means  $\pm$  SEM from triplicate wells in four separate experiments. Statistical analysis was performed using two-way ANOVA with Dunnett's *post hoc* test. \* =  $p < 0.05$  compared to  $0\mu\text{M}$  STS.

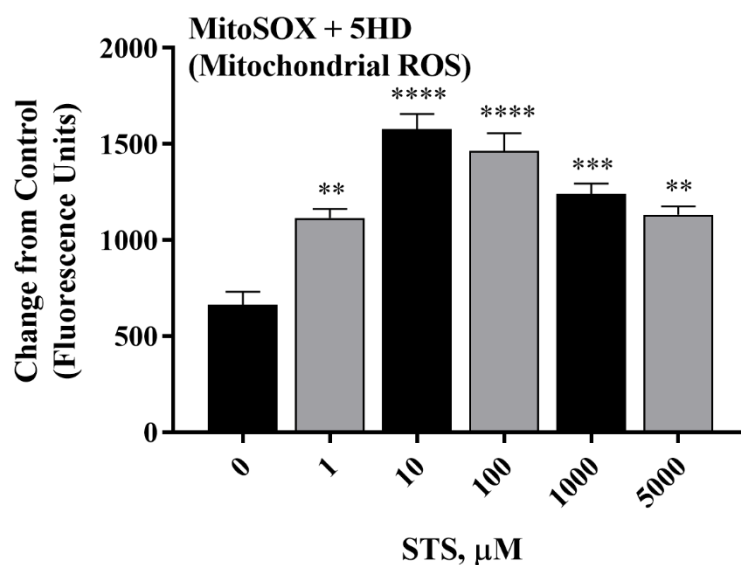


Figure 33: Intracellular mitochondrial ROS production in response to increasing doses of  $\text{H}_2\text{S}$  with the mito- $\text{K}_{\text{ATP}}$  inhibitor, 5-HD. Cells were loaded with MitoSOX and incubated with increasing doses of  $\text{H}_2\text{S}$ . Change in fluorescent intensities was measured after 30 minutes and normalized to cell number. Data are presented as the means  $\pm$  SEM from triplicate wells in four separate experiments. Statistical analysis was performed using two-way ANOVA with Dunnett's *post hoc* test. \*\* =  $p < 0.01$ , \*\*\* =  $p < 0.001$ , \*\*\*\* =  $p < 0.0001$  compared to  $0\mu\text{M}$  STS.

## CHAPTER 5: TEST WHETHER EXOGENOUS H<sub>2</sub>S ALTERS THE RESPONSE OF CELLS DURING ENDOTOXEMIA *IN VITRO*.

### 5.1 Abstract

Associations between the degree of mitochondrial dysfunction and outcomes of sepsis in both animal and patient studies are well-recognized. Although correlations do not confirm causation, it does suggest new routes to investigate for therapeutic interventions for patients of sepsis and septic shock with the focus on mitochondrial protection or stimulation of mitochondrial biogenesis. It is well understood that the excessive degree of inflammation triggers multiple downstream pathways but the precise pathophysiological mechanisms underlying the development of MOF remains unclear. While impaired circulation and tissue hypoperfusion are important contributors to the development of MOF, organ failure can still occur even in the absence of vascular dysfunction. Impaired blood flow perfusion can lead to insufficient oxygen at the mitochondrial level to drive oxidative phosphorylation of ADP to ATP and critically low levels of oxygen can potentially trigger cell death pathways. The present study was designed to examine the effects of both exogenous and endogenous hydrogen sulfide (H<sub>2</sub>S) on mitochondrial function and dynamics and cytoskeleton morphology *in vitro* an endotoxin model of sepsis using confocal microscopy and Western blot protein analysis. We observed that endotoxemia causes mitochondrial membrane depolarization and is attenuated with inhibition of endogenous H<sub>2</sub>S. Exogenous H<sub>2</sub>S leads to potentiated stress fiber formation and mitochondrial fission in LPS-treated cells.

## 5.2 Introduction

Sepsis represents a deranged and exaggerated systemic inflammatory response to infection that can lead to multi-organ dysfunction. Activation of inflammatory, immune, hormonal, metabolic, and bioenergetic responses are all involved in the pathogenesis of sepsis. Though impaired circulation leads to inadequate blood flow to tissues and is a major contributor to the development of multiple organ failure (MOF), organ failure can still occur even without abnormalities in the vasculature. Many organs manifest inflammation as indicated with the migration of inflammatory cells, chiefly macrophages and neutrophils, increased interstitial fluid leading to capillary leak and disruption in the epithelium, there is surprisingly very little cell death [94].

All cell types, excluding erythrocytes, possess mitochondria. These double-membraned organelles provide the bulk of the energy in the currency of ATP required for normal cellular and metabolic functions, including the ability to respond to pathophysiological stresses. As the primary site of total body oxygen consumption, mitochondria have many other roles in addition to generating ATP, including calcium regulation, thermoregulation, and production of reactive oxygen species (ROS) [171]. Since mitochondria are the main producers of ROS, they have an antioxidant system in place to maintain redox balance and mitochondrial function. These organelles have important quality control mechanisms to eliminate damaged and dysfunctional mitochondria to maintain oxidative phosphorylation as well as the integrity of mitochondrial function, thus, preserves the overall health of the cell.

Under stress conditions, cells adapt to maintain viability. Defense mechanisms include a decrease in oxygen and energy use, ATP demand, basal cellular functions, and

an activation of damage repair mechanisms. It is crucial to modulate the oxidative state of cells since an increase in the total amount of mitochondria and the degradation of damaged mitochondria are essential in maintaining an adequate capacity of oxidative phosphorylation for ATP generation. Metabolic stress induces cells to respond to situations of increased energy demand, promote programmed cell death. In addition, mitochondria are constantly undergoing dynamic changes, such as fission, fusion, mitophagy, and mitogenesis, to maintain a network of healthy, functional mitochondria [35, 253].

The generation of ATP in the mitochondria is a regulated process in which substrates provided by oxidative metabolism of glucose, lipids, and amino acids. Pyruvate enter the mitochondria where they it is converted to acetyl CoA, which enters the Krebs's cycle that donates electrons to complex I and complex II via NADH and FADH<sub>2</sub> of the electron transport chain (ETC), respectively. Electrons are transferred down the chain, passing through complex III and then complex IV, where molecular oxygen is the terminal electron acceptor and is reduced to water. This process creates an electrochemical gradient to enable ATP synthase to generate ATP from ADP. Incomplete reduction of oxygen increases ROS formation, specifically superoxide, mainly at the site of complex III but also complex I. Fortunately, the mitochondria have intrinsic defense mechanisms to protect against ROS through its antioxidant system [249]. However, pathological processes that generate excessive amounts of ROS can overwhelm the mitochondria even with a defense mechanism in place.

Numerous morphological changes occur in mitochondrial dynamic events. Mitochondrial fusion and fission play important roles in cell division and proliferation, as

well as in the elimination of damaged and dysfunctional mitochondria, as observed in the process of mitophagy. Dynamin-related protein 1 (DRP1) drive fission events and have been shown to be related to changes in mitochondrial membrane potential and reduced oxygen consumption [138]. Fission increases in conditions of cellular stress and plays an important role in the quality control mechanism of removing dysfunctional mitochondria before they release cytochrome *c* into the cytosol to initiate cell death pathways.

Impaired blood flow perfusion that occurs in sepsis results in insufficient oxygen at the mitochondrial level and critically low levels may trigger apoptosis. In addition, the generation of excess amounts of ROS and endogenous gases, including nitric oxide (NO), carbon monoxide (CO), and H<sub>2</sub>S can directly inhibit mitochondrial oxidative phosphorylation and cause damage to the mitochondria proteins and membrane structure [15, 132, 242]. Furthermore, genes transcribing mitochondrial proteins have been shown to be downregulated in human volunteers receiving endotoxin and in critically ill patients [32, 34].

The internal surface of blood vessels, known as the endothelium, serves as a barrier to separate the inner space of the blood vessel from underlying tissues to control the exchange of solutes and macromolecules. Dysfunction of the vascular endothelium barrier is important in the pathogenesis of numerous disease states, including sepsis [51, 178, 191]. Vascular endothelial cadherin (VE-cadherin) is a type cell adhesion molecule of the endothelium and is critical to endothelial permeability [53]. Existing in two forms, actin is the most abundant and highly conserved protein in all eukaryotic cells. Filamentous actin (F-actin) typically assembles at cadherin adhesion sites and can influence endothelial cell morphology, adhesion of cells to the extracellular matrix, and

intercellular connections [22]. Inflammatory insults induce rapid reorganization of actin structures, resulting in the formation of stress fibers and increases in vascular endothelial cell permeability. Stress fibers significantly influence the rate and size of the endothelial cell gaps, making them an important contributor to vascular endothelial cell leakiness that is observed in the pathogenesis of sepsis [59].

This present study was designed to determine the effects of exogenous and endogenous H<sub>2</sub>S on endothelial cell mitochondria *in vitro* using cultured human umbilical vein endothelial cells (HUVECs). Using intravital confocal microscopy, we demonstrated that mitochondrial membrane depolarization is induced in an endotoxic model of sepsis and further investigation of mitochondrial dynamic proteins revealed that LPS pretreatment lead to an upregulation of mitophagy machinery. Moreover, we demonstrated that inhibiting endogenous H<sub>2</sub>S abrogated F-actin stress fiber formation in endotoxemia.

### 5.3 Materials and Methods

**HUVEC Cell Culture:** HUVECs, obtained from ATCC (Manassas, Virginia), were cultured in vascular cell basal medium (ATCC) supplemented with an endothelial cell growth kit (5ng/mL vascular endothelial growth factor, 5ng/mL endothelial growth factor, 5ng/mL fibroblast growth factor, 15ng/mL insulin-like growth factor, 10mM L-glutamine, 0.75U/mL heparin sulfate, 1µg/mL hydrocortisone, 50µg/mL ascorbic acid), 10% penicillin-streptomycin, and 10% FBS. Cells were maintained in a T75 tissue culture-treated flask and seeded on collage-coated 24-well tissue culture-treated plates at a density of  $0.05 \times 10^6$  cells per well and allowed to attach overnight. Cells were

quiesced the following day in 0.1% FBS medium overnight. On the day of the experiment, medium was refreshed with 1% FBS medium. For experiments investigating mitochondrial dynamics, cells were seeded in 6-well tissue culture-treated plates at a density of  $0.3 \times 10^6$  cells per well. For intravital confocal microscopy experiments, cells were seeded in 6-well tissue culture-treated plates containing collagen-coated 25mm glass coverslips at a density of  $0.3 \times 10^6$  cells per well. For cytoskeleton morphology experiments, cells were seeded in 24-well tissue culture-treated plates containing collagen-coated glass coverslips at a density of  $0.05 \times 10^6$  cells per well. Cells were allowed to attach overnight for all experiments and were quiesced the following day in 0.1% FBS medium overnight. On the day of the experiment, medium was refreshed with 1% FBS medium. All cells were maintained in 5% CO<sub>2</sub>/95% air at 37°C.

**Reagents:** Sodium thiosulfate (STS) and lipopolysaccharide (LPS) (E. Coli, serotype 026:B6), endothelin-1 (ET-1) were purchased from Sigma-Aldrich (St. Louis, Missouri). Hoechst, 2',7-dichlorofluorescein diacetate (DCF-DA), and MitoSOX were purchased from ThermoFisher.

**Preparation for Intravital Microscopy *In Vitro*:** Mitochondria and nonviable cells were fluorescently labeled using Rhodamine123 (Rh123) and Propidium Iodide (PI) respectively. Since Rh123 is a cationic dye, it distributes electrophoretically into the mitochondrial matrix in response to the electric potential across the inner mitochondrial membrane. While PI is excluded from live, cells, it permeates dead cells and stains chromosomes. Nuclei were visualized with Hoechst. Medium was removed from wells containing collagen-coated glass coverslips and cells were loaded with a 100nM Rh123 + 6μM PI + 4μM Hoechst staining solution. Cells were stained for 20 minutes and washed

once with Hank's Balanced Salt Solution (HBSS, Life Technologies, Carlsbad, California), prewarmed to 37°C. The cell-containing coverslip was gently removed from the well and mounted onto a cell-viewing chamber. 1mL of 0% FBS HUVEC cell culture medium prewarmed to 37°C was placed in the chamber.

For microscopy, the *in vitro* intravital chamber was placed on a temperature-controlled (37-38°C) microscope stage with a viewing window over the 40X UPlanApo 0,85 objective lens of an Olympus FV500 scanning confocal microscope. Laser excitation at 405nm, 488nm, and 610nm were used in rapid succession and fluorescence in blue (Hoechst staining), green (Rh123 staining), and red (PI staining) channels were visualized.

**Treatment Groups:** Coverslips containing attached HUVECs were randomly divided into one of two treatment groups: 1. Saline, 2. ET-1. Then cells were further divided into one of six treatment sub-groups: 1. Control, 2. LPS, 3. STS, 4. PAG, 5. STS/LPS, 6. PAG/LPS. For the LPS sub-group, cells were treated with LPS (250ng/mL) six hours prior to intravital confocal microscopy. To determine any effect of endogenous H<sub>2</sub>S, PAG, the inhibitor of cystathionine  $\gamma$ -lyase (CSE), was given as a pretreatment 30 minutes prior to intravital confocal microscopy. For cells receiving both LPS and PAG treatments, LPS was administered 5.5 hours prior to PAG, which was given 30 minutes prior to intravital confocal microscopy.

**H<sub>2</sub>S Treatment:** The H<sub>2</sub>S donor, STS, was used to investigate the effect of H<sub>2</sub>S on mitochondrial function. Freshly prepared STS (40 $\mu$ M) was administered directly into the intravital chamber and the mitochondria were visualized for a period of 30 minutes with the first image marking the beginning of the experiment, just prior to the start of

STS treatment. Images were recorded at the start of the experiment and again after 30 minutes using FLUOVIEW software (Shinjuku, Tokyo, Japan).

**ET-1 Treatment:** ET-1 (10nM) was administered directly into the intravital chamber and the mitochondria were visualized for a period of 30 minutes with the first image marking the beginning of the experiment, just prior to the start of STS treatment. Images were recorded at the start of the experiment and again after 30 minutes using FLUOVIEW software. Offline analysis was performed using FIJI software (Laboratory for Optical and Computational Instrumentation, Madison, Wisconsin).

**Determination of Changes in Mitochondrial Dynamics:** Cells were removed from tissue-treated culture plates prepared for protein analysis and protein concentration was determined by the BCA protein assay. Equal amounts of protein from each sample were separated on an SDS polyacrylamide gel and transferred onto a nitrocellulose membrane. After incubation with a primary antibody for the protein of interest (phosphorylated DRP1 at serine 637, pDRP1, for mitochondrial fission, LC3B I/II for mitophagy), the blots were probed with an appropriate secondary antibody and developed with enhanced with chemiluminescence reagents. The relative amount of the pDRP1 protein was normalized to DRP1 and LC3B expression was provided as the ratio of LC3BII/LC3BI and analyzed with FIJI software.

**Protein Expression Analysis:** Relative expression of target proteins were determined by Western blot and densitometric analysis with FIJI software.

**Determining Changes in Cytoskeleton Morphology:** To investigate F-actin stress fiber formation, Texas Red-X Phalloidin fluorescent staining was used. Medium was removed from tissue culture-treated plates prepared for cytoskeleton morphology and

cells were fixed with 4% paraformaldehyde and permeabilized with digitonin (100 $\mu$ M). Cells were washed three times with ice-cold Dulbecco's phosphate-buffered saline 1X (DPBS 1X) between fixing and permeabilizing steps. Cells were loaded with a 22.5 $\mu$ M 4',6-Diamidino-2-Phenylindole, Dihydrochloride (DAPI) + 1 $\mu$ M Texas Red-X Phalloidin staining solution for 20 minutes. Cells were washed once with DPBS 1X, air-dried, and mounted on microscope slides. Microscope slides were viewed using the 40X UPlanApo 0,85 objective lens of an Olympus FV500 scanning confocal microscope. Laser excitation at 405nm and 610nm were used in rapid succession and fluorescence in blue (Hoechst staining) and red (Texas Red X-Phalloidin staining) channels were visualized.

**Offline Image Analysis:** Offline image analysis was performed using FIJI software. For mitochondria membrane potential and cell viability, 40X images recorded with FITC and Texas Red filters were used. Five areas of interest were randomly selected per image. To determine the degree of mitochondrial depolarization, areas of interest were measured for standard deviation of Rh123 green fluorescence. To determine cell viability, the number of PI-positive cells were counted and divided by the total number of cells in each image. For changes in cytoskeleton morphology, 40X images recorded with Rhodamine-Phalloidin filters were used. Five areas of interest were randomly selected per image. To determine the degree of F-actin stress fiber formation, the number of red pixels were counted that exceeded a set fluorescent intensity threshold and divided by the total number of cells in each image. The same fluorescence intensity threshold was used to quantify all images.

**Statistical Analysis:** All data are presented as means  $\pm$  standard error of the mean (SEM). Statistical analysis was performed using GraphPad Prism software (San Diego,

California). Statistical significance was assessed by one- or two-way analysis of variance (ANOVA) with independent and repeated measures used where appropriate. Dunnett's or Sidak's multiple comparison *post hoc* test was used when statistical differences were detected. Statistical significance was set at  $p < 0.05$ .

#### 5.4 Results

**Effect of H<sub>2</sub>S on Mitochondrial Depolarization *In Vitro*:** We investigated the effect of H<sub>2</sub>S using the donor, STS (40μM) on mitochondrial membrane depolarization *in vitro* in endotoxemia (Figure 44). We quantified the degree of mitochondrial membrane depolarization using the standard deviation of the means of five randomly selected areas of interest following 30 minutes of STS treatment during intravital confocal microscopy. LPS treatment for 6 hours resulted in a 42.1% decrease in mitochondrial membrane polarization (\*\*\*) =  $p < 0.001$ ). Treatment with ET-1 showed mitochondrial depolarization for H<sub>2</sub>S-treated cells in endotoxemia where H<sub>2</sub>S displayed a protective effect in the absence of ET-1 (\*\* =  $p < 0.01$ ). Furthermore, visual appearances of the differences in mitochondrial membrane potential can be seen on images (Figure 45). Data were from four separate experiments.

**Effect of PAG Pretreatment on Mitochondrial Membrane Potential:** The non-competitive inhibitor of CSE, PAG, was used to examine the role of endogenous H<sub>2</sub>S on the mitochondria HUVECs during endotoxemia. We demonstrated that treatment of ET-1 depolarized the mitochondrial membrane in PAG pre-treated cells by 4.7% (Figure 46). While PAG pre-treatment alone had no significant effect on the response to ET-1, the depolarization effect of LPS was attenuated in endotoxemia, resulting in a 25.7%

reduction in mitochondrial membrane polarization (\* =  $p < 0.05$ ). Additionally, differences between treatment groups in mitochondrial membrane polarization based on can be visually observed (Figure 47). Data were from four separate experiments.

**Effect of H<sub>2</sub>S on Mitochondrial Fission Marker *In Vitro*:** Since the relationship between mitochondrial morphology and function have been shown to be involved in shaping cellular function, we assessed the degree of mitochondrial fission by Western blot analysis for pDRP1 protein expression in cultured HUVECs. DRP1 is expressed in the cytosol and is recruited to the mitochondrion and is activated through post-translational modification to initiate fission. Mitochondrial fission was expressed as the ratio of activated DRP1, pDRP1, protein expression to DRP1 protein expression (Figure 48). H<sub>2</sub>S increased mitochondrial fission by 63.6% in endotoxemia for baseline (Figure 49, \* =  $p < 0.05$ ). There were no significant differences among ET-1 treatment groups. Data were from four separate experiments.

**Effect of PAG Pretreatment on Mitochondrial Fission Marker *In Vitro*:** We assessed the degree of mitochondrial fission among treatment groups. PAG pretreatment showed no significant differences in mitochondrial fission among baseline or ET-1 treatment groups (Figure 50). Data were from four separate experiments.

**Effect of H<sub>2</sub>S Treatment on Mitophagy Marker:** Since dysfunctional mitochondrial fragments are removed from functional mitochondrial networks via mitochondrial fission and eliminated via mitophagy, we furthered our investigation on the role of mitochondrial dynamics in the progression of sepsis by examining the degree of mitophagy, quantified as the protein expression of LC3B by Western blot analysis (Figure 51). Mitophagy was expressed as the ratio of LC3BII protein expression to

LC3BI protein expression. Endotoxemia resulted in a 70.6% increase in LC3BII/LC3BI (Figure 52, \* =  $p < 0.05$ ). There were no significant differences among ET-1 treatment groups. Data were from four separate experiments.

**Effect of PAG Pretreatment on Mitophagy Marker *In Vitro*:** We assessed the role of endogenous H<sub>2</sub>S on LC3BII/LC3BI protein expression among treatment groups (Figure 53). PAG was shown to attenuate LPS-induced mitophagy for baseline, resulting in a 17.2% decrease in LC3BII/LC3BI protein expression compared to LPS. We found no significant differences among treatments for baseline or ET-1 groups. Data were from four separate experiments.

**Effect of H<sub>2</sub>S on F-actin Stress Fiber Formation in Endotoxemia *In Vitro*:** Inflammatory stress, such as sepsis, induce rapid reorganization of actin structures, leading to the formation of stress fibers. Stress fibers are responsible for increases in vascular endothelial cell permeability. Therefore, we assessed the degree of F-actin stress fiber formation by loading stimulated cells with Texas-Red X Phalloidin fluorescent stain, which has a high affinity for F-actin. We quantified the extent of stress fiber formation based on the number of red pixels per cell that exceeded a fluorescent intensity per cell. We observed a 100.9% and 134.0% increase in F-actin stress fiber formation for cells treated with LPS alone and LPS plus H<sub>2</sub>S, respectively (Figure 54, \*\*\*\* =  $p < 0.0001$ ). For ET-1 groups, H<sub>2</sub>S was shown to potentiate F-actin stress fiber formation in endotoxemia, resulting in a 65.2% increase compared to 49.0% for LPS alone (\*\* =  $p < 0.01$ , \*\*\* =  $p < 0.001$ ). Moreover, there was a clear difference between treatment groups in the formation of F-actin stress fibers based on the visual appearance

of the HUVECs stained with Texas Red X-Phalloidin (Figure 55). Data were from four separate experiments.

### **Effect of PAG Pretreatment on F-actin Stress Fiber Formation in**

**Endotoxemia *In Vitro*:** To determine the role of endogenous H<sub>2</sub>S on F-actin stress fiber formation, we pretreated cells with the inhibitor of CSE, the enzyme that synthesizes H<sub>2</sub>S. PAG pretreatment was shown to attenuate F-actin stress fiber formation in endotoxemia for both baseline, with a 59.6% increase (Figure 56, \* =  $p < 0.05$ ) versus a 100.9% increase in LPS alone (\*\*\*) =  $p < 0.001$ ), and ET-1 groups, which showed just a 0.9% increase versus 49.0% in LPS alone (\*\* =  $p < 0.01$ ). Additionally, differences between treatment groups in the formation of F-actin stress fibers based on the visual appearance of the HUVECs stained with Texas Red X-Phalloidin can be seen (Figure 57). Data were from four separate experiments.

## 5.5 Discussion

In this present study, we investigated whether hydrogen sulfide (H<sub>2</sub>S) regulates mitochondrial function and mitochondrial dynamics *in vitro* using cultured HUVECs. We demonstrated that treatment with the H<sub>2</sub>S-releasing agent, sodium thiosulfate (STS), results in depolarization of the mitochondrial membrane in endotoxemia. We show that pretreatment with DL-propargylglycine (PAG), a non-competitive inhibitor of cystathionine  $\gamma$ -lyase (CSE), the enzyme that produces H<sub>2</sub>S, attenuates LPS-induced mitochondrial membrane depolarization. STS treatment also results in an upregulation of mitochondrial fission in endotoxemia. In addition, we report that increases in filamentous actin (F-actin) stress fiber formations occur with STS and endothelin-1 (ET-

1) co-treatment in endotoxemia and these effects are attenuated with endogenous H<sub>2</sub>S inhibition.

Our *in vitro* studies yielded very different responses with PAG than our *in vivo* studies. However, the fact that our animal studies investigated responses in murine hepatocytes while our cell culture studies investigated responses in human endothelial cells explains the discrepancies. It is well known that hepatocytes, alongside colonic epithelial cells, are chief producers of endogenous H<sub>2</sub>S in contrast to human umbilical vein endothelial cells (HUVECs). Therefore, it was not a surprise that the responses to PAG were insubstantial in our *in vitro* studies since HUVECs do not synthesize an abundant amount of endogenous H<sub>2</sub>S. Since plasma H<sub>2</sub>S levels are elevated during sepsis, administering exogenous H<sub>2</sub>S allowed us to gain fundamental insight to the molecular responses the gas has on endothelial cells.

As the leading cause of death among critically ill patients, sepsis is characterized by an exaggerated systemic inflammatory response to infection or trauma. Patients who are acutely ill show a robust inflammatory response that is associated with multiple organ dysfunction syndrome (MODS) while septic shock is in addition linked with hypotension without response to fluid resuscitation and vasopressors [25, 146]. Although early diagnosis of sepsis in conjunction with antibiotic therapeutic therapy was shown to decrease mortality, post-sepsis complications have a devastating impact, including cognitive impairment, physical disabilities, and poor recovery are all associated with high mortality among survivors of sepsis [71]. The effects of inflammatory mediators and tissue hypoxia are typically associated to organ dysfunction in the progression of sepsis with little or no apoptosis or necrosis observed and preserved tissue oxygen delivery [94].

However, research studies have suggested that despite the bioavailability of oxygen, sepsis still has a dramatic impact on cellular metabolism and mitochondrial function [21, 202]. Cytopathic hypoxia, or decreased cellular respiration, has been demonstrated to be associated with cell survival but may trigger MOF later [62]. It has now become apparent that mitochondrial dysfunction accompanied with reactive oxygen species (ROS) generation is linked with the pathogenesis of sepsis.

Mitochondrial electron transport chain (ETC) protein complexes are essential for the generation of mitochondrial membrane potential and the proton gradient that is utilized to produce ATP at the site of ATP synthase, or complex V. Furthermore, the mitochondria play key roles in several crucial cellular functions, including programmed cell death pathways, calcium flux, and redox signaling [36, 73, 148, 171]. The precise mechanism behind mitochondrial dysfunction in sepsis has not been completely elucidated. However, inflammatory mediators, such as nitric oxide (NO), H<sub>2</sub>S, and ROS directly impair several components of the mitochondrial respiratory chain and subsequently, impair ATP production [86, 132].

Clinical sepsis studies have demonstrated that the degree of mitochondrial impairment is correlated with patient mortality rate [62]. Patients who died from severe sepsis had decreased muscle ATP content whereas sepsis survivors had higher ATP levels [28]. Additionally, organ dysfunction and clinical illness were associated with decreases in metabolic rate and mitochondrial mass [86]. Recovery of metabolic activity and organ function was shown to be regulated by expression of proteins involved in mitochondrial biogenesis, such as PRRgamma-coactivator-1 $\alpha$  (PGC-1 $\alpha$ ) and nuclear respiratory factors 1 and 2 (NRF-1, NRF-2). Furthermore, the most recent pre-clinical

studies indicate that not only preservation of mitochondria, but also mitochondrial biogenesis, is critical in reestablishing organ homeostasis during sepsis recovery.

Mitochondrial fusion and fission jointly work to maintain the shape, size, and number of mitochondria as well as their physiological function and the balance of mitochondrial dynamics is crucial in cellular homeostasis [35, 223]. Mitochondrial fusion is thought to function as a rescue mechanism in which dysfunctional and damaged mitochondria couple to healthy mitochondria to restore its functionality whereas mitochondrial fission induces fragmentation when the damage is too excessive to rescue the cell from impending cytochrome *c* release and programmed cell death [174]. It has been demonstrated that the imbalance between the two dynamic events in mitochondria, fission and fusion, play an important role in the progression of sepsis [80].

Using confocal intravital microscopy, we were able to visualize and quantify changes in mitochondrial membrane potential using the fluorophore, rhodamine 123 (Rh123). Since Rh123 is a cationic fluorescent stain, it partitions itself in the most electronegative parts of the cell, making it a worthy marker for visualizing mitochondria. Rh123 staining of healthy, polarized mitochondria appear punctate and the measured standard deviation of the area of interest is high in value. Depolarized mitochondria lose their electronegativity and Rh123 no longer sequesters in the mitochondria and diffuses into the cytosol, resulting in diffuse green stain throughout the entire cell and a standard deviation that is low in value.

In HUVECs, we observed a significant change in mitochondrial membrane potential in cells treated with endotoxin for 6 hours. Interestingly, our results showed that STS treatment in endotoxemia led to depolarization of the mitochondrial membrane

with ET-1 co-treatment but not in baseline groups. Previous studies have demonstrated that the degree of mitochondrial depolarization is increased following stimulation with lipopolysaccharide (LPS) in macrophages [55]. Moreover, mitochondrial structural damage and dysfunction are important in the progression of sepsis and are linked with the severity of organ dysfunction and sepsis outcome [12]. Increased levels of mitochondrial ROS during sepsis can lead to mitochondrial depolarization, inhibit oxidative phosphorylation and ATP production, which tips the balance of energy metabolism and tissue demand. This can result in systemic inflammation and MOF ensues [8, 72]. Furthermore, excessive ROS can impair mitochondrial morphology and inhibit mitochondrial biogenesis [209, 234, 262]. Inhibition of endogenous H<sub>2</sub>S with PAG did not have a significant effect in our *in vitro* studies. Since HUVECs do not produce substantial amounts of endogenous H<sub>2</sub>S [130], one would not expect an inhibitor of CSE, the enzyme that synthesizes H<sub>2</sub>S, to elicit a significant response.

We further investigated the role of exogenous H<sub>2</sub>S on mitochondrial dynamics, specifically, mitochondrial fission and mitophagy. As the main regulator of mitochondrial fission, dynamin-related protein 1 (DRP1), is a cytosolic protein and is recruited to the outer mitochondrial membrane at the site of mitochondrial fission, where it forms a multimeric ring-like structure that constricts and cleaves mitochondria in a GTPase-dependent manner [115]. Because DRP1 is activated through post-translational modification, we determined pDRP1 expression in protein isolated from harvested cells using Western blot analysis.

We observed an upregulation of mitochondrial fission, indicated by increased phosphorylated DRP1 (pDRP1) protein expression, with H<sub>2</sub>S treatment in endotoxemia.

When we assessed the effect of PAG pretreatment on mitochondrial fission to determine if there was a role for endogenous H<sub>2</sub>S, we observed no significant effect among any of the treatment groups and the lack of endogenous H<sub>2</sub>S synthesis in HUVECs is likely responsible. ET-1 did not have any significant effect for any treatment. It is thought that ET-1 leads to the upregulation of Rho-associated protein kinase 1 (ROCK1) expression, which increases LIMK2 expression and impairs DRP1-mediated mitochondrial fission in neuronal death [118]. However, this is unlikely since upregulation of LIMK2 does not fit within the time frame of our experimental time course.

Mitochondria that are damaged and dysfunctional are deleterious to the cell. Therefore, degradation of such mitochondria is crucial to the overall livelihood of the cell. Selective mitochondrial degradation is executed by mitophagy, which is regulated by several proteins, including PTEN induced putative kinase 1 (PINK1), Parkin, and light chain 3B (LC3B). PINK1 accumulates on the outer mitochondrial membrane when mitochondria become damaged, which results in recruitment of Parkin from the cytosol. Activation of Parkin induces ubiquitination of additional mitochondrial outer membrane proteins, yielding more ubiquitin substrate from PINK1 and creating a potent positive feedback amplification loop. Phosphoubiquitin chains on the outer mitochondrial membrane recruit autophagy receptors, which recruit autophagy machinery, including LC3B, to induce mitophagy [133]. In this present study, we determined the degree of mitophagy by quantifying the protein expression ratio of active LC3B (LC3BII) to inactive LC3B (LC3BI). We demonstrated by Western blot analysis that mitophagy is upregulated in cells treated with endotoxin for 6 hours, as indicated by increased LC3BII/LC3BI protein expression. Pretreatment with the CSE inhibitor, PAG, did not

result in any significant changes in LC3BII/LC3BI protein expression among any of the treatment groups.

We further investigated the role of H<sub>2</sub>S in vascular inflammation, namely vascular endothelial cell cytoskeleton morphology. Under normal physiological conditions, vascular endothelial permeability is tightly regulated by junction molecules that bridge the gap between neighboring endothelial cells. These intercellular junction molecules function in the maintenance of overall endothelial integrity to minimize leakage of plasma fluid into the interstitial space. Tight junctions and adherens are responsible for the stability of endothelial cells and this stability is dependent on actin cytoskeleton interactions. Actin dynamics which are disturbed may tip the scale from stabilizing cortical actin to destabilizing contractile stress fibers, thus resulting in endothelial barrier dysfunction and increased vascular permeability [74]. In addition, irregular actin dynamics may also be a contributor to excessive recruitment of immune cells to the sites of inflammation [204].

Hyperpermeability of the endothelial barrier is a hallmark of sepsis and actin stress fiber formation is a contributor to increased vascular permeability. Therefore, we investigated the effect of H<sub>2</sub>S on cytoskeleton rearrangement by determining the effect of the noxious gas on F-actin stress fiber formation in an endotoxin model of sepsis. Using confocal microscopy, we demonstrate that cells stimulated with LPS for 6 hours show a dramatic increase in F-actin stress fiber formation. This effect is potentiated with co-treatment of H<sub>2</sub>S and ET-1 in endotoxemia. The potentiated effect observed with the addition of ET-1 is most likely due to the downstream effects of ET-1 binding to the ET-1 receptor, resulting in constriction through the involvement of RhoA and Rho-kinase on

the actomyosin cytoskeleton [184]. Furthermore, pretreatment with PAG attenuated F-actin stress fiber formation observed in endotoxin-treated cells, suggesting a role for endogenous H<sub>2</sub>S in vascular endothelial permeability in the progression of sepsis.

The results of this study provide insight into the molecular mechanisms underlying mitochondrial dysfunction in the pathogenesis of sepsis using an endotoxin *in vitro* model. We demonstrated that LPS stimulation leads to depolarization of the mitochondrial membrane and upregulation of mitochondrial fission. In addition, we have provided evidence for a role of endogenous H<sub>2</sub>S in the increase of vascular endothelial permeability, which is a hallmark of inflammatory disease states, such as sepsis.

## 5.6 Figures

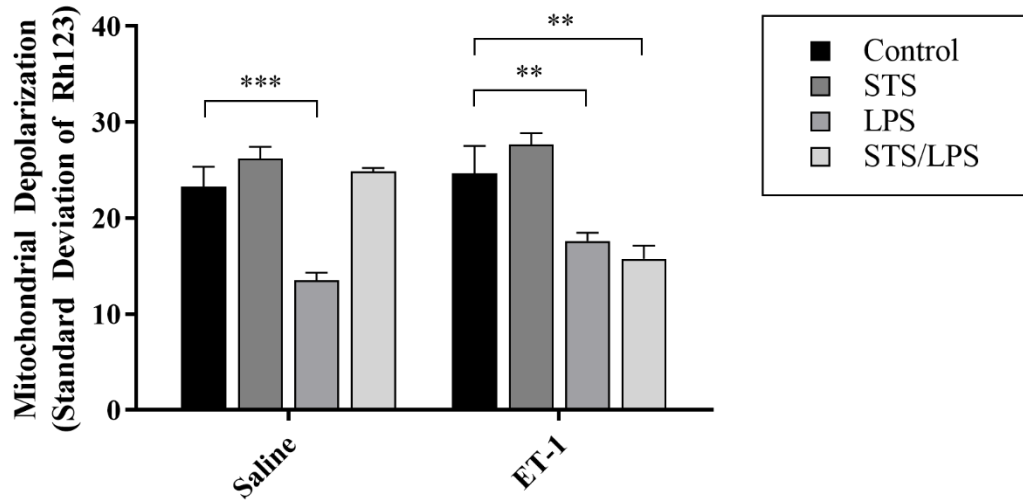


Figure 34: Effect of STS on mitochondrial depolarization *in vitro*. Images of HUVECs were recorded before and after 30 minutes following administration of H<sub>2</sub>S donor, STS. LPS treatment for 6 hours resulted in significant mitochondrial membrane depolarization, quantified as the standard deviation of Rh123 staining. STS treatment had no effect on mitochondrial depolarization in endotoxemia. Data are presented as the means  $\pm$  SEM from four separate experiments. Statistical analysis was performed using two-way ANOVA with Dunnett's *post hoc* test. \*\* =  $p < 0.01$ , \*\*\* =  $p < 0.001$ .

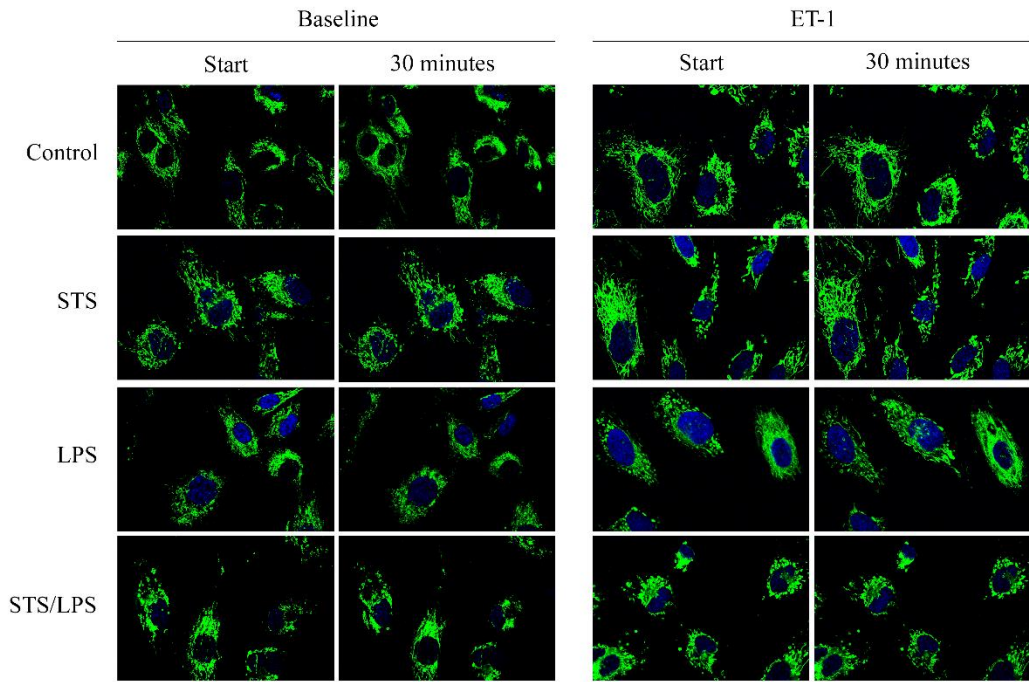


Figure 35: The effect of ET-1 and STS on mitochondrial membrane depolarization in endotoxemia *in vitro*. Mitochondria were visualized to determine the effect of ET-1 and STS on HUVECS treated with LPS for 6 hours. Representative images are shown before and after co-treatment with ET-1 (10nM) and STS (40 $\mu$ M).

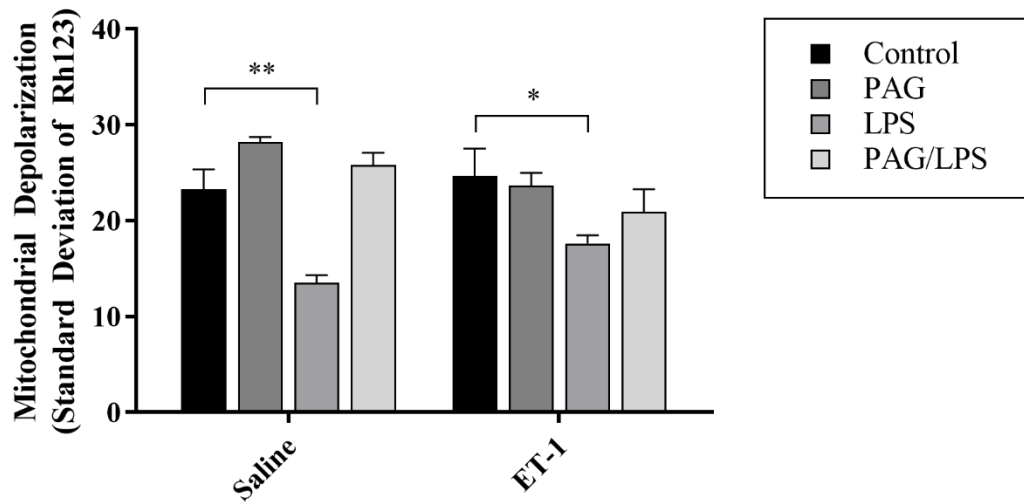


Figure 36: Effect of PAG on mitochondrial depolarization during ET-1 treatment in endotoxemia *in vitro*. HUVECs were pretreated with PAG for 30 minutes with or without LPS treatment for 6 hours. Images were recorded before and 30 minutes following administration of ET-1. PAG attenuates mitochondrial membrane depolarization during endotoxemia with or without ET-1, quantified as the standard deviation of Rh123 staining. Data are presented as the means  $\pm$  SEM from four separate experiments. Statistical analysis was performed using two-way ANOVA with Dunnett's *post hoc* test. \* =  $p < 0.05$ , \*\* =  $p < 0.01$ .

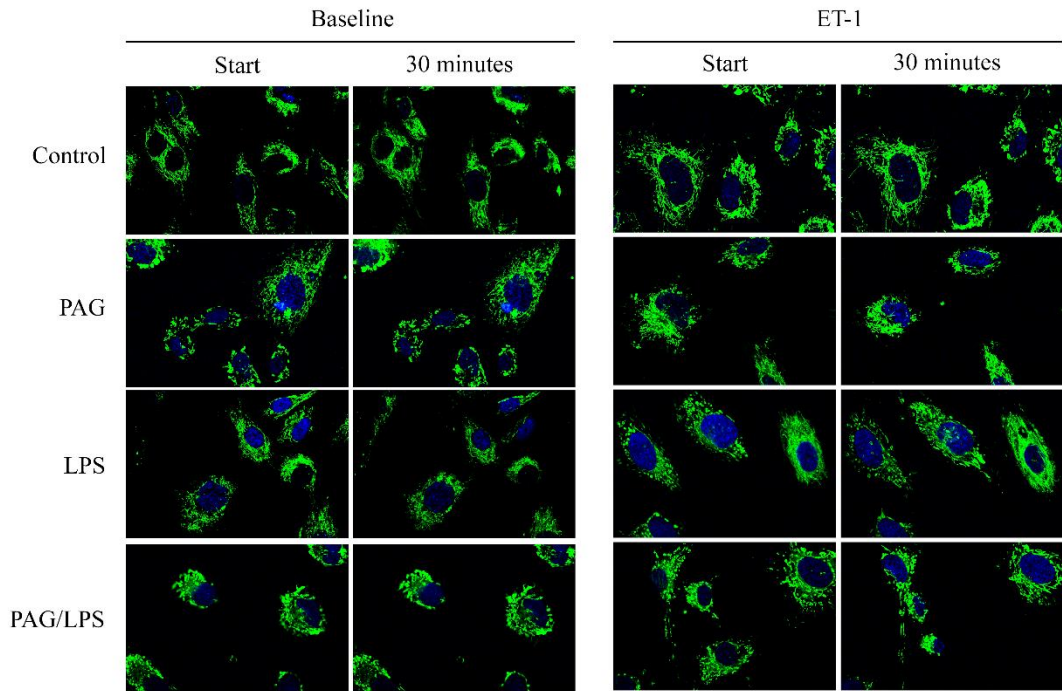


Figure 37: Effect of PAG on mitochondrial depolarization during ET-1 treatment in endotoxemia *in vitro*. HUVECs were pretreated with PAG for 30 minutes with or without LPS treatment for 6 hours. Mitochondria were visualized to determine the effect of ET-1 treatment on HUVECs treated with LPS for 6 hours, with or without the inhibitor of CSE, PAG. Representative images are shown before and after treatment with 10nM ET-1.

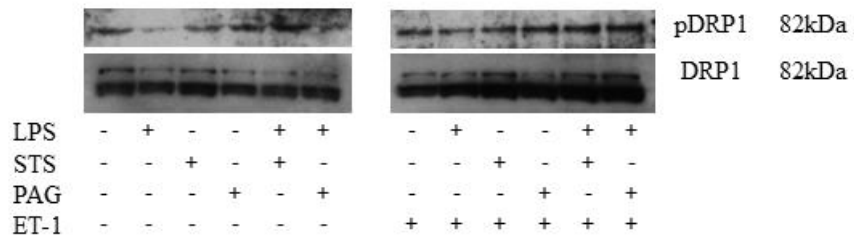


Figure 38: pDRP1 Western blot analysis *in vitro*. Total protein was determined by BCA. pDRP1 protein expression was determined by Western blot analysis on densities of pDRP1 were normalized to DRP1. Blots presented are representative of four separate experiments.

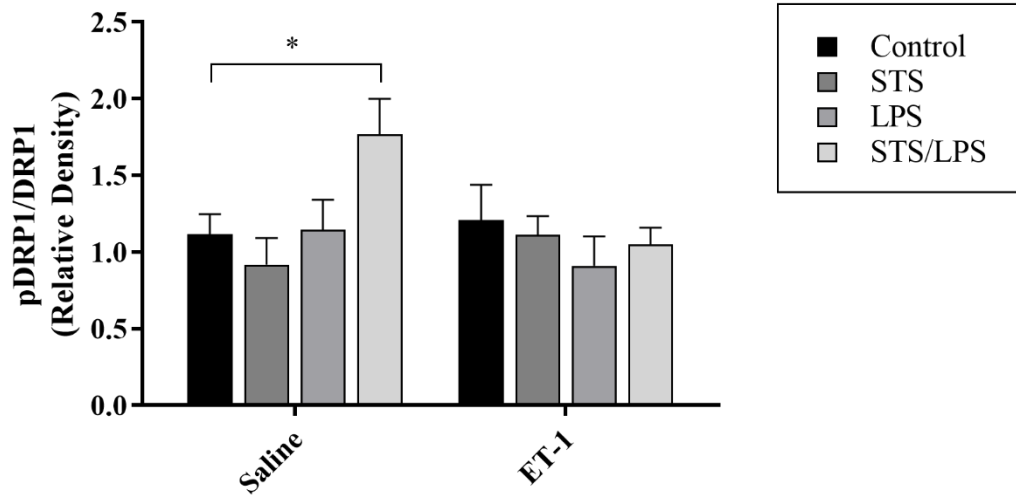


Figure 39: Effect of STS on mitochondrial fission *in vitro*. pDRP1 protein expression was determined by Western blot analysis and mitochondrial fission was expressed as the ratio of pDRP1 to DRP1 in HUVECs. STS treatment resulted in a significant decrease of mitochondrial fission in endotoxemia. Data are presented as the means  $\pm$  SEM from four separate experiments. Statistical analysis was performed using two-way ANOVA with Dunnett's *post hoc* test. \* =  $p < 0.05$ .

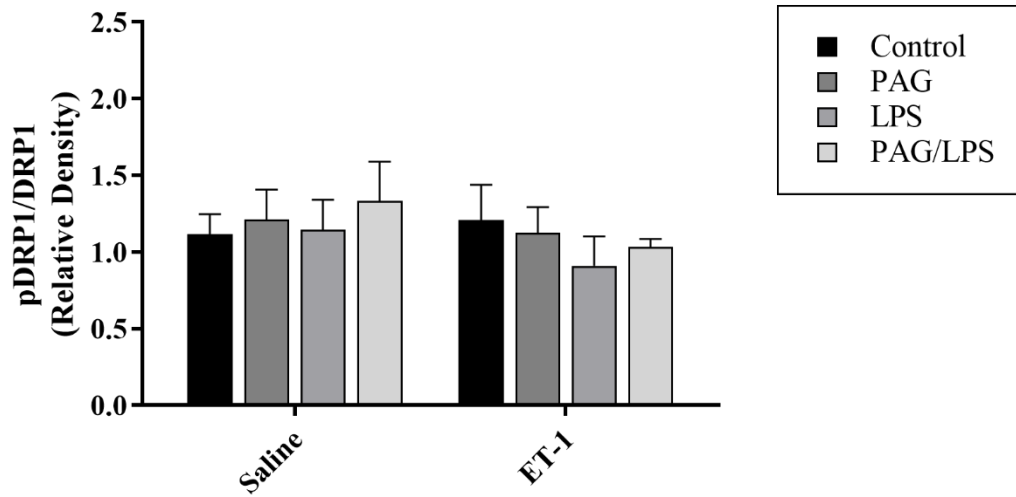


Figure 40: Effect of PAG on mitochondrial fission during ET-1 treatment during endotoxemia *in vitro*. HUVECs were pretreated with PAG for 30 minutes with or without LPS treatment for 6 hours. pDRP1 protein expression was determined by Western blot analysis and mitochondrial fission was expressed as the ratio of pDRP1 to DRP1. PAG had no effect among any treatment group. Data are presented as the means  $\pm$  SEM from four separate experiments.

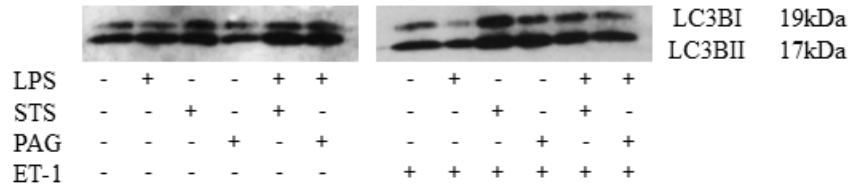


Figure 41: LC3B Western blot analysis *in vitro*. Total protein was determined by BCA. LC3BII and LC3BI protein expression was determined by Western blot analysis. Blots presented are representative of four separate experiments.

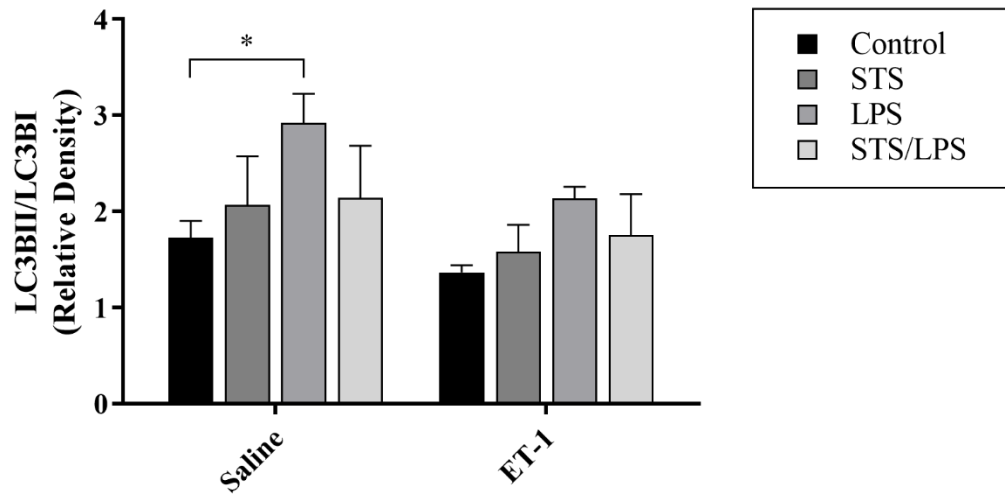


Figure 42: Effect of STS on mitophagy *in vitro*. LC3BII and LC3BI protein expression was determined by Western blot analysis on mitophagy was expressed as the ratio of LC3BII to LC3BI in HUVECs. LPS treatment for 6 hours resulting in a significant decrease of mitochondrial fission. Data are presented as the means  $\pm$  SEM from four separate experiments. Statistical analysis was performed using two-way ANOVA with Sidak's multiple comparison *post hoc* test. \* =  $p < 0.05$ .

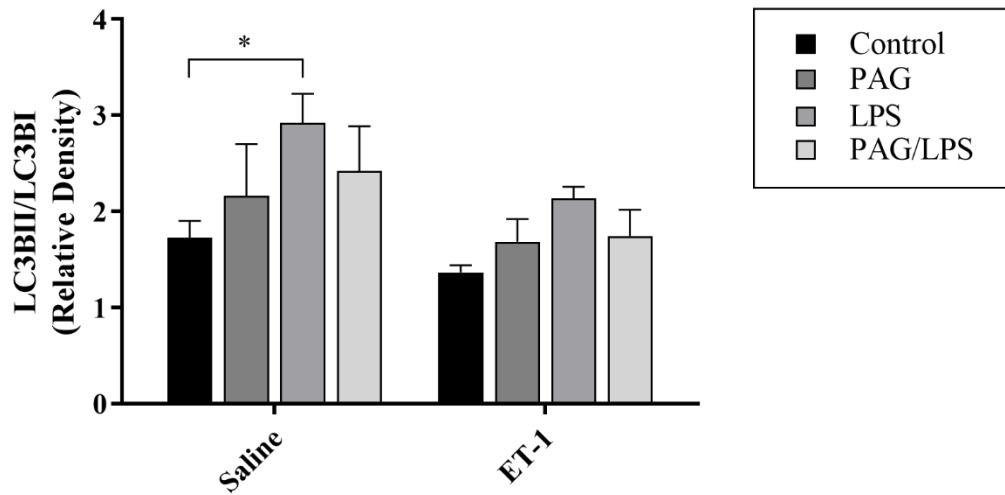


Figure 43: Effect of PAG on mitophagy during ET-1 treatment during endotoxemia *in vitro*. HUVECs were pretreated with PAG for 30 minutes with or without LPS treatment for 6 hours. LPS treatment for 6 hours resulting in a significant decrease of mitochondrial fission. Data are presented as the means  $\pm$  SEM from four separate experiments. Statistical analysis was performed using two-way ANOVA with Sidak's *post hoc* test. \* =  $p < 0.05$ .

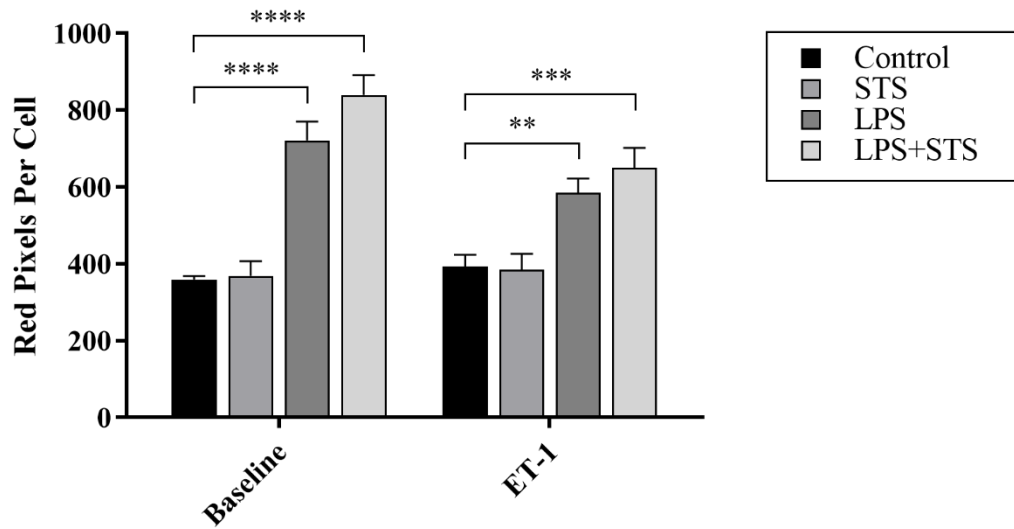


Figure 44: Effect of STS on F-actin stress fiber formation in endotoxemia *in vitro*. HUVECs were treated with the H<sub>2</sub>S donor, STS, for 30 minutes and cells were fixed, permeabilized, and loaded with Texas Red-X Phalloidin. LPS treatment for 6 hours resulting in a significant increase in F-actin stress fiber formation, quantified as the number of red pixels per cell. STS potentiated stress fiber formation in endotoxemia. Data are presented as the means  $\pm$  SEM from four separate experiments. Statistical analysis was performed using two-way ANOVA with Sidak's *post hoc* test. \*\* =  $p < 0.01$ , \*\*\* =  $p < 0.001$ , \*\*\*\* =  $p < 0.0001$ .

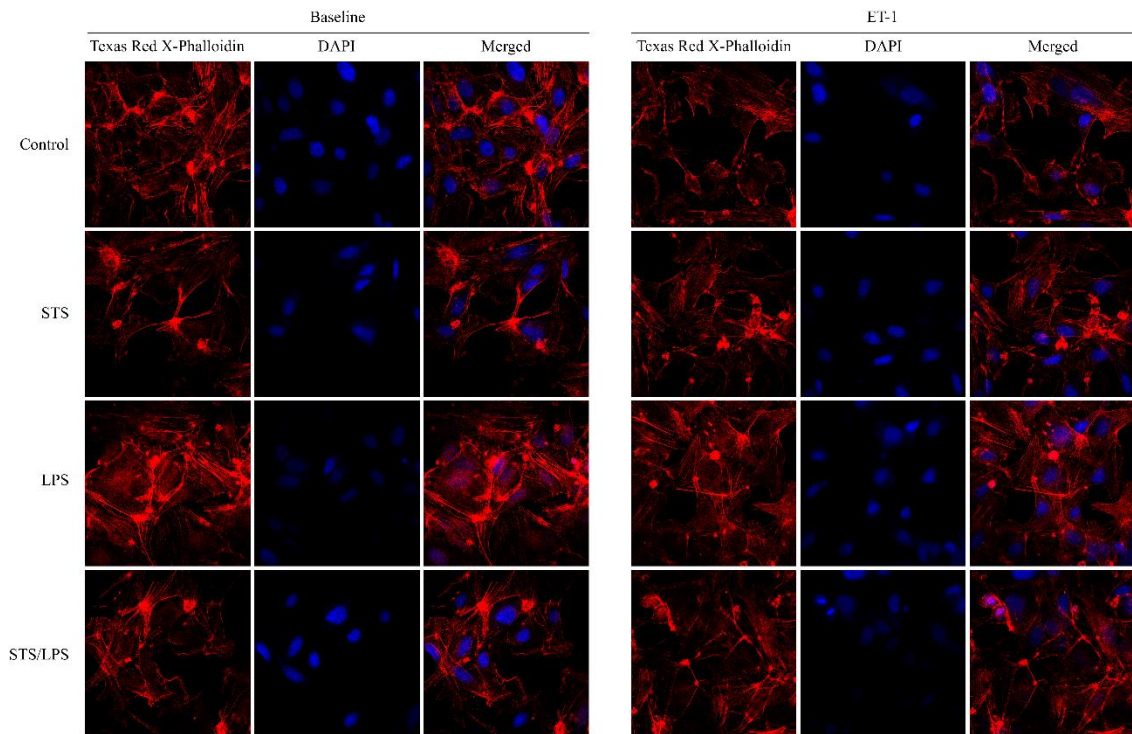


Figure 45: The effect of ET-1 and STS on F-actin stress fiber formation in endotoxemia *in vitro*. Stress fibers were visualized to determine the effect of ET-1 and STS on HUVECS treated with LPS for 6 hours. Representative images are shown with and without co-treatment with ET-1 (10nM) and STS (40 $\mu$ M).

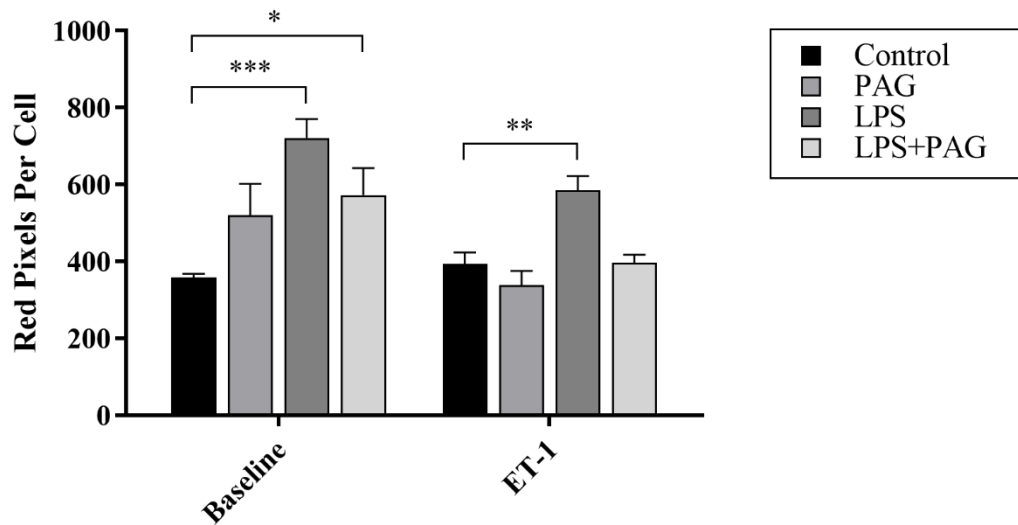


Figure 46: Effect of PAG pretreatment on F-actin stress fiber formation in endotoxemia *in vitro*. HUVECs were pretreated with PAG for 30 minutes with or without LPS treatment for 6 hours. Cells were then fixed, permeabilized, and loaded with Texas Red-X Phalloidin. LPS treatment for 6 hours resulting in a significant increase in F-actin stress fiber formation, quantified as the number of red pixels per cell. PAG pretreatment attenuated stress fiber formation in endotoxemia. Data are presented as the means  $\pm$  SEM from four separate experiments. Statistical analysis was performed using two-way ANOVA with repeated measures. \* =  $p < 0.05$ , \*\* =  $p < 0.01$ , \*\*\* =  $p < 0.001$ .

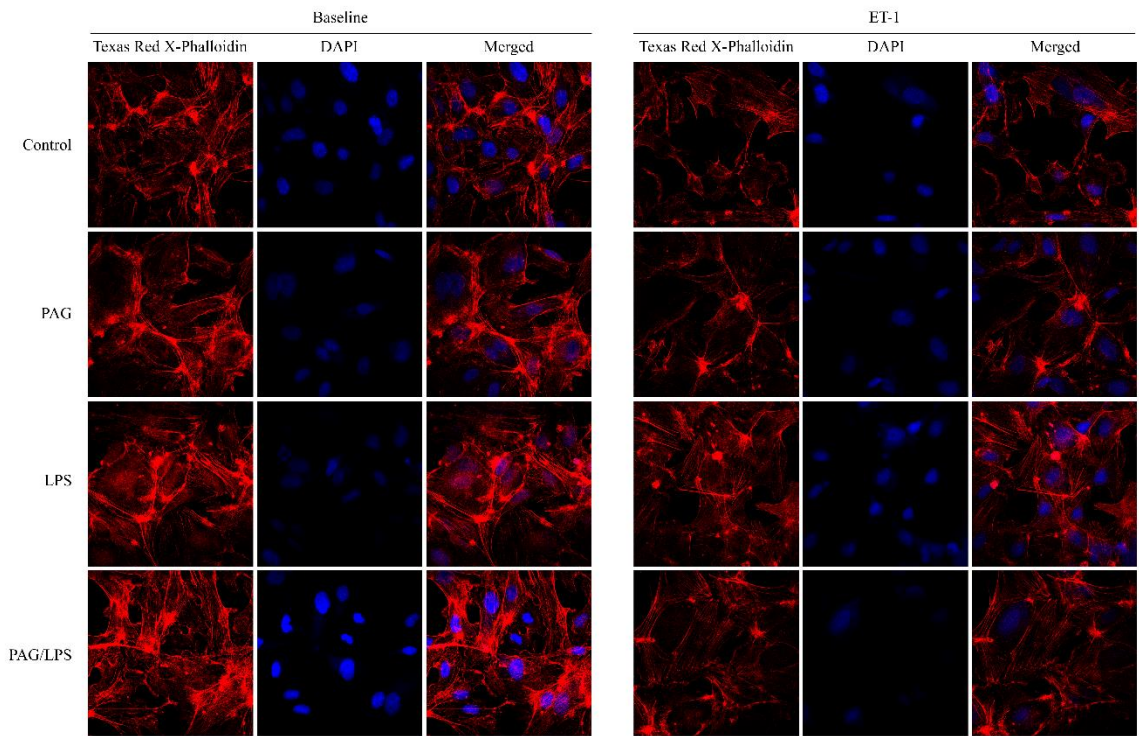


Figure 47: Effect of PAG on F-actin stress fiber formation during ET-1 treatment in endotoxemia *in vitro*. Cells were pretreated with PAG for 30 minutes with or without LPS treatment for 6 hours. Stress fibers were visualized to determine the effect of ET-1 treatment on HUVECs treated with LPS for 6 hours, with or without the inhibitor of CSE, PAG. Representative images are shown before and after treatment with 10nM ET-1.

## CHAPTER 6: DISCUSSION AND CONCLUSION

The role that hydrogen sulfide ( $H_2S$ ) plays in inflammation and disease is still not completely understood.  $H_2S$  exhibits paradoxical effects, displaying cytoprotection following hepatic ischemia/reperfusion (I/R) injury but is an important contributor to the progression of sepsis [102, 257]. It is well understood that hepatic dysfunction is a major complication that occurs in early sepsis [78]. Previous studies from our lab had a focus on the contributions of the first gaseous mediator, nitric oxide (NO), and its role in hepatic dysfunction during sepsis [42]. Research provided evidence that NO has an important role in sepsis but the complexity of the hepatic microenvironment in the progression of the disease is suggestive of a more dynamic pathophysiology. The similarities NO and  $H_2S$  share in the cardiovascular system have been reported by several studies [243]. However, these two gaseous mediators also have very major differences. More recent studies from our lab focused on the effect of  $H_2S$  in the liver during sepsis with emphasis on oxygen availability and microcirculatory dysfunction [161, 162]. Though NO effects on the liver vasculature have been thoroughly researched, there is still little investigation on the importance of  $H_2S$  in the hepatic microcirculation, particularly the molecular mechanisms underlying hepatic microcirculatory dysfunction following an inflammatory insult. Therefore, this dissertation focused on the effect of  $H_2S$  in the liver during sepsis with special emphasis on sex differences and mitochondrial dysfunction.

$H_2S$  is endogenously synthesized through the enzymatic activity of cystathionine  $\gamma$ -lyase (CSE) or cystathionine  $\beta$ -synthase (CBS), with CSE predominating  $H_2S$  production in the liver. Studies have shown that following lipopolysaccharide (LPS)

treatment or cecal ligation and puncture (CLP), hepatic CSE levels increase and result in a greater hepatic capacity to produce H<sub>2</sub>S [135, 257]. The liver is the major recipient of gastrointestinal blood flow and is exposed an exogenous source of H<sub>2</sub>S from sulfate-reducing bacteria in the gut [20]. Thus, the combination of endogenous and exogenous H<sub>2</sub>S results in elevated hepatic sulfide exposure during sepsis since it is likely that increased production of H<sub>2</sub>S from bacteria in the gut enters the portal circulation.

Colonic bacteria release large quantities of H<sub>2</sub>S, which would be highly toxic to tissues if allowed to permeate the colonic mucosa. However, the colonic mucosa possesses an efficient means of rapidly detoxifying H<sub>2</sub>S by conversion to thiosulfate. The detoxification activity of H<sub>2</sub>S has shown to be more than eight times greater for colonic mucosa than for non-colonic tissues, including liver tissue [70]. It was also reported that colonic epithelial cells metabolize H<sub>2</sub>S via mitochondrial oxidation, which serves as protection from toxic levels of sulfide derived from the gut bacteria [130]. The integrity of intestinal endothelial cells are compromised in both acute and chronic disease states and intestinal hyperpermeability has been observed in critically ill patients [188] and more specifically, in septic patients [117]. Damage to the intestinal cells in addition to elevated endogenous H<sub>2</sub>S concentrations has been demonstrated to reduce their ability to detoxify H<sub>2</sub>S, which may permit more diffusion of H<sub>2</sub>S into the hepatic portal circulation [233]. It was reported that colonic epithelial cells metabolize H<sub>2</sub>S via mitochondrial oxidation, which serves as protection from toxic levels of sulfide derived from the gut bacteria [130].

Cardiovascular dysfunction that occurs in early sepsis is characterized by a hyperdynamic state. Cardiac output is increased accompanied by modest peripheral

vasodilation, resulting in an increase in delivery oxygen to tissues [87]. However, despite the increase in delivered oxygen, it is well understood that liver dysfunction during sepsis is due, at least in part, to hypoxic injury [18, 101]. The presence of increased hepatic H<sub>2</sub>S levels requires greater H<sub>2</sub>S oxidation to prevent accumulation of the noxious gas to toxic levels. Consequently, oxygen is consumed in the process, leading to hypoxic stress and injury.

The main vasoregulatory action of H<sub>2</sub>S occurs through the activation of K<sub>ATP</sub> channels in vascular smooth muscle cells (VSMCs) and results in the relaxation of resistance vessels [264]. A vasodilatory effect of H<sub>2</sub>S on hepatic vasculature was first demonstrated using isolated livers from normal and cirrhotic rats [64]. Results from this study showed that H<sub>2</sub>S mitigated the vasopressor effects of norepinephrine (NE), independently of NO. The major complication in hepatic fibrosis and cirrhosis is portal hypertension because of increased intrahepatic resistance [13]. The vasodilatory effect of H<sub>2</sub>S may be beneficial as it acts in the portal venules to improve hepatic perfusion and reduce portal hypertension. However, during sepsis, dysfunction of the hepatic microcirculation vasculature occurs primarily at the sinusoidal level, which become hyperconstricted with heterogeneous blood flow.

In contrast to the systemic circulation where tissue perfusion is primarily regulated by VSMCs surrounding pre-capillary resistance vessels or the arterioles, perfusion in the liver is regulated at pre-sinusoidal and sinusoidal sites [17]. Like other vascular beds, vascular dysfunction of pre-sinusoidal resistance vessels following an inflammatory insult is characterized by hyporeactivity to catecholamines [180]. Numerous studies have shown that another important site of regulation of hepatic

perfusion is at the level of the sinusoid, particularly following inflammatory stress [42, 113, 181, 206]. Sinusoidal resistance is modulated primarily by the hepatic stellate cells (HSCs) [112, 260] and these specialized pericytes contract in response to vasoactive molecules including endothelin and angiotensin II [14, 95]. HSCs become activated following an inflammatory insult, leading to a switch to a myofibroblast-like phenotype and enhanced contraction in response to vasoconstrictors, especially endothelin-1 (ET-1) [198]. Furthermore, inflammatory stress leads to the uncoupling of ET-1 binding to ET<sub>B</sub> receptors and endothelial nitric oxide synthase (eNOS) activation in sinusoidal endothelial cells (SECs). This result is partly due to an increase in the inhibitory protein, caveolin-1 [128, 151, 207], and leads to an imbalance in the antagonistic relationship that exists between vasodilators and vasoconstrictors. Consequently, sinusoidal hyperconstriction ensues and leads to an increase in intrahepatic resistance in sepsis. Therefore, we investigated the effect of H<sub>2</sub>S on vascular responses at the sinusoidal level during ET-1 infusion during an endotoxic model of sepsis.

In agreement with previous studies from our lab, LPS potentiated the vasoconstrictive effect of ET-1 [162, 163]. During endotoxemia, the hepatic vasculature was hypersensitive to the vasoconstrictive effect of ET-1. Though we did not observe a statistically significant effect of H<sub>2</sub>S on ET-1-induced vasoconstriction in control or LPS-treated mice, there was a trend for increased constriction and an increase in heterogeneity, indicating an effect in the sinusoids.

Large amounts of exogenous H<sub>2</sub>S are typically required in *in vitro* experiments to elicit a biological effect, which may not be reflective of true H<sub>2</sub>S levels *in vitro* [69, 246]. Therefore, we used an inhibitor of CSE, DL-propargylglycine (PAG) [226] to determine

the effect of endogenous H<sub>2</sub>S during portal infusion of ET-1. We hypothesized that H<sub>2</sub>S causes sinusoidal constriction and is a contributor to the sensitization of the hepatic sinusoid to the vasoconstrictive effect of ET-1 during endotoxemia. To test this hypothesis, we used intravital confocal microscopy, which allows direct, real-time visualization of the hepatic sinusoids and assessment of sinusoidal perfusion *in vivo*. We did not observe any change in sinusoidal diameter with portal infusion of H<sub>2</sub>S, challenging previous reports from our lab that showed sinusoidal vasoconstriction accompanied with an increase in heterogeneity of sinusoidal perfusion [162]. However, previous studies were completed using sodium sulfide (Na<sub>2</sub>S) as the H<sub>2</sub>S donor, which has the potential to accumulate, in contrast to the donor used throughout this dissertation, which requires metabolization by tissues to produce H<sub>2</sub>S. Additionally, rats were used in previous studies, thus, there is the possibility that the observed effects are species-related. Since sinusoidal vasoconstriction plays a major role in hepatic microcirculatory failure, we investigated whether endogenous H<sub>2</sub>S contributes to the sensitization of the hepatic sinusoid to the vasoconstrictor effect of ET-1 in endotoxemia. Following co-infusion of H<sub>2</sub>S and ET-1, we observed a modest decrease, though not significant, in sinusoidal diameter. In mice treated with LPS, the effects of ET-1 were considerably different. LPS treatment lead to a greater reduction in sinusoidal diameter, including several occluded sinusoids. Moreover, sinusoidal constriction was associated with an increase in the heterogeneity of sinusoidal diameters. Increased sinusoidal heterogeneity is characterized by the presence of constricted sinusoids alongside dilated sinusoids. Increased sinusoidal heterogeneity of sinusoidal diameters is associated with heterogenous sinusoidal perfusion [107]. PAG treatment alone was similar to control for

sinusoidal diameter and heterogeneity of sinusoidal diameters. Pretreatment with PAG 30 minutes prior to surgical prep resulted in a significant improvement in sinusoidal blood flow, evidenced by less sinusoidal hyperconstriction, and less sinusoidal diameter heterogeneity following ET-1 infusion in endotoxemia.

We have shown that H<sub>2</sub>S exerts a vasoconstrictive effect on the hepatic sinusoid though the mechanism of H<sub>2</sub>S-induced vasoconstrictive remains unclear. The vasoconstrictive effect of H<sub>2</sub>S is the result of a shift in balance between vasodilators and vasoconstrictors, which regulate the contractility of hepatic stellate cells (HSCs). The effect of H<sub>2</sub>S in the sinusoid occurred rapidly, suggesting an acute effect. In addition, H<sub>2</sub>S activates K<sub>ATP</sub> channels and this is well documented in other studies. However, H<sub>2</sub>S also acts on calcium channels [153] and other ion channels by sulfhydration of cysteine residues [154]. Since H<sub>2</sub>S has been shown to increase cytosolic calcium in several cell types, including HUVECs [152], it is possible that H<sub>2</sub>S may directly cause HSC contraction through the activation of calcium channels and increased levels of cytosolic calcium. Furthermore, H<sub>2</sub>S has been shown to elicit a vasoconstrictive effect in isolated aortic rings via inhibition of cyclic adenosine monophosphate (cAMP). However, the Rho-kinase/ROCK pathway has a greater influence on HSC contractility than in smooth muscle cells [111, 215]. cAMP accumulation inhibits the Rho-kinase/ROCK pathway in HSCs and leads to the decreased contractility in response to ET-1 [213]. Additionally, ET<sub>A</sub> receptor sensitivity to ET-1 is reduced, resulting in less substrate/receptor binding and subsequently, less constriction [193]. Thus, the vasoconstrictive effect of H<sub>2</sub>S in the hepatic sinusoid may be the result of inhibiting cAMP accumulation in HSCs.

Our lab has focused on the importance of NO in hepatic microvascular dysfunction during sepsis and several studies have provided evidence for a complex relationship between NO and H<sub>2</sub>S. Specifically, *in vitro* studies have shown that a vasoinactive nitrosothiol forms from the interaction between NO and H<sub>2</sub>S. Therefore, H<sub>2</sub>S-induced vasoconstriction may be the result of a reduction in bioavailability of NO. This hypothesis is fascinating when applied to the septic liver because H<sub>2</sub>S production has been shown to be increased while NO synthesis is decreased and together, this imbalance contributes to vascular dysfunction. In support of this hypothesis, several studies have shown the involvement of NO in H<sub>2</sub>S-induced vasoconstriction. In isolated aortic rings, relaxation in response to acetylcholine is dependent of NO production by an intact endothelium [84]. Stimulation with an H<sub>2</sub>S donor, sodium hydrosulfide (NaHS), mitigates the vasorelaxant effect of acetylcholine but the vasopressor effect of H<sub>2</sub>S is lost following removal of the endothelium, suggesting an interaction with endothelial-derived NO [139]. A similar effect is observed when using the precursor of H<sub>2</sub>S, L-cysteine. L-cysteine attenuates vascular relaxation in response to acetylcholine and sodium nitroprusside, a nitric oxide donor [61, 103]. In *in vivo* studies, it was demonstrated that the vasoconstrictive effect of H<sub>2</sub>S is concentration-dependent. Low dose intravenous infusion of NaHS resulted in a transient increase in mean arterial pressure (MAP) in rats whereas high doses resulted in hypotension [6]. However, no increase in MAP was observed following treatment with a NOS inhibitor. Thus, an interaction between NO and H<sub>2</sub>S exists and a reduction in the bioavailability of NO through an interaction with H<sub>2</sub>S is of mechanistic importance in the hepatic sinusoid during sepsis.

Involved in the pathogenesis of sepsis are the activation of several responses, including inflammatory, immune, hormonal, metabolic, and bioenergetic. One of the pivotal factors in these processes is the increase of reactive oxygen species (ROS) in conjunction with antioxidant system failure. This results in irreversible oxidative stress and leads to mitochondrial dysfunction. In normal physiological conditions, ROS and antioxidant systems are in a redox balance and the loss of this balance leads to a state of oxidative stress, which is an important promoter of systemic inflammatory response. A systemic inflammatory response in conjunction with a loss of redox balance during sepsis, may lead to continuing and irreversible mitochondrial damage and dysfunction, energy depletion, and hypoxia, progressing to septic shock, severe sepsis, multiple organ failure, and death.

The three gaseous mediators, NO, carbon monoxide (CO), and H<sub>2</sub>S, are all important regulators of mitochondrial signaling [15, 132, 242]. The effects of these gaseous mediators are concentration-dependent, generating high concentrations in the pathogenesis of sepsis, resulting in greater ROS production and inhibition of mitochondrial respiration. Mitochondria can also trigger cell death pathways when ATP levels fall below a certain threshold or when mitochondria become damaged, releasing cytochrome *c* into the cytoplasm [93]. Since mitochondrial function can be assessed by monitoring changes in mitochondrial membrane potential, we utilized a cationic fluorescent stain as an indicator of mitochondrial health. Mitochondrial structural damage and dysfunction are recognized as important factors in the progression of sepsis and are associated with the severity of organ dysfunction and disease outcome [12]. Following infusion of H<sub>2</sub>S, we did not observe any significant changes in mitochondrial

membrane potential among any of the treatment groups *in vivo*. However, upon separation of male and female data, we observed mitochondrial membrane depolarization in males but not females, implicating a difference among the sexes for mitochondrial health. Further investigation of mitochondrial dynamics, namely fission and mitophagy, also showed sex-related differences. Males showed no differences among any of the treatment groups whereas females showed decreased dynamin-related protein 1 (DRP1) recruitment to the mitochondria, indicating a reduction in mitochondrial fission with inhibition of endogenous H<sub>2</sub>S. This observation suggests a protective effect with endogenous H<sub>2</sub>S inhibition since an imbalance between fusion and fission in sepsis has been reported [80]. Interestingly, portal infusion of ET-1 did not have any significant effect for any treatment for either sex for DRP1 recruitment to the mitochondria. It has been suggested that ET-1 results in the upregulation of Rho-associated protein kinase 1 (ROCK1) expression, which increases LIMK2 expression and impairs DRP1-mediated mitochondrial fission in neuronal death [118]. However, we infused ET-1 for a period of just 10 minutes, which is unlikely enough time to elicit a downstream effect on LIMK2 expression. It appears that ET-1 has a role in preventing DRP1 recruitment to the mitochondria but additional studies are needed to determine if this is true.

One of the primary targets of H<sub>2</sub>S in the mammalian system are the K<sub>ATP</sub> channels [126, 155, 177, 225, 264]. However, our knowledge of the effect of H<sub>2</sub>S on mitochondrial K<sub>ATP</sub> (mito-K<sub>ATP</sub>) channels remain incomplete. We show that exogenous H<sub>2</sub>S do not have a significant effect on total ROS at any concentration of STS administered. However, pretreatment with a specific mito-K<sub>ATP</sub> channel inhibitor resulted in a biphasic dose response curve for ROS production at all concentrations of

H<sub>2</sub>S and inhibition of mito-K<sub>ATP</sub> channels potentiated the production of ROS, particularly in the mitochondria. Therefore, the opening of the mito-K<sub>ATP</sub> channels plays an important role in the regulation of mitochondrial function and attenuates oxidative stress. Sulfur quinone reductase (SQR) is another primary target of H<sub>2</sub>S in the mitochondria, which oxidizes H<sub>2</sub>S and feeds additional electrons into the mitochondrial respiratory chain [82] and increases ROS production at the site of complex III [187]. ROS from H<sub>2</sub>S oxidation by SQR could also be a contributor to the increased ROS we observed in our studies.

Mitochondrial dysfunction in critical care diseases are frequently induced following interaction with NO and CO. Formed endogenously by NO synthase (NOS) and heme oxygenase (HO), respectively, which are both upregulated in sepsis [23, 240] and results in increased NO and CO generation. Pathogen-associated molecular patterns (PAMPs) and damage-associated molecular patterns (DAMPs) initiate inflammation. Injury to the tissues results, leading to the loss of cellular integrity and endothelial barrier function. Both NO and CO contribute to further aggravation of compromised tissue through vasoactive effects [123]. In sepsis, tissue hypoxia is caused by inflammatory mediators, which induce vasodilation and tissue edema, leading to inadequate tissue perfusion. NO and CO cause vasodilation through interaction with soluble guanylate cyclase (sGC) [98, 140]. In hypoxia, HO is induced via hypoxia-inducible factor 1 $\alpha$  (HIF-1 $\alpha$ ), resulting in enhanced CO generation [134]. Compounds containing transition metals are the major targets of NO and CO in the body. Thus, cytochrome *c* oxidase (complex IV) is the major target of NO and CO in the mitochondria, resulting in the inhibition of the protein complex and increased ROS production by the mitochondria. In

addition, NO can impair mitochondrial function through the formation of reactive nitrogen species (RNS), specifically, peroxynitrite, which causes irreversible oxidative damage to mitochondrial proteins complexes. Such damage can facilitate the opening of the mitochondrial permeability transition pore, disruption of ATP production, and apoptosis [123]. NO also stimulates ROS production in a feed-forward manner where ROS then upregulates inducible nitric oxide synthase (iNOS), leading to increased NO levels and subsequent ROS generation [245]. Like NO and CO, H<sub>2</sub>S elicits effects on the activity of the mitochondrial respiratory chain, serving as both a substrate and an inhibitor. At low concentrations, H<sub>2</sub>S is a substrate and donates electrons at the level of ubiquinone via SQR and stimulates oxidative phosphorylation and increases ATP generation. However, at high concentrations, H<sub>2</sub>S inhibits complex IV. In contrast to NO and CO, H<sub>2</sub>S inhibition of complex IV is non-competitive with respect to oxygen [182].

Given such similarities, the three gaseous mediators are expected to interact with and modulate each other. Both NO and CO can bind sGC, increasing cyclic guanosine monophosphate (cGMP), and triggering downstream effects, including mitochondrial biogenesis [43, 160, 224, 237]. Research evidence suggests an additional point of interaction involving H<sub>2</sub>S modulation of cGMP signaling by NO [186]. NO and CO have also been shown to prevent HIF-1 $\alpha$  stabilization [96], which occurs when oxygen availability to cells is low but the cells fail to detect the drop in oxygen supply due to inhibition of oxidative phosphorylation by NO and CO and subsequent decrease oxygen consumption. Other studies found that NO is a modulator of CO and H<sub>2</sub>S production. NO increases CO generation by inducing HO-1 [27] and increases H<sub>2</sub>S by increasing

CSE expression [264]. Unfortunately, very few studies have investigated the interaction between all three gaseous mediators on the mitochondria. Further work is needed to characterize the cross-talk between NO, CO, and H<sub>2</sub>S.

We furthered our mitochondrial animal studies *in vitro* using confocal intravital microscopy through utilization of a cationic fluorophore to estimate mitochondrial polarization. Similar to what was observed in male mice, endotoxin treatment for 6 hours resulted in a significant decrease in mitochondrial membrane polarization in cultured human umbilical vein endothelial cells (HUVECs). We did not investigate any sex differences in our *in vitro* studies but male HUVECs were used in all experiments. Further experimentation using cultured female HUVECs will need to be completed to elucidate any differences related to sex. On the other hand, if the sex differences are the result of hormones, such as estrogen, rather than the X versus Y chromosome, such changes would not be evident in cell culture. To further our investigation of exogenous H<sub>2</sub>S on mitochondrial fission and mitophagy. Phosphorylated DRP1 (pDRP1) protein expression was shown to be upregulated in endotoxemia. Exogenous but not endogenous H<sub>2</sub>S did appear to have a role in modulating the activation of mitochondrial fission protein, DRP1. This suggests that the effects of H<sub>2</sub>S *in vivo* are likely mediated by H<sub>2</sub>S produced by other cell types, rather than by the endothelial cells themselves. Hepatocytes and colonic epithelium are major sites of H<sub>2</sub>S oxidation, not production. However, CSE is expressed & upregulated in hepatocytes and poorly expressed in endothelial cells. As observed in our *in vitro* studies, ET-1 did not have any significant effect for any treatment, suggesting the possibility that the vasoconstrictive peptide may

preventing recruitment of DRP1 to the mitochondria. Additional studies are needed to further elucidate this.

In conclusion, the aim of this dissertation was to investigate the effect of H<sub>2</sub>S in the liver during sepsis with emphasis on microvascular and mitochondrial dysfunction. In the first half, we show that the H<sub>2</sub>S is a major contributor to the hypersensitization of the hepatic sinusoid to the constrictor effect of ET-1 during an endotoxemia model of sepsis, which leads to heterogeneity of blood flow perfusion and tissue hypoxia. Furthermore, depolarization of the mitochondrial membrane potential occurs in response to LPS treatment and H<sub>2</sub>S influences mitophagy. Moreover, we show for the first time that the hypersensitization of the hepatic sinusoid and alterations in mitochondrial dynamics are sex-related. In the second half, we provide molecular insights into the causes of vascular dysregulation in response to H<sub>2</sub>S and ET-1, in endotoxemia. We show that H<sub>2</sub>S appears to directly increase ROS but simultaneous activation of the mito-K<sub>ATP</sub> channels attenuates oxidative stress primarily in the mitochondria. Our *in vitro* studies show that LPS treatment leads to mitochondrial membrane depolarization and assembly of mitophagy machinery and the mitochondrial fission protein marker, DRP1, is activated with exogenous H<sub>2</sub>S in endotoxemia. Moreover, we show that H<sub>2</sub>S contributes to actin stress fiber formation, which leads to vascular permeability and dysfunction, in endotoxemia.

The findings of this research have translational potential. Altering our model of sepsis from endotoxemia to cecal ligation and puncture (CLP) and completing the same experimental procedures would make our study more clinically relevant. While studies using an endotoxic model of sepsis have provided a significant amount of knowledge on

the molecular mechanisms involved in the progression of the disease, it does not reflect the complex pathophysiology observed in most cases of sepsis in humans [195]. Several similarities between LPS injection and clinical sepsis exist, including similar pathophysiologic changes. However, there are also significant differences in the production of inflammatory mediators, such as the cytokines. In endotoxin models, the explosive release of cytokines into the circulation was shown to be reproducible in all species tested, including humans. This resulted in a series of anti-cytokine clinical trials, which all failed [2, 11, 65, 169]. Differences in various models of sepsis have been previously discussed [52, 63, 205]. The endotoxin model of sepsis was directly compared with a focus of infection model, or CLP [194]. CLP is a carefully characterized model of infection and was demonstrated to respond to fluid resuscitation and antibiotics [158], as observed in septic human patients. Although mortality and hematologic alterations in response to CLP and endotoxin injection were similar, the cytokine response showed significant differences. The LPS injection model of sepsis do not adequately reproduce the multifaceted, highly complex, and regulated inflammatory response of the human condition. Validation of the observations made here on an injectable model of endotoxemia in the more relevant CLP model will most likely further our understanding of clinical sepsis. Since one of the findings of this research was the attenuation of ROS production via H<sub>2</sub>S-activation of mito-K<sub>ATP</sub> channels, a potential therapeutic approach is to administer an activator of mito-K<sub>ATP</sub> channels, such as glibenclamide. Furthermore, animals must be appropriately treated with antibiotics and fluid resuscitation to mimic standard clinical therapeutic measures.

Overall, these results provide evidence for several points: 1) the deleterious effects of H<sub>2</sub>S on the microcirculation is a contributor to the deleterious effects of hepatic microcirculatory dysfunction in sepsis, 2) the effects of H<sub>2</sub>S on the hepatic microvasculature and perfusion of blood flow is a sexual dimorphism, and 3) high concentrations of H<sub>2</sub>S lead to increased ROS production which is attenuated through the activation of mito-K<sub>ATP</sub> channels since failure to activate mito-K<sub>ATP</sub> channels was shown to exacerbate ROS production by the mitochondria (Figure 48). Our results provide molecular insights into several potential therapeutic avenues for the treatment of sepsis.

6.1 Figure

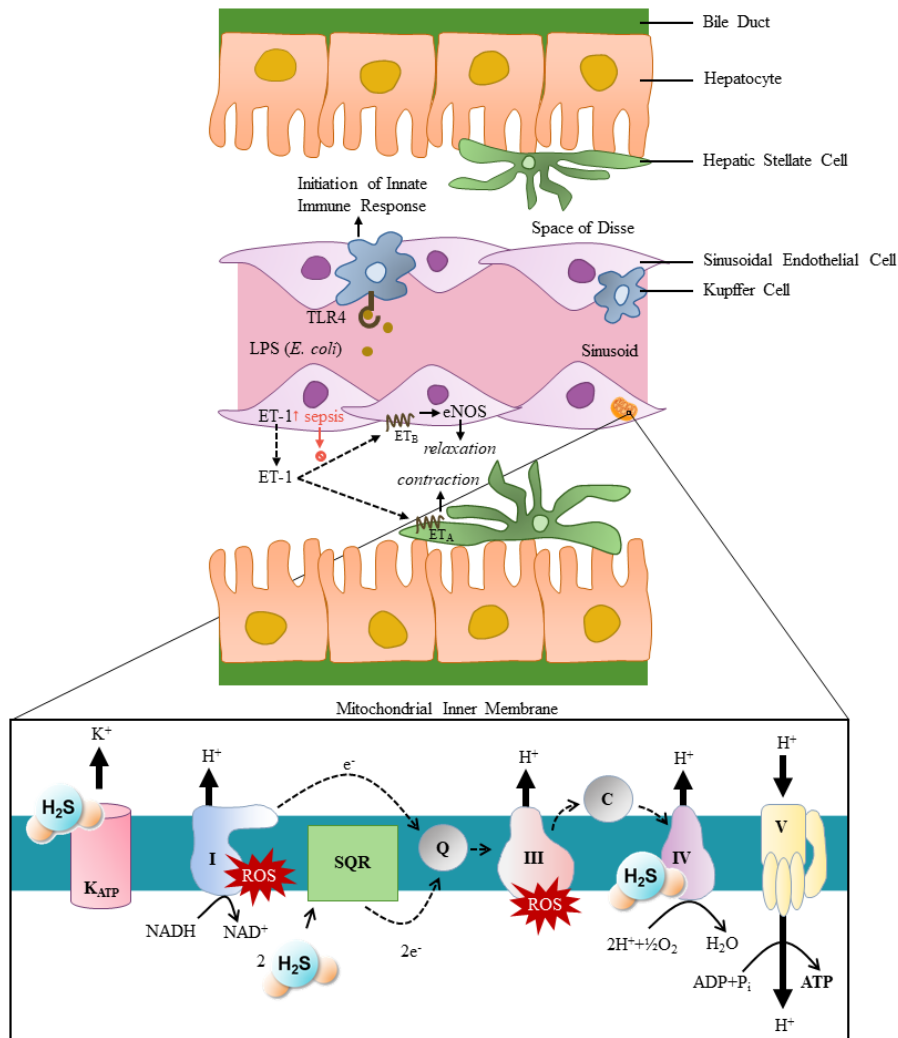


Figure 48: H<sub>2</sub>S and ET-1 effects on the septic liver. TLR4 receptors on Kupffer cells recognize PAMPs (LPS from *E. coli* in this study) and initiate an innate immune response. Under normal physiological conditions, vasoconstrictor peptide, ET-1, is in balance with vasodilator, NO. ET-1 binding to ET<sub>A</sub> receptors on HSCs promote constriction while binding to ET<sub>B</sub> receptors on SECs promote vasodilation via coupling with eNOS activation. However, in sepsis, the balance between ET-1 and NO is tipped, resulting in hypersensitization of the hepatic sinusoid to the vasoconstrictive effect of ET-1. This imbalance is mostly due to the uncoupling of ET-1 binding to ET<sub>B</sub> receptors from eNOS activation. In addition, H<sub>2</sub>S levels are increased in sepsis. H<sub>2</sub>S activation of mito-K<sub>ATP</sub> channels serves as a protective effect against ROS production by the mitochondria but excessive H<sub>2</sub>S elicits an inhibitory effect on complex IV of the respiratory chain, leading to decreased ATP production, ROS production, cytochrome *c* release, and apoptosis.

## REFERENCES

1. Abe, K. and H. Kimura, The possible role of hydrogen sulfide as an endogenous neuromodulator. *J Neurosci*, 1996. **16**(3): p. 1066-71.
2. Abraham, E., et al., Double-blind randomised controlled trial of monoclonal antibody to human tumour necrosis factor in treatment of septic shock. NORASEPT II Study Group. *Lancet*, 1998. **351**(9107): p. 929-33.
3. Adrie, C., et al., Influence of gender on the outcome of severe sepsis: a reappraisal. *Chest*, 2007. **132**(6): p. 1786-93.
4. Akao, M., et al., Mitochondrial ATP-sensitive potassium channels inhibit apoptosis induced by oxidative stress in cardiac cells. *Circ Res*, 2001. **88**(12): p. 1267-75.
5. Alam, I., et al., Hepatic tissue endothelin-1 levels in chronic liver disease correlate with disease severity and ascites. *Am J Gastroenterol*, 2000. **95**(1): p. 199-203.
6. Ali, M.Y., et al., Regulation of vascular nitric oxide in vitro and in vivo; a new role for endogenous hydrogen sulphide? *Br J Pharmacol*, 2006. **149**(6): p. 625-34.
7. Alp, N.J. and K.M. Channon, Regulation of endothelial nitric oxide synthase by tetrahydrobiopterin in vascular disease. *Arterioscler Thromb Vasc Biol*, 2004. **24**(3): p. 413-20.
8. Andrades, M., et al., Antioxidant treatment reverses organ failure in rat model of sepsis: role of antioxidant enzymes imbalance, neutrophil infiltration, and oxidative stress. *J Surg Res*, 2011. **167**(2): p. e307-13.
9. Ang, S.F., et al., Hydrogen sulfide and neurogenic inflammation in polymicrobial sepsis: involvement of substance P and ERK-NF-kappaB signaling. *PLoS One*, 2011. **6**(9): p. e24535.
10. Angus, D.C., et al., Epidemiology of severe sepsis in the United States: analysis of incidence, outcome, and associated costs of care. *Crit Care Med*, 2001. **29**(7): p. 1303-10.
11. Arndt, P. and E. Abraham, Immunological therapy of sepsis: experimental therapies. *Intensive Care Med*, 2001. **27 Suppl 1**: p. S104-15.
12. Azevedo, L.C., Mitochondrial dysfunction during sepsis. *Endocr Metab Immune Disord Drug Targets*, 2010. **10**(3): p. 214-23.
13. Bari, K. and G. Garcia-Tsao, Treatment of portal hypertension. *World J Gastroenterol*, 2012. **18**(11): p. 1166-75.

14. Bataller, R., et al., Angiotensin II induces contraction and proliferation of human hepatic stellate cells. *Gastroenterology*, 2000. **118**(6): p. 1149-56.
15. Bauer, I. and B.H. Pannen, Bench-to-bedside review: Carbon monoxide--from mitochondrial poisoning to therapeutic use. *Crit Care*, 2009. **13**(4): p. 220.
16. Bauer, M., et al., Functional significance of endothelin B receptors in mediating sinusoidal and extrasinusoidal effects of endothelins in the intact rat liver. *Hepatology*, 2000. **31**(4): p. 937-47.
17. Bauer, M., et al., ET-1 induced alterations of hepatic microcirculation: sinusoidal and extrasinusoidal sites of action. *Am J Physiol*, 1994. **267**(1 Pt 1): p. G143-9.
18. Baveja, R., et al., Potentiated hepatic microcirculatory response to endothelin-1 during polymicrobial sepsis. *Shock*, 2002. **18**(5): p. 415-22.
19. Baveja, R., et al., Endothelin 1 impairs oxygen delivery in livers from LPS-primed animals. *Shock*, 2002. **17**(5): p. 383-8.
20. Blachier, F., et al., Luminal sulfide and large intestine mucosa: friend or foe? *Amino Acids*, 2010. **39**(2): p. 335-47.
21. Boekstegers, P., et al., Peripheral oxygen availability within skeletal muscle in sepsis and septic shock: comparison to limited infection and cardiogenic shock. *Infection*, 1991. **19**(5): p. 317-23.
22. Bogatcheva, N.V. and A.D. Verin, The role of cytoskeleton in the regulation of vascular endothelial barrier function. *Microvasc Res*, 2008. **76**(3): p. 202-7.
23. Bogdan, C., Nitric oxide synthase in innate and adaptive immunity: an update. *Trends Immunol*, 2015. **36**(3): p. 161-78.
24. Boldogh, I.R. and L.A. Pon, Interactions of mitochondria with the actin cytoskeleton. *Biochim Biophys Acta*, 2006. **1763**(5-6): p. 450-62.
25. Bone, R.C., et al., Definitions for sepsis and organ failure and guidelines for the use of innovative therapies in sepsis. The ACCP/SCCM Consensus Conference Committee. American College of Chest Physicians/Society of Critical Care Medicine. *Chest*, 1992. **101**(6): p. 1644-55.
26. Bouillaud, F. and F. Blachier, Mitochondria and sulfide: a very old story of poisoning, feeding, and signaling? *Antioxid Redox Signal*, 2011. **15**(2): p. 379-91.
27. Bouton, C. and B. Demple, Nitric oxide-inducible expression of heme oxygenase-1 in human cells. Translation-independent stabilization of the mRNA and

- evidence for direct action of nitric oxide. *J Biol Chem*, 2000. **275**(42): p. 32688-93.
28. Brealey, D., et al., Association between mitochondrial dysfunction and severity and outcome of septic shock. *Lancet*, 2002. **360**(9328): p. 219-23.
  29. Brenner, C., et al., Decoding cell death signals in liver inflammation. *J Hepatol*, 2013. **59**(3): p. 583-94.
  30. Bukovska, G., V. Kery, and J.P. Kraus, Expression of human cystathionine beta-synthase in *Escherichia coli*: purification and characterization. *Protein Expr Purif*, 1994. **5**(5): p. 442-8.
  31. Calo, L., et al., Mitochondrial dynamics: an emerging paradigm in ischemia-reperfusion injury. *Curr Pharm Des*, 2013. **19**(39): p. 6848-57.
  32. Calvano, S.E., et al., A network-based analysis of systemic inflammation in humans. *Nature*, 2005. **437**(7061): p. 1032-7.
  33. Cameron, D.E., et al., Hepatocellular dysfunction in early sepsis despite increased hepatic blood flow. *Adv Shock Res*, 1981. **6**: p. 65-74.
  34. Carre, J.E., et al., Survival in critical illness is associated with early activation of mitochondrial biogenesis. *Am J Respir Crit Care Med*, 2010. **182**(6): p. 745-51.
  35. Chan, D.C., Fusion and fission: interlinked processes critical for mitochondrial health. *Annu Rev Genet*, 2012. **46**: p. 265-87.
  36. Chan, D.C., Mitochondria: dynamic organelles in disease, aging, and development. *Cell*, 2006. **125**(7): p. 1241-52.
  37. Chaudry, I.H., et al., Altered hepatocellular active transport. An early change in peritonitis. *Arch Surg*, 1982. **117**(2): p. 151-7.
  38. Cheng, Y., et al., Hydrogen sulfide-induced relaxation of resistance mesenteric artery beds of rats. *Am J Physiol Heart Circ Physiol*, 2004. **287**(5): p. H2316-23.
  39. Chiku, T., et al., H<sub>2</sub>S biogenesis by human cystathionine gamma-lyase leads to the novel sulfur metabolites lanthionine and homolanthionine and is responsive to the grade of hyperhomocysteinemia. *J Biol Chem*, 2009. **284**(17): p. 11601-12.
  40. Chun, K., et al., Microcirculatory failure determines lethal hepatocyte injury in ischemic/reperfused rat livers. *Shock*, 1994. **1**(1): p. 3-9.
  41. Clemens, M.G., et al., Regulation of glucose production from lactate in experimental sepsis. *Am J Physiol*, 1983. **244**(6): p. R794-800.

42. Clemens, M.G. and J.X. Zhang, Regulation of sinusoidal perfusion: in vivo methodology and control by endothelins. *Semin Liver Dis*, 1999. **19**(4): p. 383-96.
43. Clementi, E. and E. Nisoli, Nitric oxide and mitochondrial biogenesis: a key to long-term regulation of cellular metabolism. *Comp Biochem Physiol A Mol Integr Physiol*, 2005. **142**(2): p. 102-10.
44. Coletta, C. and C. Szabo, Potential role of hydrogen sulfide in the pathogenesis of vascular dysfunction in septic shock. *Curr Vasc Pharmacol*, 2013. **11**(2): p. 208-21.
45. Collin, M., et al., Inhibition of endogenous hydrogen sulfide formation reduces the organ injury caused by endotoxemia. *Br J Pharmacol*, 2005. **146**(4): p. 498-505.
46. Combes, A., et al., Gender impact on the outcomes of critically ill patients with nosocomial infections. *Crit Care Med*, 2009. **37**(9): p. 2506-11.
47. Cosentino, F. and Z.S. Katusic, Tetrahydrobiopterin and dysfunction of endothelial nitric oxide synthase in coronary arteries. *Circulation*, 1995. **91**(1): p. 139-44.
48. Cowley, H.C., et al., Plasma antioxidant potential in severe sepsis: a comparison of survivors and nonsurvivors. *Crit Care Med*, 1996. **24**(7): p. 1179-83.
49. d'Emmanuele di Villa Bianca, R., et al., Hydrogen sulfide-induced dual vascular effect involves arachidonic acid cascade in rat mesenteric arterial bed. *J Pharmacol Exp Ther*, 2011. **337**(1): p. 59-64.
50. Dahn, M.S., et al., Hepatic parenchymal oxygen tension following injury and sepsis. *Arch Surg*, 1990. **125**(4): p. 441-3.
51. de Punder, K. and L. Pruijboom, Stress induces endotoxemia and low-grade inflammation by increasing barrier permeability. *Front Immunol*, 2015. **6**: p. 223.
52. Deitch, E.A., Animal models of sepsis and shock: a review and lessons learned. *Shock*, 1998. **9**(1): p. 1-11.
53. Dejana, E. and D. Vestweber, The role of VE-cadherin in vascular morphogenesis and permeability control. *Prog Mol Biol Transl Sci*, 2013. **116**: p. 119-44.
54. DeLeon, E.R., G.F. Stoy, and K.R. Olson, Passive loss of hydrogen sulfide in biological experiments. *Anal Biochem*, 2012. **421**(1): p. 203-7.

55. Deng, S.Y., et al., Role of interferon regulatory factor-1 in lipopolysaccharide-induced mitochondrial damage and oxidative stress responses in macrophages. *Int J Mol Med*, 2017. **40**(4): p. 1261-1269.
56. Dimmer, K.S. and L. Scorrano, (De)constructing mitochondria: what for? *Physiology (Bethesda)*, 2006. **21**: p. 233-41.
57. Dos Santos, P., et al., Mechanisms by which opening the mitochondrial ATP-sensitive K(+) channel protects the ischemic heart. *Am J Physiol Heart Circ Physiol*, 2002. **283**(1): p. H284-95.
58. Droge, W., Free radicals in the physiological control of cell function. *Physiol Rev*, 2002. **82**(1): p. 47-95.
59. Dudek, S.M. and J.G. Garcia, Cytoskeletal regulation of pulmonary vascular permeability. *J Appl Physiol (1985)*, 2001. **91**(4): p. 1487-500.
60. Eachempati, S.R., L. Hydo, and P.S. Barie, Gender-based differences in outcome in patients with sepsis. *Arch Surg*, 1999. **134**(12): p. 1342-7.
61. Ellis, A., C.G. Li, and M.J. Rand, Differential actions of L-cysteine on responses to nitric oxide, nitroxyl anions and EDRF in the rat aorta. *British Journal of Pharmacology*, 2000. **129**(2): p. 315-322.
62. Fink, M.P., Bench-to-bedside review: Cytopathic hypoxia. *Crit Care*, 2002. **6**(6): p. 491-9.
63. Fink, M.P. and S.O. Heard, Laboratory models of sepsis and septic shock. *J Surg Res*, 1990. **49**(2): p. 186-96.
64. Fiorucci, S., et al., The third gas: H<sub>2</sub>S regulates perfusion pressure in both the isolated and perfused normal rat liver and in cirrhosis. *Hepatology*, 2005. **42**(3): p. 539-48.
65. Fisher, C.J., Jr., et al., Recombinant human interleukin 1 receptor antagonist in the treatment of patients with sepsis syndrome. Results from a randomized, double-blind, placebo-controlled trial. Phase III rhIL-1ra Sepsis Syndrome Study Group. *JAMA*, 1994. **271**(23): p. 1836-43.
66. Fitch, K.A. and R.D. Rink, Hepatic oxygen supply during early and late sepsis in the rat. *Circ Shock*, 1983. **10**(1): p. 51-9.
67. Fredriksson, K., et al., Dysregulation of mitochondrial dynamics and the muscle transcriptome in ICU patients suffering from sepsis induced multiple organ failure. *PLoS One*, 2008. **3**(11): p. e3686.

68. Fukuyama, N., et al., Clinical evidence of peroxynitrite formation in chronic renal failure patients with septic shock. *Free Radic Biol Med*, 1997. **22**(5): p. 771-4.
69. Furne, J., A. Saeed, and M.D. Levitt, Whole tissue hydrogen sulfide concentrations are orders of magnitude lower than presently accepted values. *Am J Physiol Regul Integr Comp Physiol*, 2008. **295**(5): p. R1479-85.
70. Furne, J., et al., Oxidation of hydrogen sulfide and methanethiol to thiosulfate by rat tissues: a specialized function of the colonic mucosa. *Biochem Pharmacol*, 2001. **62**(2): p. 255-9.
71. Gaieski, D.F., et al., Benchmarking the incidence and mortality of severe sepsis in the United States. *Crit Care Med*, 2013. **41**(5): p. 1167-74.
72. Galley, H.F., Oxidative stress and mitochondrial dysfunction in sepsis. *Br J Anaesth*, 2011. **107**(1): p. 57-64.
73. Galluzzi, L., O. Kepp, and G. Kroemer, Mitochondria: master regulators of danger signalling. *Nat Rev Mol Cell Biol*, 2012. **13**(12): p. 780-8.
74. Garcia-Ponce, A., et al., The role of actin-binding proteins in the control of endothelial barrier integrity. *Thromb Haemost*, 2015. **113**(1): p. 20-36.
75. Garlid, K.D., Opening mitochondrial K(ATP) in the heart--what happens, and what does not happen. *Basic Res Cardiol*, 2000. **95**(4): p. 275-9.
76. Garlid, K.D. and P. Paucek, Mitochondrial potassium transport: the K(+) cycle. *Biochim Biophys Acta*, 2003. **1606**(1-3): p. 23-41.
77. Gasparetto, A., et al., Effect of tissue hypoxia and septic shock on human skeletal muscle mitochondria. *Lancet*, 1983. **2**(8365-66): p. 1486.
78. Gimson, A.E., Hepatic dysfunction during bacterial sepsis. *Intensive Care Med*, 1987. **13**(3): p. 162-6.
79. Goldstein, J.C., et al., The coordinate release of cytochrome c during apoptosis is rapid, complete and kinetically invariant. *Nat Cell Biol*, 2000. **2**(3): p. 156-62.
80. Gonzalez, A.S., et al., Abnormal mitochondrial fusion-fission balance contributes to the progression of experimental sepsis. *Free Radic Res*, 2014. **48**(7): p. 769-83.
81. Gopalakrishna, D., et al., ET-1 Stimulates Superoxide Production by eNOS Following Exposure of Vascular Endothelial Cells to Endotoxin. *Shock*, 2016. **46**(1): p. 60-6.
82. Gubern, M., et al., Sulfide, the first inorganic substrate for human cells. *FASEB J*, 2007. **21**(8): p. 1699-706.

83. Graser, T., Y.P. Vedernikov, and D.S. Li, Study on the mechanism of carbon monoxide induced endothelium-independent relaxation in porcine coronary artery and vein. *Biomed Biochim Acta*, 1990. **49**(4): p. 293-6.
84. Griffith, T.M., et al., Isolated perfused rabbit coronary artery and aortic strip preparations: the role of endothelium-derived relaxant factor. *J Physiol*, 1984. **351**: p. 13-24.
85. Gundersen, Y., et al., The nitric oxide donor sodium nitroprusside protects against hepatic microcirculatory dysfunction in early endotoxaemia. *Intensive Care Med*, 1998. **24**(12): p. 1257-63.
86. Haden, D.W., et al., Mitochondrial biogenesis restores oxidative metabolism during *Staphylococcus aureus* sepsis. *Am J Respir Crit Care Med*, 2007. **176**(8): p. 768-77.
87. Hayes, M.A., et al., Oxygen transport patterns in patients with sepsis syndrome or septic shock: influence of treatment and relationship to outcome. *Crit Care Med*, 1997. **25**(6): p. 926-36.
88. Hildebrandt, T.M. and M.K. Grieshaber, Three enzymatic activities catalyze the oxidation of sulfide to thiosulfate in mammalian and invertebrate mitochondria. *Febs Journal*, 2008. **275**(13): p. 3352-3361.
89. Hill, B.C., et al., Interactions of sulphide and other ligands with cytochrome c oxidase. An electron-paramagnetic-resonance study. *Biochem J*, 1984. **224**(2): p. 591-600.
90. Hollenberg, S.M., et al., Effects of nitric oxide synthase inhibition on microvascular reactivity in septic mice. *Shock*, 1999. **12**(4): p. 262-7.
91. Hoppins, S., L. Lackner, and J. Nunnari, The machines that divide and fuse mitochondria. *Annu Rev Biochem*, 2007. **76**: p. 751-80.
92. Hosoki, R., N. Matsuki, and H. Kimura, The possible role of hydrogen sulfide as an endogenous smooth muscle relaxant in synergy with nitric oxide. *Biochem Biophys Res Commun*, 1997. **237**(3): p. 527-31.
93. Hotchkiss, R.S., et al., Cell death. *N Engl J Med*, 2009. **361**(16): p. 1570-83.
94. Hotchkiss, R.S., et al., Apoptotic cell death in patients with sepsis, shock, and multiple organ dysfunction. *Crit Care Med*, 1999. **27**(7): p. 1230-51.
95. Housset, C., D.C. Rokey, and D.M. Bissell, Endothelin receptors in rat liver: lipocytes as a contractile target for endothelin 1. *Proc Natl Acad Sci U S A*, 1993. **90**(20): p. 9266-70.

96. Huang, L.E., et al., Inhibition of hypoxia-inducible factor 1 activation by carbon monoxide and nitric oxide. Implications for oxygen sensing and signaling. *J Biol Chem*, 1999. **274**(13): p. 9038-44.
97. Hubacek, J.A., et al., Gene variants of the bactericidal/permeability increasing protein and lipopolysaccharide binding protein in sepsis patients: gender-specific genetic predisposition to sepsis. *Crit Care Med*, 2001. **29**(3): p. 557-61.
98. Ignarro, L.J., Endothelium-derived nitric oxide: actions and properties. *FASEB J*, 1989. **3**(1): p. 31-6.
99. Ignarro, L.J., et al., Activation of purified soluble guanylate cyclase by endothelium-derived relaxing factor from intrapulmonary artery and vein: stimulation by acetylcholine, bradykinin and arachidonic acid. *J Pharmacol Exp Ther*, 1986. **237**(3): p. 893-900.
100. Jacobi, J., et al., Exogenous superoxide mediates pro-oxidative, proinflammatory, and procoagulatory changes in primary endothelial cell cultures. *Free Radic Biol Med*, 2005. **39**(9): p. 1238-48.
101. James, P.E., et al., Endotoxin-induced liver hypoxia: defective oxygen delivery versus oxygen consumption. *Nitric Oxide*, 2002. **6**(1): p. 18-28.
102. Jha, S., et al., Hydrogen sulfide attenuates hepatic ischemia-reperfusion injury: role of antioxidant and antiapoptotic signaling. *Am J Physiol Heart Circ Physiol*, 2008. **295**(2): p. H801-6.
103. Jia, L. and R.F. Furchgott, Inhibition by sulfhydryl compounds of vascular relaxation induced by nitric oxide and endothelium-derived relaxing factor. *J Pharmacol Exp Ther*, 1993. **267**(1): p. 371-8.
104. Jin, S.M., et al., Mitochondrial membrane potential regulates PINK1 import and proteolytic destabilization by PARL. *J Cell Biol*, 2010. **191**(5): p. 933-42.
105. Kabil, O. and R. Banerjee, Redox biochemistry of hydrogen sulfide. *J Biol Chem*, 2010. **285**(29): p. 21903-7.
106. Kamoun, W.S., et al., LPS inhibits endothelin-1-induced endothelial NOS activation in hepatic sinusoidal cells through a negative feedback involving caveolin-1. *Hepatology*, 2006. **43**(1): p. 182-90.
107. Kamoun, W.S., et al., Quantification of hepatic microcirculation heterogeneity of perfusion: effects of endothelin-1. *Microvasc Res*, 2005. **69**(3): p. 180-6.
108. Kamoun, W.S., et al., Induction of biphasic changes in perfusion heterogeneity of rat liver after sequential stress in vivo. *Shock*, 2005. **24**(4): p. 324-31.

109. Kane, L.A., et al., PINK1 phosphorylates ubiquitin to activate Parkin E3 ubiquitin ligase activity. *J Cell Biol*, 2014. **205**(2): p. 143-53.
110. Karapetsa, M., et al., Oxidative status in ICU patients with septic shock. *Food Chem Toxicol*, 2013. **61**: p. 106-11.
111. Kawada, N., et al., ROCK inhibitor Y-27632 attenuates stellate cell contraction and portal pressure increase induced by endothelin-1. *Biochem Biophys Res Commun*, 1999. **266**(2): p. 296-300.
112. Kawada, N., et al., The contraction of hepatic stellate (Ito) cells stimulated with vasoactive substances. Possible involvement of endothelin 1 and nitric oxide in the regulation of the sinusoidal tonus. *Eur J Biochem*, 1993. **213**(2): p. 815-23.
113. Keller, S.A., et al., Kupffer cell ablation improves hepatic microcirculation after trauma and sepsis. *J Trauma*, 2005. **58**(4): p. 740-9; discussion 749-51.
114. Kimura, H., The physiological role of hydrogen sulfide and beyond. *Nitric Oxide*, 2014. **41**: p. 4-10.
115. Kiriya, Y. and H. Nochi, Intra- and Intercellular Quality Control Mechanisms of Mitochondria. *Cells*, 2017. **7**(1).
116. Klatt, P., et al., Structural analysis of porcine brain nitric oxide synthase reveals a role for tetrahydrobiopterin and L-arginine in the formation of an SDS-resistant dimer. *EMBO J*, 1995. **14**(15): p. 3687-95.
117. Klaus, D.A., et al., Increased plasma zonulin in patients with sepsis. *Biochem Med (Zagreb)*, 2013. **23**(1): p. 107-11.
118. Ko, A.R., et al., Endothelin-1 induces LIMK2-mediated programmed necrotic neuronal death independent of NOS activity. *Mol Brain*, 2015. **8**: p. 58.
119. Kohen, R. and A. Nyska, Oxidation of biological systems: oxidative stress phenomena, antioxidants, redox reactions, and methods for their quantification. *Toxicol Pathol*, 2002. **30**(6): p. 620-50.
120. Kosir, M. and M. Podbregar, Advances in the Diagnosis of Sepsis: Hydrogen Sulfide as a Prognostic Marker of Septic Shock Severity. *EJIFCC*, 2017. **28**(2): p. 134-141.
121. Kowaltowski, A.J., et al., Bioenergetic consequences of opening the ATP-sensitive K(+) channel of heart mitochondria. *Am J Physiol Heart Circ Physiol*, 2001. **280**(2): p. H649-57.

122. Koyano, F., et al., Ubiquitin is phosphorylated by PINK1 to activate parkin. *Nature*, 2014. **510**(7503): p. 162-6.
123. Kozlov, A.V., et al., Mitochondria-mediated pathways of organ failure upon inflammation. *Redox Biol*, 2017. **13**: p. 170-181.
124. Kreymann, G., et al., Oxygen consumption and resting metabolic rate in sepsis, sepsis syndrome, and septic shock. *Crit Care Med*, 1993. **21**(7): p. 1012-9.
125. Kubo, S., M. Kajiwara, and A. Kawabata, Dual modulation of the tension of isolated gastric artery and gastric mucosal circulation by hydrogen sulfide in rats. *Inflammopharmacology*, 2007. **15**(6): p. 288-92.
126. Kulkarni-Chitnis, M., et al., Inhibitory action of novel hydrogen sulfide donors on bovine isolated posterior ciliary arteries. *Exp Eye Res*, 2015. **134**: p. 73-9.
127. Kwok, W. and M.G. Clemens, Targeted mutation of Cav-1 alleviates the effect of endotoxin in the inhibition of ET-1-mediated eNOS activation in the liver. *Shock*, 2010. **33**(4): p. 392-8.
128. Kwok, W., et al., Caveolin-1 mediates endotoxin inhibition of endothelin-1-induced endothelial nitric oxide synthase activity in liver sinusoidal endothelial cells. *Am J Physiol Gastrointest Liver Physiol*, 2009. **297**(5): p. G930-9.
129. Labrousse, A.M., et al., C. elegans dynamin-related protein DRP-1 controls severing of the mitochondrial outer membrane. *Mol Cell*, 1999. **4**(5): p. 815-26.
130. Lagoutte, E., et al., Oxidation of hydrogen sulfide remains a priority in mammalian cells and causes reverse electron transfer in colonocytes. *Biochim Biophys Acta*, 2010. **1797**(8): p. 1500-11.
131. Lanone, S., et al., Muscular contractile failure in septic patients: role of the inducible nitric oxide synthase pathway. *Am J Respir Crit Care Med*, 2000. **162**(6): p. 2308-15.
132. Larsen, F.J., et al., Regulation of mitochondrial function and energetics by reactive nitrogen oxides. *Free Radic Biol Med*, 2012. **53**(10): p. 1919-28.
133. Lazarou, M., et al., The ubiquitin kinase PINK1 recruits autophagy receptors to induce mitophagy. *Nature*, 2015. **524**(7565): p. 309-314.
134. Lee, P.J., et al., Hypoxia-inducible factor-1 mediates transcriptional activation of the heme oxygenase-1 gene in response to hypoxia. *J Biol Chem*, 1997. **272**(9): p. 5375-81.
135. Li, L., et al., Hydrogen sulfide is a novel mediator of lipopolysaccharide-induced inflammation in the mouse. *FASEB J*, 2005. **19**(9): p. 1196-8.

136. Li, L., P. Rose, and P.K. Moore, Hydrogen sulfide and cell signaling. *Annu Rev Pharmacol Toxicol*, 2011. **51**: p. 169-87.
137. Li, L., et al., GYY4137, a novel hydrogen sulfide-releasing molecule, protects against endotoxic shock in the rat. *Free Radic Biol Med*, 2009. **47**(1): p. 103-13.
138. Liesa, M., M. Palacin, and A. Zorzano, Mitochondrial dynamics in mammalian health and disease. *Physiol Rev*, 2009. **89**(3): p. 799-845.
139. Lim, J.J., et al., Vasoconstrictive effect of hydrogen sulfide involves downregulation of cAMP in vascular smooth muscle cells. *Am J Physiol Cell Physiol*, 2008. **295**(5): p. C1261-70.
140. Lin, H. and J.J. McGrath, Vasodilating effects of carbon monoxide. *Drug Chem Toxicol*, 1988. **11**(4): p. 371-85.
141. Liu, X., et al., Induction of apoptotic program in cell-free extracts: requirement for dATP and cytochrome c. *Cell*, 1996. **86**(1): p. 147-57.
142. Liu, Y.H. and J.S. Bian, Bicarbonate-dependent effect of hydrogen sulfide on vascular contractility in rat aortic rings. *Am J Physiol Cell Physiol*, 2010. **299**(4): p. C866-72.
143. Llesuy, S., et al., Oxidative stress in muscle and liver of rats with septic syndrome. *Free Radic Biol Med*, 1994. **16**(4): p. 445-51.
144. Lopez, A., et al., Multiple-center, randomized, placebo-controlled, double-blind study of the nitric oxide synthase inhibitor 546C88: effect on survival in patients with septic shock. *Crit Care Med*, 2004. **32**(1): p. 21-30.
145. Madden, J.A., et al., Precursors and inhibitors of hydrogen sulfide synthesis affect acute hypoxic pulmonary vasoconstriction in the intact lung. *J Appl Physiol* (1985), 2012. **112**(3): p. 411-8.
146. Martin, G.S., et al., The epidemiology of sepsis in the United States from 1979 through 2000. *N Engl J Med*, 2003. **348**(16): p. 1546-54.
147. Matsuda, N., et al., PINK1 stabilized by mitochondrial depolarization recruits Parkin to damaged mitochondria and activates latent Parkin for mitophagy. *J Cell Biol*, 2010. **189**(2): p. 211-21.
148. McBride, H.M., M. Neuspiel, and S. Wasiak, Mitochondria: more than just a powerhouse. *Curr Biol*, 2006. **16**(14): p. R551-60.
149. McCuskey, R.S., R. Urbaschek, and B. Urbaschek, The microcirculation during endotoxemia. *Cardiovasc Res*, 1996. **32**(4): p. 752-63.

150. Meissner, C., et al., The mitochondrial intramembrane protease PARL cleaves human Pink1 to regulate Pink1 trafficking. *J Neurochem*, 2011. **117**(5): p. 856-67.
151. Merkel, S.M., et al., LPS inhibits endothelin-1-mediated eNOS translocation to the cell membrane in sinusoidal endothelial cells. *Microcirculation*, 2005. **12**(5): p. 433-42.
152. Moccia, F., et al., Hydrogen sulfide regulates intracellular Ca<sup>2+</sup> concentration in endothelial cells from excised rat aorta. *Curr Pharm Biotechnol*, 2011. **12**(9): p. 1416-26.
153. Munaron, L., et al., Hydrogen sulfide as a regulator of calcium channels. *Cell Calcium*, 2013. **53**(2): p. 77-84.
154. Mustafa, A.K., et al., H<sub>2</sub>S signals through protein S-sulfhydration. *Sci Signal*, 2009. **2**(96): p. ra72.
155. Mustafa, A.K., et al., Hydrogen sulfide as endothelium-derived hyperpolarizing factor sulfhydrates potassium channels. *Circ Res*, 2011. **109**(11): p. 1259-68.
156. Napolitano, L.M., et al., Gender differences in adverse outcomes after blunt trauma. *J Trauma*, 2001. **50**(2): p. 274-80.
157. Narendra, D.P., et al., PINK1 is selectively stabilized on impaired mitochondria to activate Parkin. *PLoS Biol*, 2010. **8**(1): p. e1000298.
158. Newcomb, D., et al., Antibiotic treatment influences outcome in murine sepsis: mediators of increased morbidity. *Shock*, 1998. **10**(2): p. 110-7.
159. Nicholls, P. and J.K. Kim, Sulphide as an inhibitor and electron donor for the cytochrome c oxidase system. *Can J Biochem*, 1982. **60**(6): p. 613-23.
160. Nisoli, E., et al., Mitochondrial biogenesis in mammals: the role of endogenous nitric oxide. *Science*, 2003. **299**(5608): p. 896-9.
161. Norris, E.J., et al., The liver as a central regulator of hydrogen sulfide. *Shock*, 2011. **36**(3): p. 242-50.
162. Norris, E.J., et al., Hydrogen sulfide modulates sinusoidal constriction and contributes to hepatic microcirculatory dysfunction during endotoxemia. *Am J Physiol Gastrointest Liver Physiol*, 2013. **304**(12): p. G1070-8.
163. Norris, E.J., et al., Hydrogen sulfide differentially affects the hepatic vasculature in response to phenylephrine and endothelin 1 during endotoxemia. *Shock*, 2013. **39**(2): p. 168-75.

164. Olson, K.R., Hydrogen sulfide and oxygen sensing: implications in cardiorespiratory control. *J Exp Biol*, 2008. **211**(Pt 17): p. 2727-34.
165. Olson, K.R., Is hydrogen sulfide a circulating "gasotransmitter" in vertebrate blood? *Biochim Biophys Acta*, 2009. **1787**(7): p. 856-63.
166. Olson, K.R., et al., Thiosulfate: a readily accessible source of hydrogen sulfide in oxygen sensing. *Am J Physiol Regul Integr Comp Physiol*, 2013. **305**(6): p. R592-603.
167. Olson, K.R., et al., Hydrogen sulfide as an oxygen sensor/transducer in vertebrate hypoxic vasoconstriction and hypoxic vasodilation. *J Exp Biol*, 2006. **209**(Pt 20): p. 4011-23.
168. Olson, K.R., et al., Hypoxic pulmonary vasodilation: a paradigm shift with a hydrogen sulfide mechanism. *Am J Physiol Regul Integr Comp Physiol*, 2010. **298**(1): p. R51-60.
169. Opal, S.M., et al., Confirmatory interleukin-1 receptor antagonist trial in severe sepsis: a phase III, randomized, double-blind, placebo-controlled, multicenter trial. The Interleukin-1 Receptor Antagonist Sepsis Investigator Group. *Crit Care Med*, 1997. **25**(7): p. 1115-24.
170. Ordureau, A., et al., Defining roles of PARKIN and ubiquitin phosphorylation by PINK1 in mitochondrial quality control using a ubiquitin replacement strategy. *Proc Natl Acad Sci U S A*, 2015. **112**(21): p. 6637-42.
171. Osellame, L.D., T.S. Blacker, and M.R. Duchen, Cellular and molecular mechanisms of mitochondrial function. *Best Pract Res Clin Endocrinol Metab*, 2012. **26**(6): p. 711-23.
172. Osellame, L.D., et al., Cooperative and independent roles of the Drp1 adaptors Mff, MiD49 and MiD51 in mitochondrial fission. *J Cell Sci*, 2016. **129**(11): p. 2170-81.
173. Palmer, C.S., et al., MiD49 and MiD51, new components of the mitochondrial fission machinery. *EMBO Rep*, 2011. **12**(6): p. 565-73.
174. Palmer, C.S., et al., The regulation of mitochondrial morphology: intricate mechanisms and dynamic machinery. *Cell Signal*, 2011. **23**(10): p. 1534-45.
175. Pannen, B.H., et al., Endotoxin pretreatment enhances portal venous contractile response to endothelin-1. *Am J Physiol*, 1996. **270**(1 Pt 2): p. H7-15.
176. Pannen, B.H., et al., A time-dependent balance between endothelins and nitric oxide regulating portal resistance after endotoxin. *Am J Physiol*, 1996. **271**(5 Pt 2): p. H1953-61.

177. Papapetropoulos, A., et al., Hydrogen sulfide is an endogenous stimulator of angiogenesis. *Proc Natl Acad Sci U S A*, 2009. **106**(51): p. 21972-7.
178. Park-Windhol, C. and P.A. D'Amore, Disorders of Vascular Permeability. *Annu Rev Pathol*, 2016. **11**: p. 251-81.
179. Partikian, A., et al., Rapid diffusion of green fluorescent protein in the mitochondrial matrix. *J Cell Biol*, 1998. **140**(4): p. 821-9.
180. Pastor, C.M. and T.R. Billiar, Nitric oxide causes hyporeactivity to phenylephrine in isolated perfused livers from endotoxin-treated rats. *Am J Physiol*, 1995. **268**(1 Pt 1): p. G177-82.
181. Paxian, M., et al., Functional link between ETB receptors and eNOS maintain tissue oxygenation in the normal liver. *Microcirculation*, 2004. **11**(5): p. 435-49.
182. Petersen, L.C., The effect of inhibitors on the oxygen kinetics of cytochrome c oxidase. *Biochim Biophys Acta*, 1977. **460**(2): p. 299-307.
183. Pickrell, A.M. and R.J. Youle, The roles of PINK1, parkin, and mitochondrial fidelity in Parkinson's disease. *Neuron*, 2015. **85**(2): p. 257-73.
184. Pinzani, M. and F. Marra, Cytokine receptors and signaling in hepatic stellate cells. *Semin Liver Dis*, 2001. **21**(3): p. 397-416.
185. Poderoso, J.J., et al., Nitric oxide inhibits electron transfer and increases superoxide radical production in rat heart mitochondria and submitochondrial particles. *Arch Biochem Biophys*, 1996. **328**(1): p. 85-92.
186. Pong, W.W. and W.D. Eldred, Interactions of the gaseous neuromodulators nitric oxide, carbon monoxide, and hydrogen sulfide in the salamander retina. *J Neurosci Res*, 2009. **87**(10): p. 2356-64.
187. Prieto-Lloret, J., et al., Role of reactive oxygen species and sulfide-quinone oxoreductase in hydrogen sulfide-induced contraction of rat pulmonary arteries. *Am J Physiol Lung Cell Mol Physiol*, 2018. **314**(4): p. L670-L685.
188. Puleo, F., et al., Gut failure in the ICU. *Semin Respir Crit Care Med*, 2011. **32**(5): p. 626-38.
189. Pun, P.B., et al., Gases in the mitochondria. *Mitochondrion*, 2010. **10**(2): p. 83-93.
190. Quayle, J.M., M.T. Nelson, and N.B. Standen, ATP-sensitive and inwardly rectifying potassium channels in smooth muscle. *Physiol Rev*, 1997. **77**(4): p. 1165-232.

191. Rajendran, P., et al., The vascular endothelium and human diseases. *Int J Biol Sci*, 2013. **9**(10): p. 1057-69.
192. Rasmussen, I., et al., Splanchnic and total body oxygen consumption in experimental fecal peritonitis in pigs: effects of dextran and iloprost. *Circ Shock*, 1992. **36**(4): p. 299-306.
193. Reinehr, R., R. Fischer, and D. Haussinger, Regulation of endothelin-A receptor sensitivity by cyclic adenosine monophosphate in rat hepatic stellate cells. *Hepatology*, 2002. **36**(4 Pt 1): p. 861-73.
194. Remick, D.G., et al., Comparison of the mortality and inflammatory response of two models of sepsis: lipopolysaccharide vs. cecal ligation and puncture. *Shock*, 2000. **13**(2): p. 110-6.
195. Remick, D.G. and P.A. Ward, Evaluation of endotoxin models for the study of sepsis. *Shock*, 2005. **24 Suppl 1**: p. 7-11.
196. Renga, B., et al., Reversal of Endothelial Dysfunction by GPBAR1 Agonism in Portal Hypertension Involves a AKT/FOXO1 Dependent Regulation of H<sub>2</sub>S Generation and Endothelin-1. *PLoS One*, 2015. **10**(11): p. e0141082.
197. Rockey, D.C., et al., Cellular localization of endothelin-1 and increased production in liver injury in the rat: potential for autocrine and paracrine effects on stellate cells. *Hepatology*, 1998. **27**(2): p. 472-80.
198. Rockey, D.C. and R.A. Weisiger, Endothelin induced contractility of stellate cells from normal and cirrhotic rat liver: implications for regulation of portal pressure and resistance. *Hepatology*, 1996. **24**(1): p. 233-40.
199. Roller, J., et al., Heme oxygenase (HO)-1 protects from lipopolysaccharide (LPS)-mediated liver injury by inhibition of hepatic leukocyte accumulation and improvement of microvascular perfusion. *Langenbecks Arch Surg*, 2010. **395**(4): p. 387-94.
200. Rosser, D.M., et al., Endotoxin reduces maximal oxygen consumption in hepatocytes independent of any hypoxic insult. *Intensive Care Med*, 1998. **24**(7): p. 725-9.
201. Rosser, D.M., et al., Oxygen tension in the bladder epithelium rises in both high and low cardiac output endotoxemic sepsis. *J Appl Physiol (1985)*, 1995. **79**(6): p. 1878-82.
202. Sair, M., et al., Tissue oxygenation and perfusion in patients with systemic sepsis. *Crit Care Med*, 2001. **29**(7): p. 1343-9.

203. Sakr, Y., et al., The influence of gender on the epidemiology of and outcome from severe sepsis. *Crit Care*, 2013. **17**(2): p. R50.
204. Schnoor, M., Endothelial actin-binding proteins and actin dynamics in leukocyte transendothelial migration. *J Immunol*, 2015. **194**(8): p. 3535-41.
205. Schultz, M.J. and T. van der Poll, Animal and human models for sepsis. *Ann Med*, 2002. **34**(7-8): p. 573-81.
206. Shah, V., et al., Liver sinusoidal endothelial cells are responsible for nitric oxide modulation of resistance in the hepatic sinusoids. *J Clin Invest*, 1997. **100**(11): p. 2923-30.
207. Shah, V., et al., Impaired endothelial nitric oxide synthase activity associated with enhanced caveolin binding in experimental cirrhosis in the rat. *Gastroenterology*, 1999. **117**(5): p. 1222-8.
208. Shibuya, N., et al., 3-Mercaptopyruvate sulfurtransferase produces hydrogen sulfide and bound sulfane sulfur in the brain. *Antioxid Redox Signal*, 2009. **11**(4): p. 703-14.
209. Shokolenko, I., et al., Oxidative stress induces degradation of mitochondrial DNA. *Nucleic Acids Res*, 2009. **37**(8): p. 2539-48.
210. Siebert, N., et al., H<sub>2</sub>S contributes to the hepatic arterial buffer response and mediates vasorelaxation of the hepatic artery via activation of K(ATP) channels. *Am J Physiol Gastrointest Liver Physiol*, 2008. **295**(6): p. G1266-73.
211. Singer, M. and D. Brealey, Mitochondrial dysfunction in sepsis. *Biochem Soc Symp*, 1999. **66**: p. 149-66.
212. Sivarajah, A., M.C. McDonald, and C. Thiemermann, The production of hydrogen sulfide limits myocardial ischemia and reperfusion injury and contributes to the cardioprotective effects of preconditioning with endotoxin, but not ischemia in the rat. *Shock*, 2006. **26**(2): p. 154-61.
213. Sohail, M.A., et al., Adenosine induces loss of actin stress fibers and inhibits contraction in hepatic stellate cells via Rho inhibition. *Hepatology*, 2009. **49**(1): p. 185-94.
214. Sonin, N.V., et al., Patterns of vasoregulatory gene expression in the liver response to ischemia/reperfusion and endotoxemia. *Shock*, 1999. **11**(3): p. 175-9.
215. Soon, R.K., Jr. and H.F. Yee, Jr., Stellate cell contraction: role, regulation, and potential therapeutic target. *Clin Liver Dis*, 2008. **12**(4): p. 791-803, viii.

216. Spapen, H., Liver perfusion in sepsis, septic shock, and multiorgan failure. *Anat Rec (Hoboken)*, 2008. **291**(6): p. 714-20.
217. Spiller, F., et al., Hydrogen sulfide improves neutrophil migration and survival in sepsis via K<sup>+</sup>ATP channel activation. *Am J Respir Crit Care Med*, 2010. **182**(3): p. 360-8.
218. Srinivasan, S. and N.G. Avadhani, Cytochrome c oxidase dysfunction in oxidative stress. *Free Radic Biol Med*, 2012. **53**(6): p. 1252-63.
219. Stidwill, R.P., D.M. Rosser, and M. Singer, Cardiorespiratory, tissue oxygen and hepatic NADH responses to graded hypoxia. *Intensive Care Med*, 1998. **24**(11): p. 1209-16.
220. Stipanuk, M.H. and P.W. Beck, Characterization of the enzymic capacity for cysteine desulphhydration in liver and kidney of the rat. *Biochem J*, 1982. **206**(2): p. 267-77.
221. Stojanovski, D., et al., Levels of human Fis1 at the mitochondrial outer membrane regulate mitochondrial morphology. *J Cell Sci*, 2004. **117**(Pt 7): p. 1201-10.
222. Stuehr, D., S. Pou, and G.M. Rosen, Oxygen reduction by nitric-oxide synthases. *J Biol Chem*, 2001. **276**(18): p. 14533-6.
223. Suen, D.F., K.L. Norris, and R.J. Youle, Mitochondrial dynamics and apoptosis. *Genes Dev*, 2008. **22**(12): p. 1577-90.
224. Suliman, H.B., et al., A new activating role for CO in cardiac mitochondrial biogenesis. *J Cell Sci*, 2007. **120**(Pt 2): p. 299-308.
225. Sun, J.M., et al., Reduction of isoproterenol-induced cardiac hypertrophy and modulation of myocardial connexin43 by a KATP channel agonist. *Mol Med Rep*, 2015. **11**(3): p. 1845-50.
226. Sun, Q., et al., Structural basis for the inhibition mechanism of human cystathionine gamma-lyase, an enzyme responsible for the production of H<sub>2</sub>S. *J Biol Chem*, 2009. **284**(5): p. 3076-85.
227. Szabo, C., Hydrogen sulphide and its therapeutic potential. *Nat Rev Drug Discov*, 2007. **6**(11): p. 917-35.
228. Szabo, C. and K. Modis, Pathophysiological roles of peroxynitrite in circulatory shock. *Shock*, 2010. **34** **Suppl 1**: p. 4-14.
229. Szabo, C., et al., Regulation of mitochondrial bioenergetic function by hydrogen sulfide. Part I. Biochemical and physiological mechanisms. *Br J Pharmacol*, 2014. **171**(8): p. 2099-122.

230. Tang, D., et al., PAMPs and DAMPs: signals that spur autophagy and immunity. *Immunol Rev*, 2012. **249**(1): p. 158-75.
231. Tang, G., et al., Direct stimulation of K(ATP) channels by exogenous and endogenous hydrogen sulfide in vascular smooth muscle cells. *Mol Pharmacol*, 2005. **68**(6): p. 1757-64.
232. Tang, G., et al., H<sub>2</sub>S is an endothelium-derived hyperpolarizing factor. *Antioxid Redox Signal*, 2013. **19**(14): p. 1634-46.
233. Taniguchi, E., et al., Rhodanese, but not cystathionine-gamma-lyase, is associated with dextran sulfate sodium-evoked colitis in mice: a sign of impaired colonic sulfide detoxification? *Toxicology*, 2009. **264**(1-2): p. 96-103.
234. Tsutsui, H., S. Kinugawa, and S. Matsushima, Oxidative stress and mitochondrial DNA damage in heart failure. *Circ J*, 2008. **72 Suppl A**: p. A31-7.
235. Twig, G. and O.S. Shirihai, The interplay between mitochondrial dynamics and mitophagy. *Antioxid Redox Signal*, 2011. **14**(10): p. 1939-51.
236. VanderMeer, T.J., H. Wang, and M.P. Fink, Endotoxemia causes ileal mucosal acidosis in the absence of mucosal hypoxia in a normodynamic porcine model of septic shock. *Crit Care Med*, 1995. **23**(7): p. 1217-26.
237. Vieira, H.L., C.S. Queiroga, and P.M. Alves, Pre-conditioning induced by carbon monoxide provides neuronal protection against apoptosis. *J Neurochem*, 2008. **107**(2): p. 375-84.
238. Viridis, A., et al., Cyclooxygenase-2 inhibition improves vascular endothelial dysfunction in a rat model of endotoxic shock: role of inducible nitric-oxide synthase and oxidative stress. *J Pharmacol Exp Ther*, 2005. **312**(3): p. 945-53.
239. Vollmar, B., et al., Hepatic microcirculatory perfusion failure is a determinant of liver dysfunction in warm ischemia-reperfusion. *Am J Pathol*, 1994. **145**(6): p. 1421-31.
240. Waltz, P., et al., Lipopolysaccharide induces autophagic signaling in macrophages via a TLR4, heme oxygenase-1 dependent pathway. *Autophagy*, 2011. **7**(3): p. 315-20.
241. Wang, R., The gasotransmitter role of hydrogen sulfide. *Antioxid Redox Signal*, 2003. **5**(4): p. 493-501.
242. Wang, R., Physiological implications of hydrogen sulfide: a whiff exploration that blossomed. *Physiol Rev*, 2012. **92**(2): p. 791-896.

243. Wang, R., Two's company, three's a crowd: can H<sub>2</sub>S be the third endogenous gaseous transmitter? *FASEB J*, 2002. **16**(13): p. 1792-8.
244. Webster, N.R. and J.F. Nunn, Molecular structure of free radicals and their importance in biological reactions. *Br J Anaesth*, 1988. **60**(1): p. 98-108.
245. Weidinger, A., et al., Vicious inducible nitric oxide synthase-mitochondrial reactive oxygen species cycle accelerates inflammatory response and causes liver injury in rats. *Antioxid Redox Signal*, 2015. **22**(7): p. 572-86.
246. Whitfield, N.L., et al., Reappraisal of H<sub>2</sub>S/sulfide concentration in vertebrate blood and its potential significance in ischemic preconditioning and vascular signaling. *Am J Physiol Regul Integr Comp Physiol*, 2008. **294**(6): p. R1930-7.
247. Yanagisawa, M., et al., A novel potent vasoconstrictor peptide produced by vascular endothelial cells. *Nature*, 1988. **332**(6163): p. 411-5.
248. Yang, G., et al., H<sub>2</sub>S as a physiologic vasorelaxant: hypertension in mice with deletion of cystathionine gamma-lyase. *Science*, 2008. **322**(5901): p. 587-90.
249. Yin, F., H. Sancheti, and E. Cadenas, Mitochondrial thiols in the regulation of cell death pathways. *Antioxid Redox Signal*, 2012. **17**(12): p. 1714-27.
250. Yokoyama, Y., et al., Endothelin receptor remodeling induces the portal venous hyper-response to endothelin-1 following endotoxin pretreatment. *Shock*, 2002. **17**(1): p. 36-40.
251. Yokoyama, Y., et al., Altered endothelin receptor subtype expression in hepatic injury after ischemia/reperfusion. *Shock*, 2000. **13**(1): p. 72-8.
252. Yong, R. and D.G. Searcy, Sulfide oxidation coupled to ATP synthesis in chicken liver mitochondria. *Comp Biochem Physiol B Biochem Mol Biol*, 2001. **129**(1): p. 129-37.
253. Youle, R.J. and A.M. van der Bliek, Mitochondrial fission, fusion, and stress. *Science*, 2012. **337**(6098): p. 1062-5.
254. Zellweger, R., et al., Females in proestrus state maintain splenic immune functions and tolerate sepsis better than males. *Crit Care Med*, 1997. **25**(1): p. 106-10.
255. Zhang, H., S.M. Moochhala, and M. Bhatia, Endogenous hydrogen sulfide regulates inflammatory response by activating the ERK pathway in polymicrobial sepsis. *J Immunol*, 2008. **181**(6): p. 4320-31.

256. Zhang, H., et al., Endogenous hydrogen sulfide regulates leukocyte trafficking in cecal ligation and puncture-induced sepsis. *J Leukoc Biol*, 2007. **82**(4): p. 894-905.
257. Zhang, H., et al., Role of hydrogen sulfide in cecal ligation and puncture-induced sepsis in the mouse. *Am J Physiol Lung Cell Mol Physiol*, 2006. **290**(6): p. L1193-201.
258. Zhang, J., et al., Role of hydrogen sulfide in severe burn injury-induced inflammation in mice. *Mol Med*, 2010. **16**(9-10): p. 417-24.
259. Zhang, J.X., M. Bauer, and M.G. Clemens, Vessel- and target cell-specific actions of endothelin-1 and endothelin-3 in rat liver. *Am J Physiol*, 1995. **269**(2 Pt 1): p. G269-77.
260. Zhang, J.X., W. Pegoli, Jr., and M.G. Clemens, Endothelin-1 induces direct constriction of hepatic sinusoids. *Am J Physiol*, 1994. **266**(4 Pt 1): p. G624-32.
261. Zhang, Q., et al., Hydrogen sulfide preconditioning protects rat liver against ischemia/reperfusion injury by activating Akt-GSK-3beta signaling and inhibiting mitochondrial permeability transition. *PLoS One*, 2013. **8**(9): p. e74422.
262. Zhang, Q., K. Itagaki, and C.J. Hauser, Mitochondrial DNA is released by shock and activates neutrophils via p38 map kinase. *Shock*, 2010. **34**(1): p. 55-9.
263. Zhang, Q., et al., Circulating mitochondrial DAMPs cause inflammatory responses to injury. *Nature*, 2010. **464**(7285): p. 104-7.
264. Zhao, W., et al., The vasorelaxant effect of H<sub>2</sub>S as a novel endogenous gaseous K(ATP) channel opener. *EMBO J*, 2001. **20**(21): p. 6008-16.
265. Zhao, Y., T.D. Biggs, and M. Xian, Hydrogen sulfide (H<sub>2</sub>S) releasing agents: chemistry and biological applications. *Chem Commun (Camb)*, 2014. **50**(80): p. 11788-805.
266. Zou, P., et al., Coordinated Upregulation of Mitochondrial Biogenesis and Autophagy in Breast Cancer Cells: The Role of Dynamin Related Protein-1 and Implication for Breast Cancer Treatment. *Oxid Med Cell Longev*, 2016. **2016**: p. 4085727.